MECHANISMS OF ACTION OF MOOD-STABILIZING DRUGS

Elena Di Daniel
Department of Biology
University College London

Supervisors:
Professor Anne W Mudge
Dr Peter R Maycox

Thesis submitted for the degree of Doctor of Philosophy (PhD)
University of London

January 2007

ProQuest LLC
789 East Eisenhower Parkway
P.O. Box 1346
Ann Arbor, MI 48106-1346

ABSTRACT

Bipolar disorder or manic-depression is a severe and common psychiatric illness that is often treated with mood-stabilizing drugs. Several molecular targets and signalling pathways have been implicated in the pathophysiology of the illness and in the mechanism of action of these drugs. However, the precise targets that are responsible for the therapeutic action and side-effects of the drugs are not known.

In this PhD thesis we have analysed some of the potential drug targets, in particular extracellular signal-regulated kinase mitogen-activated protein kinase (ERK/MAPK) and glycogen synthase kinase-3 (GSK3), which mood stabilizers are believed to regulate. We showed, using cell and biochemical assays, that the effects of lithium, valproate or carbamazepine on ERK/MAPK are not always observed in a given cell type. In addition, only lithium inhibits GSK3 directly and modulation of this kinase with potent and selective inhibitors does not mimic the effects of mood stabilizers on cortical and sensory neuron growth cone morphology.

A major part of my thesis focused on the enzyme prolyl oligopeptidase (PO), which is thought to modulate the phosphatidylinositol pathway, as shown from studies in *Dictyostelium discoideum* and human astroglioma cells. PO inhibitors alone have no effect on sensory neuron growth cone morphology, but reverse the growth cone changes induced by mood stabilizers, mimicking addition of *myo*-inositol to the culture media. We studied PO null-mutant mice and analysed the effects of mood stabilizers on the morphology of growth cones from these mice. Unexpectedly, the PO null-mutant phenotype itself resembled wild-type neurons treated with a mood stabilizer and each drug had no further effect on growth cone morphology. These results show that PO is a critical component of signalling pathways involved in mood-stabilizing drug action on growth cones. Using viral delivery of native or catalytically-dead PO, we showed that each restored the wild-type phenotype. In order to better understand PO function, a yeast-two-hybrid screen (Y2H) was also performed at GlaxoSmithKline to determine protein interactors for PO, and we analysed one of these interactors, namely GAP43. We showed that both the native and the catalytically-dead PO co-precipitate with the neuronal protein GAP43. These results show that there are additional biological effects of PO independent of its catalytic domain.

DECLARATION

I declare that all the work presented in this thesis is entirely my own. When reagents were generated elsewhere, or part of the experiment was performed in collaboration with someone else, this is indicated in the text.

Elena Di Daniel

ACKNOWLEDGEMENTS

My very first and big acknowledgement is for Dr Carol Scorer, former Head of the Schizophrenia and Bipolar Disorder Department four years ago, who offered me the great opportunity to enrol for a PhD, while still working full-time in her Department.

I also would like to greatly acknowledge Drs Ceri Davies, Declan Jones and Jim Hagan for their input and support throughout these years.

Thanks to my excellent manager Peter Maycox who identified a superb supervisor at UCL, Professor Anne Mudge, with great drive and enthusiasm in the Bipolar Disorder research area. Both Peter and Anne have taught me a lot throughout these years and have always been present for me to discuss data and a way forward.

It has been a pleasure to work within the Molecular and Cellular Neurobiology team with my colleagues Melanie Robbins, Isabel Benzel, Olga Krylova, Colin Glover, and I would like to thank each of them for their support and discussions.

I also would like to thank Ajit Shah for the neurochemical analysis of inositol levels, Andrew Lloyd for helping me with the statistical analysis, Barbara Barbato from Information Management for drug information data, my good friends Mark and Steve for thesis proof-reading and formatting.

Thanks to Giovanna Lalli, Antonella Riccio and Dan Cutler for their suggestions and advice, their encouragement and time with me when at UCL, particularly during my third year presentation.

And finally I must thank my family: my mum Ilva, my brother Andrea and my dad PierLuigi for encouraging me during all these years abroad.

TABLE OF CONTENTS

LIST OF FIGURES AND TABLES

ABBREVIATIONS

AA:	arachidonic acid
bcl-2:	B-cell lymphoma leukemia-2
BD:	bipolar disorder
BDNF:	brain-derived neurotrophic factor
CBZ:	carbamazepine
CDP-DAG:	cytidine diphosphate-diacylglycerol
CNS:	central nervous system
COX:	cyclooxygenase
CREB:	cyclic AMP-response element binding protein
DAG:	diacylglycerol
DAT:	dopamine transporter
dic:	day in culture
DMEM:	Dulbecco's modified Eagle's medium
DMSO:	dimethyl sulfoxide
DRG:	dorsal root ganglion
ECL:	enhanced chemiluminescence
ECT:	electroconvulsive therapy
EDTA:	ethylenediaminetetraacetic acid
EGTA:	ethylene glycol tetraacetic acid (glycol-bis(2-aminoethylether)-N,N,N',N'-tetraacetic acid)
ERK MAPK:	extracellular signal-regulated kinase/mitogen-activated protein kinase
FBS:	foetal bovine serum
GAP43:	growth-associated protein 43
GPT:	gabapentin
GS:	glycogen synthase

GSK3:	glycogen synthase kinase-3
HBSS:	Hank's balanced-salt solution
HCl:	hydrochloric acid
HMIT:	H^+ dependent *myo*-inositol transporter
5-HT:	serotonin
ICC:	immunocytochemistry
IHC:	immunohistochemistry
IMPase:	inositol monophosphatase
IP:	immunoprecipitation
$InsP_3$ or IP_3:	inositol 1,4,5-trisphosphate
IPPase:	inositol polyphosphate-1-phosphatase
LiCl:	lithium chloride
LTG:	lamotrigine
MARCKS:	myristoylated alanine-rich C-kinase substrate
MInsPP:	multiple inositol polyphosphate phosphatase
MIP-synthase:	*myo*-inositol-1-phosphate synthase
MW:	molecular weight
NMDA:	N-methyl-D-aspartate
PA:	phosphatidic acid
PBS:	phosphate-buffered saline
PCR:	polymerase chain reaction
PFA:	paraformaldehyde
PKC:	protein kinase C
PIns:	phosphatidylinositol
PI4-kinase:	phosphatidylinositol synthase kinase
PIP5-kinase:	phosphatidylinositol 4-phosphate 5-kinase
PIP_2 or $PI(4,5)P_2$:	phosphatidylinositol 4,5-bisphosphate

PLC:	phospholipase C
PO:	prolyl oligopeptidase
PTN:	phenytoin
RNA:	ribonucleic acid
RT-PCR:	reverse transcription polymerase chain reaction
SDS-PAGE:	sodium-dodecyl-sulphate polyacrylamide gel electrophoresis
sem:	standard error of the mean
SMIT:	sodium-dependent *myo*-inositol transporter
SNP:	single nucleotide polymorphism
SSRI:	selective serotonin reuptake inhibitor
TBS:	Tris-buffered saline
TBST:	Tris-buffered saline with Tween 20
TRPM2:	melastatin-like transient receptor potential 2 channel
TSA:	trychostatin A
VPA:	sodium valproate (valproic acid sodium salt)
Y2H:	yeast-two-hybrid

CHAPTER 1
Introduction

1.1 Bipolar disorder

In 1896 Emil Kraepelin differentiated the major psychoses into dementia praecox and manic-depressive illness. In particular, he referred to dementia praecox (named today as schizophrenia) as an illness with a deteriorating course, in contrast to manic-depressive illness, which was believed to be episodic, with full recovery between episodes and with good prognosis.

A more recent description of manic-depressive illness, also named bipolar disorder (BD), has revealed that this is a severe, chronic, and often life-threatening illness, and that the favourable long-term outcome may only represent the situation for a minority of individuals (Goodwin & Jamison, 1990). Kraepelin's classification still survives in the current classification of Diagnostic and Statistical Manual of Mental Disorders (DSM-IV) (DSM-IV, 2000). Current estimates suggest that BD affects about 1.5 % of the world population (Goodwin & Jamison, 1990), it is equally distributed between men and women, and the median age of onset is in the early twenties (Weissman *et al.*, 1996). It has been shown that BD individuals with a history of major traumatic events in childhood (about one-third) are more difficult to treat, have a more severe course of the illness and an increased incidence of suicide attempts (Leverich *et al.*, 2002). There is an increased risk of onset in the post-partum period, therefore indicating that changes in hormonal levels may trigger the illness (Blehar *et al.*, 1998). In addition, for women with BD, the post-partum period is a time of considerable risk of relapse.

Two almost diametrically opposite mood states characterise BD: mania and depression - and individuals cycle between these two opposite mood poles. Mania is characterised by a hyper-aroused state (either euphoric or dysphoric), decreased need for sleep, increased motor activity, racing thoughts and increased optimism that can become so extreme that the individual's judgement is impaired. Individuals in the manic phase are prone to gamble and make inappropriate decisions, which may have a devastating impact on their lives. The depressive phases of the illness are characterised by a depressive mood, anhedonia and impaired sleep. These symptoms do not differ substantially from those observed in unipolar depression and are more recurrent than manic episodes. As highlighted in longitudinal studies, about two-thirds of BD individuals are greatly impacted by the illness

and they spend about one-third of their life time in a depressive state (Post *et al.*, 2003a; Post *et al.*, 2003b). BD is defined in DSM-IV as the occurrence of a major depressive episode in the context of having experienced at least one manic (BD type I) or hypo-manic (BD type II) episode. A longitudinal (20 years long) study has shown that BD-I and BD-II have similar demographic characteristics and ages of onset, with BD-II much more prevalent than type I and more difficult to diagnose (Judd *et al.*, 2003b; Judd *et al.*, 2003a). BD-II has a higher prevalence of anxiety disorders and social phobia compared with BD-I. The occurrence of four or more episodes of depression or mania within a 12-month period is referred to as 'rapid cycling', and the depressive episodes predominate. BD individuals cycle between these different phases and experience intervals of euthymia when they are asymptomatic, but they still maintain vulnerability to mood episodes. These periods of apparent clinical recovery are marked by subtle social, occupational, and cognitive impairments (Altshuler *et al.*, 2004; El Badri *et al.*, 2001). Recently, results from a meta-analysis study have indicated that euthymic BD individuals present marked impairment in some aspects of executive function and verbal memory (Robinson *et al.*, 2006). BD is diagnosed, on average, eight years after the first episode due to frequent misdiagnosis as unipolar depression (37% of BD individuals) (Ghaemi *et al.*, 2000). The illness has afflicted many famous musicians, writers and political leaders and it has been linked to creativity and success (Jamison, 1995). However, there is evidence that only the early phase of mania contributes to creativity, whereas full-blown mania usually becomes destructive to many aspects of life. As a result, many BD individuals are concerned that the pharmacological treatment of their mood swings may reduce their creativity, and many of them use or abuse alcohol or addictive drugs as self-medication (Jamison, 1996).

1.2 Genetics

Family and twin studies have demonstrated a strong genetic basis for BD (~80%) (Craddock & Forty, 2006; MacKinnon *et al.*, 1997; McGuffin *et al.*, 2003), yet classical genetic linkage analyses have not clearly identified the genes involved in the illness. A possible explanation for this lack of success so far is because BD is probably caused by the interaction of numerous genes, each of which exerts a modest increase in relative risk. Several genome regions of interest have been repeatedly implicated in individual studies, as indicated below:

4p16	**6q**	**12q23-24**	**18q21** **18q22** **18 centromere**	**21q22**
(Blackwood *et al.*, 1996)	(McQueen *et al.*, 2005)	(Craddock *et al.*, 1993)	(Stine *et al.*, 1995) (Straub *et al.*, 1994) (Berrettini *et al.*, 1994)	(Straub *et al.*, 1994)

Table 1.1 Chromosomal regions implicated in BD.

Furthermore, a meta-analysis study has shown strong evidence for susceptibility loci on chromosome 13q and 22q (Badner & Gershon, 2002) and the study by Segurado *et al.* showed a modest level of support for regions on chromosomes 9p22.3-21.1, 10q11.21-22.1 and 14q24.1-32.12 (Segurado *et al.*, 2003).

Candidate genes that have been implicated in BD are brain-derived neurotrophic factor (BDNF), melastatin-like transient receptor potential 2 channel (TRPM2), G72, glycogen synthase kinase-3 (GSK3) and the dopamine transporter (DAT), amongst others.

Of these, the neurotrophin BDNF has drawn particular attention as it modulates synaptic activity, survival and differentiation, which may all be altered in BD subjects. Moreover, two drugs used to treat BD, lithium (Li^+) and valproic acid (VPA), each increase BDNF levels in the rat cortex and hippocampus (Einat *et al.*, 2003). A single nucleotide polymorphism (SNP) has been identified in the BDNF gene (chromosome 11p13), causing

a Val66Met change, with the Val allele considered as a risk allele for BD (Sklar *et al.*, 2002; Green & Craddock, 2003). An earlier age of onset of BD has been reported for Val Val genotype carriers compared with Val Met (Rybakowski *et al.*, 2003). The Val/Met polymorphism seems also to affect the therapeutic response to lithium, with the Met polymorphism more frequent in lithium responders (Rybakowski *et al.*, 2005). At the cellular level, the Val Met polymorphism has been shown to impact intracellular trafficking and activity-dependent secretion of BDNF (Rybakowski *et al.*, 2005; Rybakowski *et al.*, 2003; Egan *et al.*, 2003). A recent study in a population of ~3,000 BD individuals has shown no association of Val Met BDNF polymorphism with BD, except for a subpopulation of rapid cycling subtypes (Green *et al.*, 2006). These findings show that further functional and genetic studies are needed to understand the involvement of this gene in the illness, as it is possible that other, yet to be analysed, SNPs may be associated with BD.

Another gene with a very strong genetic association with BD is TRPM2 (located on chromosome 21) (Xu *et al.*, 2006). Interestingly, alterations in TRPM2 levels associated with increased calcium concentration have been reported in BD blood cells (Yoon *et al.*, 2001). However, very limited studies have been performed in relation to BD and the relevance of these findings to the illness is not clear at present.

The most frequently replicated locus for BD to date is the higher primate-specific gene, G72 (on chromosome 13q33) (Schumacher *et al.*, 2004; Chen *et al.*, 2004; Hattori *et al.*, 2003). Recombinant G72 interacts with D-amino-acid oxidase (DAAO). DAAO oxidises D-serine, which is a potent activator of the N-methyl-D-aspartate glutamate receptor (NMDA). Interestingly, the G72 gene has also been associated with schizophrenia, therefore suggesting that the two illnesses may share some common susceptibility loci for some overlapping symptom domains (Schumacher *et al.*, 2004). A caveat, however, is that G72 mRNA and protein have not yet been detected in human tissues.

Another genetically associated, although biologically controversial gene for BD is GSK3. The α and β isoforms are mapped to human chromosome 19q13.1-13.2 and 3q13.3-21.1, respectively (Shaw *et al.*, 1998), regions that are weakly linked to BD (Badenhop *et al.*, 2002). One single nucleotide substitution in the promoter region of GSK3β at -50 T/C has

been associated with therapeutic response to lithium in a group of BD-I subjects (Benedetti *et al.*, 2005). In particular, carriers of the T/T genotype were less responsive to lithium treatment and had an earlier age of onset of the illness (Benedetti *et al.*, 2004a). In another study by the same group, 60 BD depressed individuals with the C/C genotype showed improved mood in response to total sleep deprivation (Benedetti *et al.*, 2004b). These findings suggest that the C/C genotype may be associated with a milder form of the disorder, and may have a protective role in respect to BD. Inhibition of GSK3β has been linked with effects on neuronal survival and neuroprotection (Jope & Bijur, 2002). However, the functional consequences of the C/C genotype on the above cellular effects have not been studied as yet. Overall, the biological and genetic data point to GSK3 as an interesting candidate target for BD.

An imbalance in the dopaminergic system has been hypothesized to contribute to the pathogenesis of a number of psychiatric illnesses, including BD. In particular, the dopamine transporter, DAT, plays a crucial role in striatal dopaminergic neurotransmission, as it modulates synaptic levels of dopamine and thus controls the concentration of active neurotransmitter. Two missense substitutions were identified in the DAT gene (chromosome 5p15.3) and were associated with BD: the Ala559Val mutant protein, which was shown to be functional, and the Glu602Gly mutant, which was not functional due to a failure in transport to the cell surface (Horschitz *et al.*, 2005). More recently, other variants have been reported that seem to associate with BD (Greenwood *et al.*, 2006). Interestingly, DAT knock-down mutant mice are hyper-active and VPA significantly attenuates the hyperactivity, therefore suggesting that the dopamine transporter is involved in manic behaviour.

Other genes more weakly associated with BD are indicated in the table below:

Neuregulin-1 (NRG)	**Disrupted in schizophrenia 1 (DISC1)**	**Catechol-O-Methyltransferase (COMT)**	**G-protein Receptor Kinase 3 (GRK3)**	**Inositol Monophosphatase (IMPA2)**
8p12	1q42	22q11	22q12.1	18p11.2
(Green *et al.*, 2005)	(Thomson *et al.*, 2005)	(Shifman *et al.*, 2004)	(Barrett *et al.*, 2003)	(Sjoholt *et al.*, 2004)

Table 1.2 Candidate genes associated with BD.

However, the role of these genes in the illness requires further investigation, such as replication of genetic association from well-controlled samples.

It is interesting to note that some susceptibility genes have been associated with both BD and schizophrenia or depression. In particular, of the above-mentioned genes, G72, DISC1 and neuregulin-1 have been associated with BD and unipolar depression, therefore indicating that these illnesses may have shared susceptibility for some overlapping symptoms domains (Craddock *et al.*, 2005). It is not unusual for a BD proband to have first-degree relatives diagnosed with schizophrenia and, to a lesser extent, unipolar depression. These findings show that there is a more complex relationship between the mood disorders than that reflected in the conventional Kraepelin dichotomy.

1.3 Pharmacological treatment of BD

Several drugs are currently used in the clinic to treat BD and are efficacious in the different phases of mania or depression. These drugs are known as 'mood stabilizers', a term that was not clearly defined until recently. Charles Bowden and Gary Sachs each suggest different definitions of 'mood stabilizer'. According to Bowden, a 'mood stabilizer' is a drug that alleviates the frequency and or intensity of manic, hypomanic, depressive or mixed episodes in BD individuals and that does not increase the frequency or severity of any of these types of BD episodes (Bowden, 1998). According to Sachs a 'mood stabilizer' is a drug that decreases the vulnerability to subsequent episodes of mania or depression and that does not exacerbate the current acute episode when administered during the acute, continuation or maintenance phase of treatment (Sachs, 1996). Both definitions seem to converge on a key feature that a 'mood stabilizer' should not cause an affective switch. The summary of the two definitions is the 'liberal definition', which states that a 'mood stabilizer' is an agent with efficacy in at least one of the three phases of BD (acute mania, acute depression or maintenance) and it should neither cause an affective switch to the opposite mood state nor should it worsen the acute episode (Ghaemi, 2001). Joseph Calabrese, instead, proposed a 'conservative definition', which states that a 'mood stabilizer' should be effective as monotherapy for the acute treatment of depression and mania and mixed states and for the prevention of relapse and recurrence (Calabrese & Rapport, 1999). Therefore, it becomes clear that different drugs are, or are not, considered as mood stabilizers depending on the definition used and this has caused great confusion in the field. Nassir Ghaemi, recently proposed an intermediate definition, which states that a 'mood stabilizer' is an agent with efficacy in two of the three phases of BD, namely acute mania, acute depression or prophylaxis of mania and depression (Ghaemi, 2001).

Following this definition the three most-commonly used mood stabilizers are Li^+, VPA and carbamazepine (CBZ), which are all approved for mania and BD prophylaxis by the Food and Drug Administration (FDA), the European Agency for the Evaluation of Medicinal Products (EMEA) and the Medicines and Healthcare Products Regulatory Agency in the UK (MHRA). More recently, olanzapine has been approved by the FDA and EMEA for the treatment of mania in 2000 and 2002, respectively, and for the maintenance therapy of BD in 2004 and, therefore, can be considered a mood stabilizer. Additionally, lamotrigine (LTG) is a potential mood stabilizer (Calabrese *et al.*, 2006; Goodwin *et al.*, 2004; Muzina

et al., 2005) and registration in the US is expected shortly. Mood stabilizer structures are very different and range from a cation (Li^+) to a tricyclic molecule (CBZ) (Fig. 1.1).

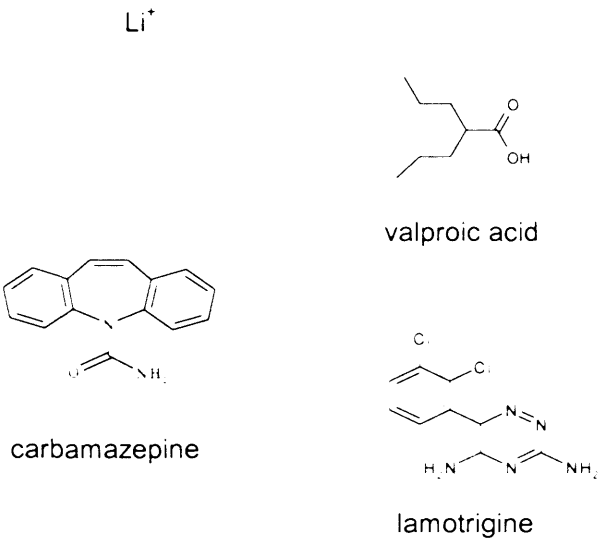

Fig. 1.1 Structure of the most-commonly used mood-stabilizing drugs.

The recommended use of drugs in the treatment of BD is covered by UK or US guidelines (Goodwin & Young, 2003) and sometimes discrepancies exist between the two that point towards professional and cultural differences (Vestergaard, 2004).

The discovery of lithium as an efficacious mood-stabilizing agent by Cade in 1949 and its introduction as a therapy by Mogens Schou revolutionised the treatment of BD. Lithium was approved for the treatment of acute mania in the US in 1970, and for the maintenance therapy in 1974. It shows some limited efficacy in the treatment of acute bipolar depression, and it has a strong anti-suicidal effect (Kessing *et al.*, 2005; Muller-Oerlinghausen *et al.*, 2005). It continues to be the "gold standard" for the treatment of BD, both for the acute manic phase and in preventing the frequency of episodes of mania and depression. There is, however, some evidence suggesting that certain groups of subjects do not respond adequately to lithium therapy, in particular those with rapid cycling, family history of affective illness in first-degree relatives, and co-morbid substance abuse (Calabrese & Woyshville, 1995). Lithium has a narrow therapeutic index (0.8 to 1.4 mEq/l) (Bowden, 1996) due to toxic effects on renal, neurological and cardiovascular systems. Other side-effects include gastric disturbances, diabetes insipidus, weight gain, flattened mood and loss of creativity. The intracellular concentrations of lithium, VPA and CBZ

have not been clearly determined, nor is the mechanism by which they cross the cell membrane. Some literature on lithium reported efflux and influx studies using lithium sensitive microelectrodes. Lithium is believed to accumulate into cells via the voltage-dependent sodium channel and the sodium/potassium exchange pump and possibly via calcium channels and extruded in an active manner using a sodium/lithium exchanger. The influx of lithium appears to be rapid and linear with time, while the rate of lithium efflux is slower. Cellular accumulation of lithium was reported to be accompanied by an approximately equimolar loss of potassium (O'Day & Phillips, 1991). An intra to extracellular ratio of about 0.7 was obtained in motorneurons, and similarly in cultured neurons, and lithium did not seem to ever equilibrate (Gow & Ellis, 1996; Grafe *et al.*, 1982). Overall, it looks like there are different ways of influx and efflux for lithium, generally involving exchange with sodium ions.

A series of anticonvulsant compounds has emerged as the major anti-manic or maintenance alternative to lithium, namely VPA, CBZ and LTG.

Divalproex (commercialised as Depakote: 1:1 molar ratio of sodium valproate and valproic acid) is at least as effective as lithium in acute mania (Bowden *et al.*, 1994) and more efficacious than lithium in mania accompanied by symptoms of depression (mixed states) (Swann *et al.*, 1997). It was approved for the treatment of acute mania in the US in 1995 and in the UK in 2001. Side-effects of VPA include nausea, vomiting, hepatotoxicity and teratogenicity with an increased risk of spina bifida and cardiac malformations. VPA has the propensity to induce weight gain (Owens & Nemeroff, 2003). VPA is metabolised into at least 14 different species via conjugation with glucuronic acid and oxidation and some of these metabolites exhibit pharmacological activity (Kakee *et al.*, 2002).

CBZ displays at least comparable efficacy to lithium (Okuma *et al.*, 1990) and to VPA (Nasrallah *et al.*, 2006) in acute mania and it was approved for this indication by the FDA in 2004. CBZ is less effective than lithium in preventing depressive breakthrough compared to manic relapse (Goodwin, 2003; Malhi *et al.*, 2003). CBZ is metabolised by cytochrome P450 3A3/4 and the main metabolite, epoxide, is also biologically active. Drug side-effects include rash, white cell suppression, transient hepatic enzyme elevations and neurotoxicity. Like VPA, CBZ is also teratogenic.

The sodium channel blocker LTG appears to be useful in monotherapy or combination therapy with another mood stabilizer for the treatment of BD depression without increasing cycling or provoking a switch into mania (Calabrese *et al.*, 1996; Calabrese *et al.*, 2002; Calabrese *et al.*, 2003); moreover, it is also efficacious in prophylaxis of depressive episodes (Yatham, 2004). A meta-analysis of 5 studies (performed by GlaxoSmithKline) (4 of which did not find a statistically significant effect as underpowered) found evidence of a modest, but clinically worthwhile, benefit for LTG in BD depression (Geddes *et al.*, 2006). LTG, instead, does not appear to have significant efficacy in treating acute mania (Calabrese *et al.*, 2003). It is well tolerated and it has a good side-effect profile (Bhagwagar & Goodwin, 2005). In all BD clinical trials, the rate of serious rash was 0.1% (0.1% also for placebo). Rash seems to occur when the initial dose is too high and the risk can be reduced with proper dose titration (GlaxoSmithKline filed data). It received FDA approval in 2003 for the maintenance treatment of BD, but it is not currently widely used in the UK (NICE guidelines).

Another anticonvulsant that has shown positive results in rapid-cycling BD subjects and in those refractory to conventional treatments is topiramate (Suppes, 2002). Further studies are required, however, to confirm its clinical efficacy. No evidence for efficacy in BD has been reported for the anticonvulsants gabapentin and phenytoin, at least as monotherapy (Yatham, 2004).

The atypical antipsychotic drugs, in particular olanzapine, aripiprazole, risperidone and ziprasidone, have all been approved by the FDA for the treatment of acute mania. Interestingly, the antipsychotic drug quetiapine has shown efficacy in depression as well as in manic episodes and it has just received approval from the FDA (Dando & Keating, 2006; Post *et al.*, 2003b).

Tricyclic antidepressants and selective serotonin reuptake inhibitors (SSRI) are used for the treatment of depressive episodes in BD; however, there is still some controversy about whether they represent an appropriate treatment. In particular, the 2002 American Psychiatry Association Guidelines recommended a more conservative use of antidepressant drugs, which was criticised by the more 'liberal' Munich group (Moller & Grunze, 2000). According to Ghaemi *et al.*, antidepressant drugs do not have a high risk of inducing mood

cycling and switch to mania; they are not proven to prevent suicide (unlike lithium) or to be better than a mood stabilizer in the long-term treatment of BD depression (Ghaemi *et al.*, 2003). The American Psychiatry Association Guidelines recommend that antidepressant drugs should be reserved for severe BD depression only and discontinued immediately after recovery. However, antidepressant drugs are generally prescribed earlier and more frequently than mood stabilizers due to misdiagnosis and ~20% of individuals experience a new or worsening rapid cycling (Ghaemi *et al.*, 2000). A previous study supporting the American Psychiatry Association recommendations has shown that 35% of individuals with BD had manic episodes rated as likely to have been antidepressant drug-induced. Furthermore, cycle acceleration has been reported in 26% of subjects after antidepressant drug treatments (Altshuler *et al.*, 1995). Younger age at first treatment was a predictor of vulnerability to antidepressant drug-induced cycle acceleration and it was more likely to occur in women with BD-II (Altshuler *et al.*, 1995). A more recent study has shown that newer antidepressant drugs do not have lower rates of negative outcomes compared with tricyclic antidepressant drugs (Ghaemi *et al.*, 2004). Overall, the data suggest that antidepressant drugs are probably overused and mood stabilizers underused and that development of better treatments for bipolar depression presents a "niche" in BD treatment.

In the search for better treatments it is also important to consider drugs that have little efficacy on their own but may be effective in BD through ability to potentiate other primary therapies. For example, olanzapine and other atypical antipsychotic drugs may possess mild to moderate antidepressant properties as an add-on with an antidepressant drug (Ghaemi, 2000). Finally, electroconvulsive therapy (ECT) is efficacious both in mania and depression, but it is used only in severe cases of the illness (Fink, 2006).

Despite extensive clinical use of the drugs described above, the cellular mechanisms modulated by these compounds still remain to be elucidated. In particular, knowing the clinically-relevant targets for treating BD would indicate which signalling pathways are critical for mood control. Focusing on these pathways would then allow identification of targets towards which more potent and selective drugs could be designed. Several molecules or pathways are known to be directly modulated by mood stabilizers and the literature points to GSK3 and to the phosphoinositide signalling pathway as a possible

common target pathway affected by mood stabilizers. Additional secondary targets that may be involved in the mechanism of action of mood stabilizers are the extracellular signal-regulated kinase mitogen-activated protein kinase, the *myo*-inositol transporters, *myo*-inositol synthase, protein kinase C (PKC) and prolyl oligopeptidase (PO). I have touched on all these targets in the course of this thesis, but have focussed my investigation primarily on the biological function of PO.

1.4 Mood stabilizers and the phosphoinositide signalling pathway

Inositol phospholipids play a major role in receptor-mediated signal transduction pathways and are implicated in a diverse range of cellular processes in the central nervous system (CNS), such as enzyme activation, cytoskeletal changes, endocytosis, exocytosis, ion-channel activation, spine morphology and production of various second messengers (Fig. 1.2) (McLaughlin & Murray, 2005).

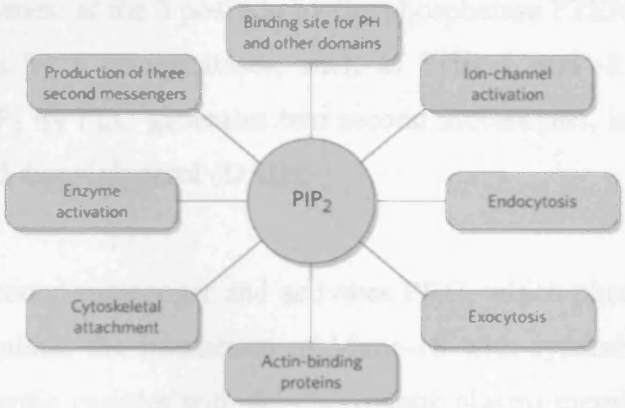

Fig. 1.2 Schematic of different functions of PIP_2. Source: (McLaughlin & Murray, 2005).

Activation of a variety of G-protein-linked neurotransmitter receptor subtypes and electrical activity (Micheva *et al.*, 2001) induce the hydrolysis of membrane phospholipids, in particular of phosphatidylinositol-4,5-bisphosphate (PIP_2, also named $PI(4,5)P_2$ or $PtdIns(4,5)P_2$), by phospholipase C (PLC). The 11 mammalian PLC isozymes can be divided into three structural groups: β, γ and δ and they are differentially distributed (Phillis & O'Regan, 2004). Two PLC isoforms, PLC-β activated by G proteins, and, PLC-γ activated by receptor tyrosine kinases, catalyse the PIP_2 reaction. Protein surfaces that interact with phosphoinositides can consist either of clusters of basic residues within unstructured regions, such as those found in many actin regulatory proteins (e.g. profilin) or of folded molecules, such as the pleckstrin homology (PH) domain (Di Paolo & De Camilli, 2006). PLC has an absolute requirement for calcium and it has at least two potential lipid-binding domains: the PH and the C2 domains. PIP_2 is a key regulator of the actin cytoskeleton and increased levels of presynaptic PIP_2 have been linked to abnormalities in both the presynaptic actin cytoskeleton and the organisation of the

synaptic vesicle pool (Osborne *et al.*, 2001). Moreover, a recent study has shown that PIP_2 is enriched in dendritic spines and the amount of PIP_2 affects spine morphology (Calabrese, B. and Halpain, S. 06). PIP_2 is dephosphorylated by the phosphatase synaptojanin, a nerve terminal inositol 5-phosphatase that interacts with the endocytic machinery via its proline-rich domain (Slepnev & De Camilli, 2000). Another fate of PIP_2 is conversion to $PIns(3,4,5)P_3$ by class I phosphoinositide 3-kinase (PI3-kinases). This lipid is present in negligible amounts in resting cells, but can be dramatically increased in response to growth factor stimulation. $PIns(3,4,5)P_3$ is subsequently dephosphorylated by two types of enzymes: at the 3 position by the phosphatase PTEN to generate $PI(4,5)P_2$ and at the 5 position by 5 phosphatases, such as SHIP-1 and -2 to generate $PIns(3,4)P_2$. Hydrolysis of PIP_2 by PLC generates two second messengers, inositol-1,4,5-trisphosphate (IP_3 or $InsP_3$) and diacylglycerol (DAG).

DAG acts as a second messenger and activates PKC, which phosphorylates Munc-18 and, subsequently regulates the interaction of Munc-18 with syntaxin and the docking and/or the fusion of synaptic vesicles with the presynaptic plasma membrane (Fujita *et al.*, 1996). Munc-18 is specifically localised in nerve cells (and not in glia) and it is highly distributed in axons (Kalidas *et al.*, 2000). It therefore seems to be a key component in the regulation of synaptic function. More recently, other DAG targets have been identified, which include protein kinase D (PKD), diacylglycerol kinases β and γ, ras guanine nucleotide releasing proteins (RasGRP), chimaerins and Munc-13. In particular, Munc-13 proteins are specifically localised to the presynaptic active zone and are essential for synaptic vesicle priming by activation of the SNARE protein syntaxin. It has recently been shown that the increase in neurotransmitter release induced by phorbol esters in primary neurons is mediated exclusively by Munc-13 and not by PKC (Brose *et al.*, 2004).

In the cytosol, IP_3 stimulates the mobilisation of calcium from intracellular stores by binding to IP_3 receptors in the endoplasmic reticulum. IP_3 can be phosphorylated by kinases to high inositol phosphate molecules (ortho- and pyro-phosphate inositol), whose functions as intracellular messengers are still unclear as their levels do not seem to change in response to cell stimulation (Bennett *et al.*, 2006). IP_5 and IP_6 are generally assumed to have "housekeeping" functions rather than being second messengers (Berridge & Irvine, 1989). Moreover, IP_3 can be phosphorylated by $Ins(1,4,5)P_3$ 3-kinase to $Ins(1,3,4,5)P_4$,

which is then dephosphorylated to Ins(1,3,4)P_3. IP_4 is a second messenger in its own right as it can influence IP_3-regulated calcium homeostasis (Irvine *et al.*, 2006). IP_3 can be dephosphorylated to IP_2, IP_1 and *myo*-inositol by phosphatases. In particular, the inositol polyphosphate-1-phosphatase (IPPase) converts IP_2 to IP_1 and the inositol monophosphatase (IMPase) dephosphorylates IP_1 (Ins(1)P, Ins(3)P or Ins(4)P) to *myo*-inositol (Fig. 1.3).

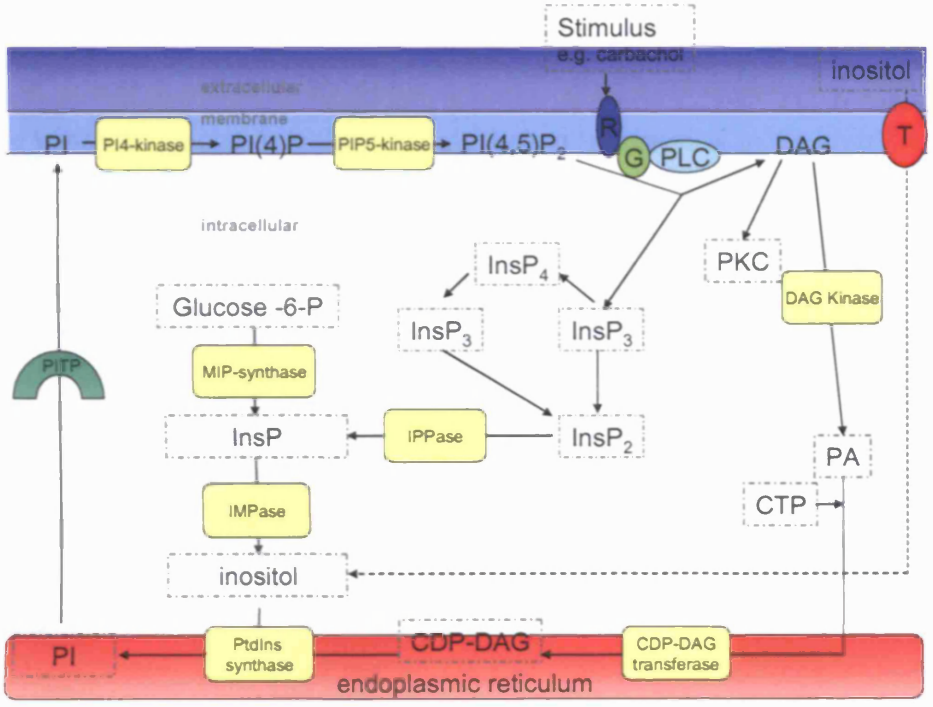

Fig. 1.3 Schematic of the PIns signalling pathway.
T = transporter; the other components of the pathway are indicated in the text.

Inositol is a cyclic hexitol, which can exist as nine isomeric forms. *Myo*-inositol is the most common form found in mammals and it has one axial and five equatorial hydroxyls (Fisher *et al.*, 2002) (Fig. 1.4). It is a major brain osmolyte, mostly derived from diet. *Scyllo*-inositol, an isomer in which all six of the hydroxyl groups are equatorial (representing only 8% of the total brain inositol) is the other most abundant inositol in the brain.

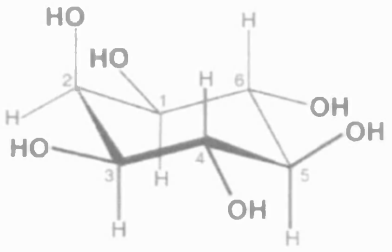

Fig. 1.4 *Myo*-inositol structure. Source: (Irvine, 2005).

De-phosphorylated *myo*-inositol is incorporated into PI and PIP_2 via a reaction involving activated phosphatidic acid (PA), named cytidine diphosphate-diacylglycerol (CDP-DAG) (Heacock & Agranoff, 1997). More precisely, DAG is phosphorylated at the plasma membrane to PA via the action of DAG kinase; subsequently, PA is converted to CDP-DAG. PI is converted to phosphatidylinositolphosphate (PIP) by the phosphatidylinositol kinase PI4-kinase and to PIP_2 by the phosphatidylinositol 4-phosphate 5-kinase (PIP5-kinase) (Halstead *et al.*, 2005). PI is formed in the endoplasmic reticulum and PI transfer proteins (PITP) then transport the newly synthesised PI to the plasma membrane (Cockcroft, 2001). How this works in synapses is unclear at present.

The ability of a cell to maintain sufficient levels of *myo*-inositol is crucial for the resynthesis of phosphoinositides and for the maintenance and efficiency of signal transduction. Differences in phosphatidylinositol (PIns) signalling exist amongst species and in different tissues and some confusion exists in the literature (Fig 1.5).

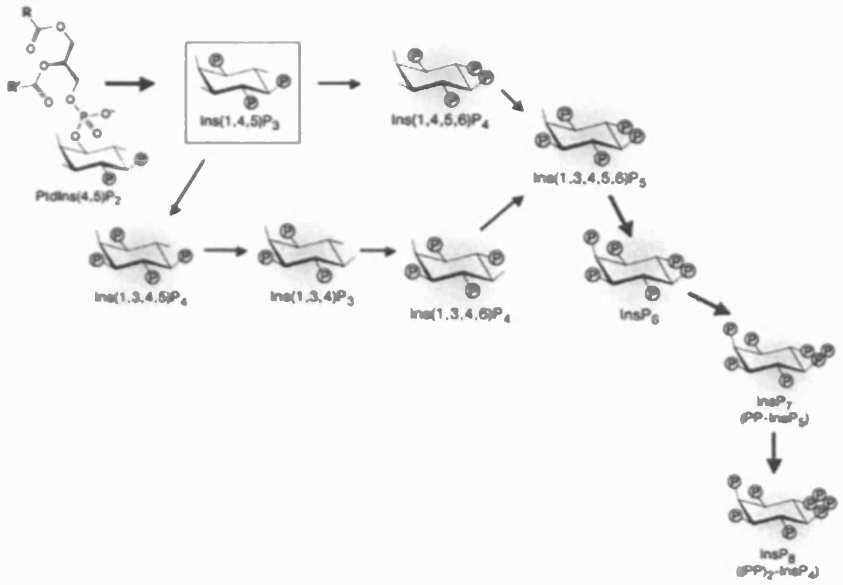

Fig. 1.5 Two likely pathways for $InsP_6$ synthesis in mammalian cells.
Source: (Irvine *et al.*, 2006). The upper pathway is found in yeasts and may exist in mammals.

Clinical studies have revealed modest and often contradictory abnormalities in the PIns signalling pathway in BD individuals. A magnetic resonance spectroscopy study showed that lithium induced *myo*-inositol reductions in the frontal cortex of BD individuals after five days of drug administration, at a time when the clinical state of the subjects was completely unchanged (Moore *et al.*, 1999). Furthermore, Silverstone *et al.* did not observe any differences in *myo*-inositol levels in control and BD individuals; however, they showed that chronic treatment with both lithium and VPA may normalise the altered PIns cycle activity observed in BD (Silverstone *et al.*, 2002). These studies point to the involvement of the PIns cycle in BD, however, it is still not clear at which level it occurs.

Moreover, some preliminary studies suggest that some genes encoding proteins belonging to the PIns pathway may be genetically associated with BD e.g. phosphoinositide 3-kinase class 3 (PIK3C3), phosphatidylinositol 4-kinase (PIK4CA) and phosphatidylinositol 4-phosphate 5-kinase II α (PIP5K2A) (Halstead *et al.*, 2005).

1.4.1 Mood stabilizers and IMPase/IPPase

Allison & Stewart showed that lithium treatment resulted in a 30% reduction in *myo*-inositol concentration in the rat cerebral cortex, which was accompanied by an increase in IP_1, suggesting that the drug inhibited the enzyme IMPase, which converts *myo*-inositol 1 (or 4)-phosphate (D or L) to *myo*-inositol (Allison & Stewart, 1971). It was subsequently confirmed that lithium inhibits IMPase directly with a K_i of 0.8 mM (Hallcher & Sherman, 1980), which is within the therapeutic plasma levels of lithium (0.6 - 1.2 mM) (Bowden, 1996). Lithium appears to inhibit the enzyme following substrate hydrolysis by occupying the second magnesium binding site before the phosphate group can dissociate from its interaction with the magnesium site (Atack *et al.*, 1995). There are at least two IMPase genes in mammals, IMPA1 and IMPA2 (Shamir *et al.*, 2001) and it is still not clear whether functional differences between the two genes exist. IMPA1 mRNA seems to be expressed at levels several fold higher than IMPA2, both in mice and human frontal cortex (Agam *et al.*, 2002) (also see Allan Brain Gene Atlas at http://www.brainatlas.org).

Ohnishi *et al.* suggested that IMPA2 has a distinct function from IMPA1, as it has lower activity towards *myo*-inositol monophosphate than IMPA1 and it shows different kinetics of lithium inhibition. No other substrates for IMPA2 have been identified so far (Ohnishi *et al.*, 2006). Very recently, an IMPA2 null-mutant mouse was generated and its behaviour analysed. The behaviour of the IMPA2 null-mutant mouse did not mimic the effects of lithium treatment in the forced swim, tail suspension, elevated zero-maze and open field tests, therefore suggesting that IMPA2 is not the key target for mood control (Cryns *et al.*, 2006).

IMPA1 therefore seems to be the predominant lithium-sensitive enzyme in the brain (Gee *et al.*, 1988; Parthasarathy *et al.*, 1994; Ragan *et al.*, 1988). The inhibition by lithium is uncompetitive. It also suggests that lithium does not bind to the enzyme directly, but rather to the enzyme-substrate complex. Interestingly, this finding also means that lithium is most effective when substrate levels are high. Vadnal & Parthasarathy reported that CBZ stimulates IMPase, while VPA does not have any direct effects (Vadnal & Parthasarathy, 1995). More recently, Mudge & Thomas did not observe any inhibition of IMPase by CBZ (personal communication), suggesting that IMPase inhibition may be specific to lithium.

Moreover, IMPA1 mRNA expression was reported to be decreased (two-third reduction) in lymphoblastoid cell lines from drug-free BD compared with control subjects and increased (two-fold) by treatment with lithium (Nemanov *et al.*, 1999), therefore suggesting that chronic inhibition of the enzyme by lithium results in up-regulation of the gene at the transcriptional level.

Lithium also directly inhibits the phosphatase immediately upstream of IMPase, called IPPase in an uncompetitive manner with a K_i of 0.3 mM (Ragan *et al.*, 1988). These findings suggest that the effects of lithium on PIns signalling are more pronounced in cells undergoing the highest rates of PIP_2 hydrolysis as opposed to quiescent cells (Nahorski *et al.*, 1991). Berridge *et al.* originally proposed the inositol depletion hypothesis in order to explain the efficacy of lithium in the treatment of BD (Berridge *et al.*, 1989; Berridge & Irvine, 1989). This theory was refined in 1995 to state that lithium slows down the rate of the PIns cycle rather than depleting intracellular concentrations of inositol (Batty & Downes, 1995). In fact, it seems that inositol concentrations in neurons can reach mM levels, as it accumulates from the cerebrospinal fluid and the plasma, where inositol concentrations are ~300 μM and ~30 μM, respectively, via the transporters SMIT1, SMIT2 and possibly HMIT (Agranoff & Fisher, 2001; Shetty *et al.*, 1995).

1.4.2 Mood stabilizers and MIP-synthase

The mood stabilizer VPA also modulates the PIns cycle, although via a different mechanism than lithium, as it does not affect IMPase and IPPase (Murray & Greenberg, 2000; Vadnal & Parthasarathy, 1995). In contrast to lithium, VPA decreases inositol phosphate levels (Vaden *et al.*, 2001) and it does so by decreasing the *in vivo* activity of *myo*-inositol-1-phosphate synthase in mammalian brain (MIP-synthase, known as ino-1 in yeast) (Shaltiel *et al.*, 2004; Agam *et al.*, 2002). MIP-synthase catalyses the reaction that converts D-glucose-6-phosphate to D-*myo*-inositol-3-phosphate (also named L-*myo*-inositol-1-phosphate (Berridge & Irvine, 1989)). The reaction is NAD-dependent and the activity is decreased 30-fold when inositol is added (Ju *et al.*, 2004). Postmortem human brain MIP-synthase activity is inhibited indirectly in a non-competitive manner by VPA with a K_i of 0.21 mM (Shaltiel *et al.*, 2004). The purified recombinant human enzyme is, however, not inhibited directly by VPA (Ju *et al.*, 2004), suggesting that either a metabolite of VPA is the true inhibitor or that VPA targets an additional protein required for MIP-synthase activity. MIP-synthase protein has been reported to be expressed in the periphery in testes and within the brain, to be associated mainly with the endothelium and the vasculature (Wong *et al.*, 1987) (see Allan Brain Gene Atlas at http://www.brainatlas.org); its involvement in the mechanism of action of mood stabilizers is therefore not clear.

1.4.3 Mood stabilizers and inositol transporters

Brain inositol levels are regulated via three main pathways: synthesis from glucose-6-phosphate to inositol-1-phosphate by the enzyme MIP synthase (see section 1.4.2), recycling from PIP_2 breakdown, and transport from the blood and cerebrospinal fluid. Key components of this third route are the inositol transporters, of which three are known. The sodium-dependent *myo*-inositol transporter 1 (SMIT1, SLC5A3) has been reported to be inhibited by lithium, VPA or CBZ after long-term treatment of astrocytes (at least 8 days treatment) (van Calker & Belmaker, 2000). Moreover, all three mood stabilizers decreased SMIT1 mRNA levels in astrocytes dissected from different brain areas or in human astrocytoma cell lines, but only after very prolonged treatment (8 to 14 days), indicating that SMIT1 may not be the primary target for the action of mood stabilizers (Lubrich & van Calker, 1999). A more recent study by the same group showed increased SMIT1 mRNA levels in neutrophils from BD-I individuals when compared with healthy subjects and decreased SMIT1 expression in neutrophils from BD individuals treated with lithium (Willmroth *et al.*, 2006). The relevance and correlation of these findings to the brain are not clear. SMIT1 mRNA expression is increased in neural tissue following brain injury (Guo *et al.*, 1997); moreover, in the mature brain the highest levels of SMIT1 expression are in the choroid plexus (Guo *et al.*, 1997). SMIT1 is regulated by osmolarity and it is expressed also in the periphery, especially in the kidney (Yamauchi *et al.*, 1995). SMIT1 null-mutant mice die soon after birth due to central apnoea (Berry *et al.*, 2003). The fetuses have a 92% reduction in brain inositol levels with no change in phosphatidylinositol levels. Maternal treatment with inositol prevents lethality (Chau *et al.*, 2005). Heterozygote mice were also analysed and they showed no effect on lithium-sensitive behaviour (e.g. forced swim test). These results led the authors to rule out the inositol depletion hypothesis (Shaldubina *et al.*, 2006b). In addition, a second sodium-dependent *myo*-inositol transporter has been described, SMIT2 (SLC5A13), which is widely distributed in peripheral tissues and also in the brain (Coady *et al.*, 2002). Little is known, however, about this isoform, except that it is regulated by osmolarity (Bissonnette *et al.*, 2004).

Uldry *et al.* recently described a H^+ dependent *myo*-inositol transporter (HMIT), which has a more restricted tissue distribution than SMIT, and is expressed in several brain regions, including neurons in the frontal cortex and in the hippocampus (Uldry *et al.*, 2001) (see Allan Brain Gene Atlas at http://www.brainatlas.org). Interestingly, HMIT is inserted into

the neuronal plasma membrane from a vesicular compartment in an activity-dependent manner, suggesting that HMIT may be involved in regulating neuronal PIns synthesis during periods of high activity (Eldry *et al.*, 2001).

1.4.4 Mood stabilizers and PKC

The PKC family is subdivided into three subfamilies: the conventional, novel, and atypical PKCs (cPKC, nPKC, and aPKC, respectively). cPKCs are activated by calcium and DAG, nPKCs are activated by DAG, but not by calcium, and aPKCs are not activated by either of these molecules. PKCs are heterogeneously distributed in the brain with particularly high levels in presynaptic terminals. Several PKC isoforms play a major role in the regulation of neuronal excitability and long-term alterations in gene expression and plasticity (Nishizuka, 1995). Chronic lithium treatment has been shown to significantly decrease membrane-associated PKC levels in the rat hippocampus and frontal cortex (Chen *et al.*, 2000a). Exposure of immortalised hippocampal cells to lithium induced a isozyme-selective decrease in PKC α and or ε levels, isoforms involved in facilitating neurotransmitter release, and a decrease in the levels of the PKC substrate myristoylated alanine-rich C-kinase substrate (MARCKS) (Lenox *et al.*, 1992; Watson & Lenox, 1996). Addition of *myo*-inositol completely reversed the lithium-induced down-regulation of MARCKS, indicating a link with the PIns pathway (Watson & Lenox, 1996). The mood stabilizer, VPA, produced strikingly similar effects to lithium on PKC α and ε isozymes, and on MARCKS (Chen *et al.*, 1994), but neither lithium nor VPA affect PKC activity directly. Another PKC downstream target is the growth-associated protein 43 (GAP43, also called B-50, p57, neuromodulin, pp46 or F1) (Benowitz & Routtenberg, 1997). GAP43 is a cytoplasmic protein involved in neuronal plasticity and it is a major constituent of growth cones. It has been suggested that attenuation of PKC activity may play a role in the anti-manic effects of lithium and VPA. A pilot study found that tamoxifen (a non-steroidal anti-oestrogen known to be a PKC inhibitor at higher concentrations) may indeed possess anti-manic efficacy (Bebchuk *et al.*, 2000); however, the study was very small and there have been no further data to support these findings. Overall, it seems that alterations in PKC signalling may be relevant to BD - it may not be PKC itself, but other components of the pathway that are affected by mood stabilizers.

1.4.5 Mood stabilizers and PO

Prolyl oligopeptidase (PO or PREP) is an enzyme (EC 3.4.21.26, 710 amino acids, ~80 kDa) that belongs to a class of serine peptidases, family S9A. The human PO gene is located on chromosome 6q22 (Goossens *et al.*, 1996). PO was first identified in human uterus as an oxytocin-cleaving enzyme (Koida & Walter, 1976). Subsequently, it was shown to cleave a number of neuropeptides, including substance P, thyrotropin-releasing hormone (TRH), and arginine-vasopressin at the carboxyl of the proline residue *in vitro*. For this reason it was originally termed post-proline cleaving enzyme. PO cannot hydrolyse peptides containing more than about 30 amino acids, the reason for which is evident from its crystal structure (see Chapter 4). Other members of this serine peptidase family include dipeptidyl peptidase IV, oligopeptidase B and acylaminoacyl peptidase, some of which are of pharmaceutical interest (Polgar, 2002). More recently Szeltner *et al.* identified a new member of the PO family, the prolyl endopeptidase-like protein, PREPL, which lacks enzymatic activity and shares only ~20% similarity with PO (Szeltner *et al.*, 2005). PREPL exists as a homodimer and possesses negligible hydrolytic activity. PREPL has high homology with oligopeptidase B. Interestingly, lower PREPL mRNA expression levels have recently been reported in the orbitofrontal cortex of BD individuals when compared with controls, whereas PO levels did not change significantly (Ryan *et al.*, 2006).

PO is highly conserved through evolution from bacteria, eukaryocytes and plants (Harwood *et al.*, 1997). Human and porcine PO share ~97% amino acid identity. PO cellular localisation (intracellular versus secreted) has changed through evolution (Venalainen *et al.*, 2004). Specifically, mammalian PO does not contain any predicted transmembrane domain sequences or signal peptides and is mainly a cytosolic enzyme. However, a membrane-bound form of PO has been identified in synaptosomal and myelin membranes (O'Leary & O'Connor, 1995; O'Leary *et al.*, 1996). This particulate form has an apparent molecular weight of ~87 kDa, is 10-fold less active than cytosolic PO and differs in terms of sensitivity to inhibitors and affinity for peptide substrates (Irazusta *et al.*, 2002). PO is synthesised as an active peptidase and it is not found as a zymogen or proenzyme. Moreover, two proteins with PO activity have been detected in bovine and human plasma, whose origins are not clear: PO and an enzyme that is activity-resistant to the specific PO inhibitor Z-Gly-Pro-Prolinal (Breen *et al.*, 2004; Cunningham & O'Connor,

1997); this second enzyme has been called ZIP, as Z-Gly-Pro-Prolinal Insensitive Protease. PO and ZIP cleave substrates differentially. They both cleave TRH, but ZIP fails to hydrolyse substance P and vasopressin for reasons which are not clear. ZIP forms a homodimer with molecular weight more than twice that of monomeric PO (Birney & O'Connor, 2001).

PO is widely distributed in the rat, mouse and human periphery and CNS, as indicated by PO activity and mRNA expression studies. Rossner *et al.* studied PO activity in mouse and found the highest levels of activity in the cerebellum, and an increase in hippocampal PO activity in aged mice (Rossner *et al.*, 2005). In contrast, in the rat brain, a reduction in PO activity was reported during development (Agirregoitia *et al.*, 2003). Analysis of human PO brain activity revealed the highest levels in the cortex, and the lowest in cerebellum. The temporal profile of these alterations was, however, area specific and differences in the activity between the soluble and particulate forms of PO were observed (Agirregoitia *et al.*, 2003). PO activity in the CNS is higher than in peripheral tissues, such as skin (Kusuhara *et al.*, 1993), muscle and testes (Kato *et al.*, 1980; Irazusta *et al.*, 2002).

PO mRNA expression in the rat has been analysed in detail by Bellemere *et al.* who reported high expression levels in cerebellar Purkinje and granule cells, in hypothalamic nuclei, in pyramidal neurons of Ammon's horn, in granule cells of the dentate gyrus, and within the amygdala. Moderate levels were observed in the cerebral cortex, the anterior thalamic group, the septal region and substantia nigra (Bellemere *et al.*, 2004).

PO has been implicated in memory and cognition and in several illnesses. Naturally occurring PO inhibitors have been obtained from several sources (e.g. wine, plant extracts, green tea and fungi). Several PO inhibitors have also been chemically synthesised and some of these showed memory enhancement in pre-clinical and human studies. For example, the potent and selective PO inhibitor, S-17092, improved memory impairment in 1-methyl-4-phenyl-1,2,3,6-tetrahydropyridine (MPTP)-treated monkeys (Schneider *et al.*, 2002) and increased memory performance in humans (Morain *et al.*, 2000). Another inhibitor, JTP-4819, reversed scopolamine-induced amnesia in the passive avoidance test in rats, ameliorated memory deficits in rats with middle cerebral artery occlusion in the Morris water maze, and increased cortical and hippocampal levels of substance P and TRH

immunoreactivity in aged rats (Shinoda *et al.*, 1995; Shinoda *et al.*, 1999; Toide *et al.*, 1995; Toide *et al.*, 1997). Five PO inhibitors have entered clinical trials at phase II, although none have progressed to the market.

Interestingly, abnormal PO plasma and activity levels have been measured in individuals with affective disorders. In particular, PO serum activity was increased (~14%) in manic and schizophrenic individuals (Maes *et al.*, 1995). In contrast, decreased serum PO activity has been observed in individuals suffering from depression (Maes *et al.*, 1994). Interestingly, in depressed subjects, plasma PO activity was significantly increased during treatment with antidepressant drugs, such as fluoxetine, whereas, in manic subjects, short-term treatment with VPA decreased PO activity (Maes *et al.*, 1995). An important control that is missing from these studies is the assessment of the drug effect in control conditions, which could be easily performed *in vitro* by treating blood cells from healthy controls with drugs. A more recent study by Breen *et al.* showed a ~25% decrease in PO activity in BD euthymic subjects under lithium treatment compared with controls (Breen *et al.*, 2004). However, this study lacks the untreated-BD sample control making interpretation of these data difficult. In addition, two sets of data are presented in an unconventional way, with or without a "quenching correction", which resembles the standard sample blank, which is conventionally subtracted in enzymatic assays. Moreover, no controls for the effect of lithium on PO levels in cells were performed.

Since its identification, the mechanism of action of PO has been related to the cleavage of neuropeptides. To support this mechanism, it has been demonstrated that orally administered PO inhibitors increase substance P, vasopressin and TRH levels in the rat brain (Nakajima *et al.*, 1992; Toide *et al.*, 1995). However, only very recently it has been emphasised that mammalian PO is a cytosolic enzyme and, therefore, it is located in a different cellular compartment to neuropeptides, which are generated in vesicles and then secreted (Schulz *et al.*, 2005). There are only very limited data on the intracellular signalling pathways modulated by PO at present and the precise intracellular targets remain unknown. A study in *Dictyostelium discoideum* showed that ablation of the PO gene (DpoA) resulted in a 3-fold increase in IP_3 levels and induced resistance to the morphological effects of lithium. Similar effects were observed with a selective PO inhibitor (Williams *et al.*, 1999). These data suggest that the PO mechanism of action is

somehow related to the PIns signalling pathway. The increase in IP_3 levels via PO inhibition may derive from regulation of the activity of the enzyme multiple inositol polyphosphate phosphatase (MInsPP) (Harwood, 2005). However, there is no evidence that PO inhibits MInsPP directly. MInsPP generates IP_3 from IP_6, a very abundant inositol phosphate present in cells, which may act as a cellular store of inositol and phosphates in *Dictyostelium discoideum* (Harwood, 2003; Harwood & Agam, 2003). However, MInsPP is localised in the endoplasmic reticulum in mammals, whereas PO is a cytosolic protein; moreover, there is no evidence that MInsPP is involved in signalling events in particular in the regulation of IP_3 levels. Furthermore, the intracellular signalling in *Dictyostelium discoideum* differs substantially from mammalian systems; therefore, it is critical to confirm these findings in neurons. For example, Mudge & Saiardi did not find any evidence that IP_5 and IP_6 levels change when neurons are treated with the muscarinic agent carbachol used to stimulate the PIns signalling pathway (personal communication).

Of the mood stabilizers, only VPA inhibits recombinant PO directly, whereas lithium and CBZ are without direct effect on the enzyme (Cheng *et al.*, 2005). The fact that VPA inhibits PO directly (Cheng *et al.*, 2005), but its effects on growth cone size are reversed by PO inhibitors (Williams *et al.*, 2002), seems at first contradictory. However, the authors hypothesised that VPA may act as an inhibitor or an activator of PO depending on the intracellular signalling conditions and this would, therefore, explain the dual action of VPA in stabilizing mood from 'above' or from 'below' baseline levels (Cheng *et al.*, 2005). Their model suggests that euthymic mood may be dependent on stable PIns signalling and VPA may limit mood swings to mania by decreasing PIns signalling, and it may limit mood swings to depression by inhibiting PO and thus increasing PIns signalling.

1.5 Mood stabilizers and GSK3

The serine-threonine kinase GSK3 is a central component in many intracellular signalling pathways, in particular in the Wnt and in the PI3K/Akt pathways (Fig. 1.6).

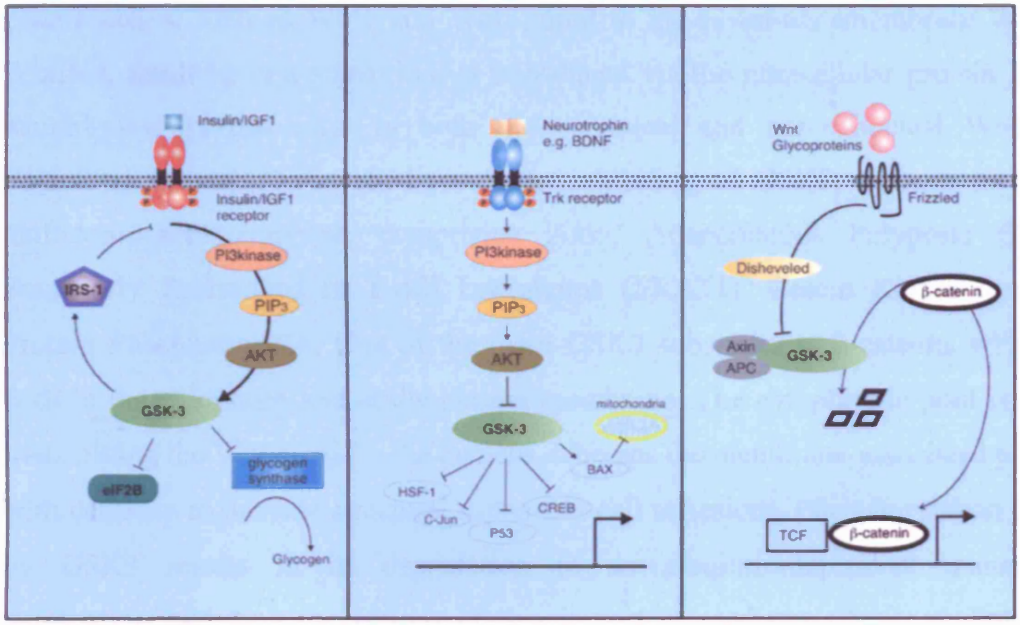

Fig. 1.6 GSK3 and intracellular signalling pathway. Source: (Gould & Manji, 2005).

Wnt signalling is often subdivided into canonical and non-canonical pathways. In humans, the Wnt protein family is composed of at least 15 secreted glycoproteins. The non-canonical pathway is activated by Wnt5a and Wnt11. This pathway branches into two cascades: the Wnt JNK pathway, which involves c-Jun N-terminal kinase (JNK) and the Wnt Ca^{2+} pathway, which involves PKC. In the canonical Wnt pathway, Wnt glycoproteins, such as Wnt1 and Wnt3, bind to the seven-transmembrane Wnt receptor, Frizzled, resulting in a signal that is transduced via the intracellular protein Dishevelled, which plays pivotal roles in both the canonical and non-canonical Wnt pathways. Signalling through Dishevelled results in inhibition of GSK3, through formation of a multicomponent complex, comprising Axin, Adenomatous Polyposis Coli (APC), Frequently Rearranged in T-cell Lymphoma (FRAT1), Casein Kinase I epsilon, and Protein Phosphatase-2A. One of the main GSK3 substrates is β-catenin, which is found both in the cytoplasm and at the plasma membrane. The cytoplasmic pool is involved in transmitting the Wnt signal to the nucleus, whereas the membrane-associated pool interacts with cadherin to provide structural support in cell adhesions. Phosphorylation of β-catenin by GSK3 results in its degradation in an ubiquitin-dependent manner, thereby terminating inhibiting the actions of this important mediator (Peifer & Polakis, 2000). Unphosphorylated β-catenin binds to the T-cell factor Lymphoid enhancer factor (Tcf Lef) that translocates to the nucleus and acts as a transcription factor at Tcf Lef promoter sites in a number of genes (Novak & Dedhar, 1999).

GSK3 is also a component of the PI3K Akt (also known as PKB) pathway, which is activated by growth factors, such as insulin. Insulin binds to a tyrosine kinase receptor, inducing receptor autophosphorylation at several intracellular tyrosine residues. This leads to the recruitment of the lipid PI3K to the plasma membrane and in close proximity to its physiological substrate PIP_2, which is then phosphorylated to PIP_3. A key effector of PIP_3 in insulin signalling is PKB. PKB has a PH domain located in the N-terminal domain, which binds to PIP_3. This results in recruitment of PKB from the cytosol to the plasma membrane, where PIP_3 is located. Once activated, PKB dissociates from the plasma membrane and phosphorylates numerous substrates both in the cytoplasm and in the nucleus, including GSK3.

Two isoforms of GSK3 are known, namely α and β, which share nearly identical sequences in their kinase domains. GSK3 is constitutively active within cells, and phosphorylation at Ser9 or Ser21 (GSK3β or α, respectively) by PKB, decreases GSK3 activity (Cross *et al.*, 1995). Other kinases are capable of phosphorylating GSK3β Ser9, such as p70 S6 kinase, p90Rsk, PKC and PKA (Fang *et al.*, 2000; Sutherland *et al.*, 1993). Phosphorylation of GSK3β on Tyr216, in contrast, increases its activity (Hughes *et al.*, 1993; Wang *et al.*, 1994). GSK3 has a preference for phosphorylating substrates that have been pre-phosphorylated or "primed" by other kinases e.g. β-catenin pre-phosphorylated by casein kinase. GSK3 is known to regulate the activation states of several transcription factors, including heat shock factor-1, cyclic AMP-response element binding protein (CREB), c-jun, NF-KB, Myc and AP-1, among others (Grimes & Jope, 2001). Of these transcription factors particularly noteworthy is CREB, a nuclear phosphoprotein that controls the expression of genes containing promoters with the cyclic AMP-response element. CREB plays a critical role in long-term memory, synaptic plasticity and cell survival (Shaywitz & Greenberg, 1999). Another interesting downstream GSK3 target is glycogen synthase, which is phosphorylated and, therefore, inactivated by GSK3, resulting in inhibition of glycogen formation (Plyte *et al.*, 1992). This effect has stimulated the development of GSK3 inhibitors for the treatment of diabetes and several compounds are presently undergoing clinical trials.

GSK3 inhibitors are currently in development also for the treatment of Alzheimer's disease, as GSK3 directly modulates the phosphorylation state and, therefore, the function of several microtubule-associated proteins, including tau and MAP-1B. This results in loss and or unbundling of stable axonal microtubules (Lee *et al.*, 2003; Lucas *et al.*, 1998; Sang *et al.*, 2001).

GSK3 is highly expressed in the adult brain (Ali *et al.*, 2001), in the cytoplasm, nucleus and mitochondria of both neurons and glia (Jope & Johnson, 2004). Cytosolic GSK3 inhibits protein synthesis and destabilises microtubules, while the nuclear enzyme inhibits expression of anti-apoptotic proteins and promotes p53-dependent apoptosis. In mitochondria, GSK3 can regulate energy production, but its precise mechanism is still unknown.

GSK3 is involved in several neuronal processes, such as apoptosis, neurite outgrowth and growth cone morphology. Inhibition of GSK3 with synthetic inhibitors has been shown to protect from cell death induced by several apoptotic stimuli in different cell systems, whereas transient over-expression of GSK3β induces spontaneous apoptosis in cell lines, such as PC12 (Hetman *et al.*, 2000; Pap & Cooper, 1998). Similar neuroprotective results were obtained in rat sympathetic neurons (Crowder & Freeman, 2000) and in rat cerebellar granule neurons (Maggirwar *et al.*, 1999).

Of the mood stabilizers, lithium directly inhibits GSK3, with an IC_{50} of approximately 2 mM (above therapeutic plasma concentrations) (Klein & Melton, 1996; Phiel & Klein, 2001) and inhibition occurs via competition for a low-affinity magnesium binding site (Ryves & Harwood, 2001). Importantly, however, lithium inhibits GSK3 also indirectly by increasing the phosphorylation of Akt, which phosphorylates Ser9 and inhibits GSK3. The direct and indirect effects of lithium on GSK3 act in concert to influence crucial GSK3-regulated functions (Chalecka-Franaszek & Chuang, 1999; Jope, 2003). As a result of GSK3 inhibition, lithium reduces MAP-1B and tau phosphorylation levels (Lovestone *et al.*, 1999; Lucas & Salinas, 1997), decreases glycogen synthase phosphorylation and increases β-catenin levels. Interestingly, O'Brien *et al.* and Gould *et al.* have shown that the antidepressant effect of lithium in the forced swim test is mimicked by the GSK3 inhibitor AR-A014418 and in mice lacking one copy of the GSK3β gene (Gould *et al.*, 2004; O'Brien *et al.*, 2004).

It is interesting to note that other group II cations, such as beryllium and zinc can also inhibit GSK3, but are not efficacious in the treatment of BD (Ilouz *et al.*, 2002; Ryves *et al.*, 2002).

Conflicting reports indicate that VPA directly or indirectly (via Akt and Ser9 phosphorylation) inhibits GSK3 (Chen *et al.*, 1999a; Hall *et al.*, 2002; Kim *et al.*, 2005a; Werstuck *et al.*, 2004), or does not have any effects at all (De Sarno *et al.*, 2002; Eickholt *et al.*, 2005; Jin *et al.*, 2005; Phiel *et al.*, 2001; Williams *et al.*, 2002).

Of the mood stabilizers, CBZ has been shown very recently not to affect GSK3 either directly or indirectly (Ryves *et al.*, 2005). LTG, instead, attenuated staurosporine- and heat

shock-induced caspase 3 activity in a cell line over-expressing GSK3 (Bijur *et al.*, 2000), although there is no evidence for a direct effect of LTG on GSK3. ECT treatment, used for severe depression and mania, has been reported to alter phosphorylation of GSK3, amongst other intracellular effects (Roh *et al.*, 2003).

Moreover, acute treatment with several antipsychotic drugs e.g. risperidone, olanzapine, clozapine, quetiapine, and ziprasidone, has been shown to inhibit indirectly GSK3 by increasing Ser9 phosphorylation in the mouse cortex, hippocampus, striatum, and cerebellum in a concentration-dependent manner, therefore showing that antipsychotic drugs, as well as mood stabilizers, modulate GSK3 activity (Li *et al.*, 2006).

1.6 Mood stabilizers and ERK/MAPK

Mitogen-activated protein kinases (MAPKs) transmit extracellular signals to the nucleus, where the transcription of specific genes is induced by the synthesis, phosphorylation and activation of transcription factors. Three MAPK signal transduction pathways have been identified in mammalian cells: extracellular-signal regulated kinase 1 2 (ERK1 2), JNK and p38 (Gutkind, 1998) (Fig. 1.7). In particular, the ERK MAPK pathway is sometimes activated by neurotrophic factors to regulate neurogenesis, neurite outgrowth, and neuronal survival (Skaper & Walsh, 1998). Activation of the JNK pathway has also been linked to neurite outgrowth and branching (Xiao *et al.*, 2006; Xiao & Liu, 2003; Xiao *et al.*, 2006).

MAP kinases are abundant in the brain, and a broad role for the MAPK cascade in regulating gene expression in long-term forms of synaptic plasticity has been amply demonstrated (Roberson *et al.*, 1999).

The mood stabilizer VPA has been shown to strongly activate ERK MAPK in SH-SY5Y cells (Yuan *et al.*, 2001). The effect was blocked by the MEK inhibitor PD098059, as well as by dominant negative-Ras and dominant negative-Raf, suggesting the involvement of the Ras Raf MAPK kinase pathway in the mechanism of action of VPA. VPA also increased ERK MAPK phosphorylation in neurons of the rat anterior cingulate and in cultured cortical cells (Hao *et al.*, 2004). More recently, lithium was also shown to activate ERK MAPK in rat cerebellar granule neurons, but to exert the opposite effect in astrocytes (Kopnisky *et al.*, 2003; Pardo *et al.*, 2003). Chronic lithium or VPA treatment also increased levels of activated ERK MAPK in the rat hippocampus and frontal cortex, and this resulted in behavioural changes that mimic anti-manic effects. In fact, lithium was shown to reverse the effects of the ERK MAPK inhibitor SL327 in the open field test by decreasing locomotor activity (Einat *et al.*, 2003). Only one report suggests that CBZ modulates the ERK MAPK pathway and the study was performed in SH-SY5Y cells, therefore making the relevance to the brain unclear (Mai *et al.*, 2002).

Activation of the ERK MAPK pathway inhibits cell death and promotes survival by inducing the phosphorylation (and inactivation) of Bad, and increasing the expression of the B-cell lymphoma leukemia-2 gene (bcl-2), most likely through CREB activation

(Riccio *et al.*, 1999). Bcl-2 is expressed in the rodent and mammalian nervous system and is localised to the outer mitochondrial membrane, endoplasmic reticulum and nuclear membrane. Although the precise mechanisms of action of bcl-2 are unknown, it is now clear that bcl-2 is a protein that inhibits both apoptotic and necrotic cell death induced by diverse stimuli (Adams & Cory, 1998). Lithium exerts neuroprotective effects in a variety of preclinical *in vitro* assays e.g. NMDA receptor activation, ageing, serum/nerve growth factor deprivation, ouabain, thapsigargin, β-amyloid and these effects may be related to its effects on bcl-2 (Manji *et al.*, 2000). Lithium was shown to increase levels of bcl-2 in the rat dentate gyrus and striatum (Manji *et al.*, 2000), in rat cerebellar granule neurons (Chen & Chuang, 1999) and in SH-SY5Y cells (Lai *et al.*, 2006). Moreover, lithium reduced levels of the pro-apoptotic protein p53 both in cerebellar granule neurons (Chen & Chuang, 1999) and in SH-SY5Y cells (Lu *et al.*, 1999). Importantly, cytoprotective effects were observed *in vivo* as well. Treatment with lithium attenuated the biochemical deficits produced by kainic acid and ibotenic acid infusion and forebrain cholinergic system lesions, exerted dramatic protective effects against middle cerebral artery occlusion (Nonaka & Chuang, 1998) and enhanced hippocampal neurogenesis in the adult rodent (Chen *et al.*, 2000b).

VPA is also neuroprotective in *in vitro* systems, such as serum deprivation and oxidative stress (Lai *et al.*, 2006; Manji & Chen, 2002; Wang *et al.*, 2003; Yuan *et al.*, 2001) and the effects may be related to bcl-2. In fact, chronic treatment of rodents with therapeutic doses of lithium and VPA has been reported to produce a doubling of bcl-2 levels in the frontal cortex, as reflected in a marked increase in the number of bcl-2 immunoreactive cells in layers II and IV of the cortex (Chen *et al.*, 1999b). VPA protected cerebellar granule neurons against excitotoxic agents (Bruno *et al.*, 1995), apoptosis induced by low potassium (Mora *et al.*, 2002), as well as injury to rat hippocampal neurons caused by β-amyloid and glutamate (Mark *et al.*, 1995).

Neuroplasticity underlies diverse processes of vital importance by which the brain perceives, adapts to and responds to a variety of internal and external stimuli. The manifestation of neuroplasticity in the adult CNS has been characterised as including alterations of dendritic function, synaptic remodelling, long-term potentiation, axonal sprouting, neurite extension, synaptogenesis and even neurogenesis. Recent brain

morphometric studies are beginning to lead to a fuller appreciation of the magnitude of the neuroplastic events involved in the pathophysiology of BD (Duman *et al.*, 2000). Some reports suggest regional reduction in CNS volume, as well as reduction in the number and or sizes of glia and neurons in discrete brain areas of BD individuals; however, results have been inconsistent. The most robust finding from a meta-analysis of 26 studies in BD brains is enlargement of the right lateral ventricle; no other regional volumetric deviations were measured (McDonald *et al.*, 2004). Strong heterogeneity existed, however, for several regions, including the third ventricle, left subgenual prefrontal cortex, bilateral amygdala and thalamus.

A clinical study using proton magnetic resonance spectroscopy to quantitate N-acetyl-aspartate levels (putative neuronal marker, localised to mature neurons and not found in mature glial cells, cerebrospinal fluid or blood (Tsai & Coyle, 1995)) reported that chronic lithium administration at therapeutic doses increased N-acetyl-aspartate concentrations in the human brain (Moore *et al.*, 2000). It is therefore intriguing to speculate that chronic lithium treatment may not only exert robust neuroprotective effects, but also neurotrophic effects in humans.

The development of novel treatments for BD, which more directly target molecules involved in critical CNS cell survival and cell death pathways, has the potential to enhance neuroplasticity and cellular resilience, thereby modulating the long-term course of the illness.

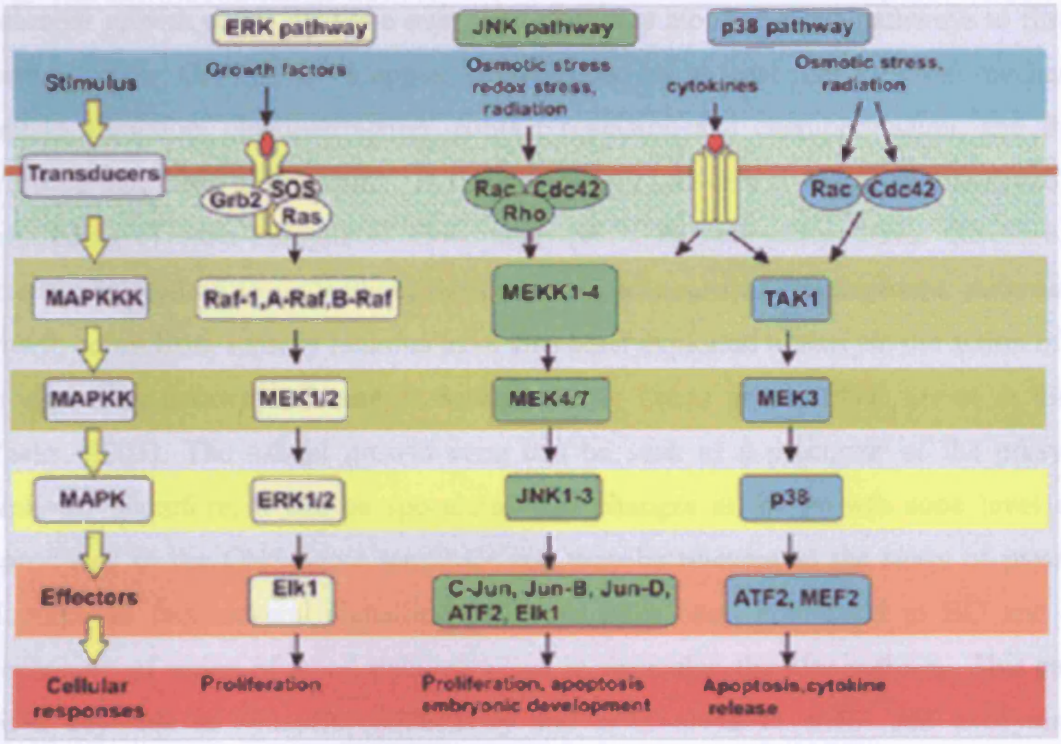

Fig. 1.7 Schematic of the MAPK pathways. Source: Cell Signalling web site (adapted).

1.7 Mood stabilizers and growth cone morphology

Neuronal growth cones navigate over long distances along specific pathways to find their correct targets. Growth cones appear to be guided by at least four different mechanisms: contact attraction, chemoattraction, contact repulsion and chemorepulsion, and there is evidence that these mechanisms act simultaneously and in a coordinated manner to direct pathfinding (Tessier-Lavigne & Goodman, 1996). Growth cones have, therefore, been extensively studied to understand the processes of neuronal development. Alternatively, growth cones from sensory neurons have also been exploited to analyse the action of drugs on signalling pathways (Lucas & Salinas, 1997; Lucas *et al.*, 1998; Owen & Gordon-Weeks, 2003). The axonal growth cone can be seen as a precursor of the presynaptic terminal. Therefore, it can be speculated that changes at the growth cone level can be reproduced in the CNS nerve terminals and may be relevant to the study of psychiatric illnesses. In fact, several signalling pathways have been implicated in BD and in the mechanism of action of mood stabilizers and, in particular, the PIns pathway. This pathway has a key role in synaptic connectivity and is involved in endo- and exocytosis, all processes that occur at the growth cone.

Growth cones were first described by Ramon y Cajal in 1890 as conical expansions at the tips of developing axons and dendrites. They are dynamic structures, as they extend and retract by sensing the environment during processes of neurite outgrowth and axonal pathfinding. Growth cones use receptors to sense extracellular cues and to transduce information to the cellular machinery that mediates growth cone turning responses. One of the key players to regulate the growth cone motility is calcium. Calcium signals localised to one side of the growth cone can cause asymmetric activation of enzymes to direct the growth cone and high calcium levels can inhibit growth cone motility and arrest growth. Gradients of NGF, BDNF, netrin-1 and myelin associated glycoprotein (MAG) all induce growth cone turning responses that depend on their concentration (Tessier-Lavigne, 2002; Tessier-Lavigne & Goodman, 1996). Growth cones migrate by assembly and disassembly of filamentous actin (F-actin) and microtubules, and cycle between fast moving, elongated forms with a contracted appearance and slow moving, spread forms. Steering depends on intact filopodia and F-actin, whereas extension requires intact microtubules. Briefly, microtubules are eukaryotic cytoskeletal organelles involved in several cellular processes,

such as cell division and transport of vesicles. Microtubules are formed by tubulin, which is a heterodimer of two polypeptide chains, called α and β. Different genes encode for six α and seven β isoforms, which differ in localisation (Bianchi *et al.*, 2005). Microtubules are functionally modified by post-translational modifications, including tyrosination, detyrosination, acetylation, phosphorylation and glutamylation. These modifications usually affect the carboxyl-terminal domain. In contrast, acetylation occurs at Lys 40 of α-tubulin. Acetylated-tubulin is currently considered a marker of stable microtubules, in contrast to tyrosinated-tubulin representing dynamic microtubules (Table 1.3) (Bianchi *et al.*, 2005).

	Comment
Tubulin α and β isotypes	
α1 α2	• Highly expressed during brain development • Associated with neurite outgrowth
α4	• Only isotype without a C-terminal tyrosine residue
β I βI	• Highly expressed during brain development
βIII	• Neuronal specific • Marker of post-mitotic neurons
βVa b	• Highly expressed during brain development
α-Tubulin modifications	
Tyrosination detyrosination	• Marker of dynamic microtubules • Involved in neuronal plasticity events
Acetylation	• Marker of stable microtubules
Glutamylation	• Representing 90% of brain tubulin
Phosphorylation	• Involved in neuronal differentiation?
MAPs	
MAP-1A	• Involved in neuronal differentiation?
MAP-1B	• Highly expressed during brain development
MAP-2a b	• Specifically expressed in dendrites
MAP-2c	• Expressed only during brain development
MAP-4	• Expressed also in non neuronal cells
TAU	• Specifically expressed in axons

Table 1.3 Overview of the microtubular system in mammalian brain.

The growth cone peripheral domain is devoid of cytoplasmic organelles, but includes filopodia and lamellipodia, which are flattened veils between filopodia. The thicker, central domain is rich in vesicles and organelles. F-actin and microtubules are arranged as parallel bundles in the neurite shaft but splay apart and turn as they enter the growth cone central domain. Microtubules dominate the central domain of the growth cone, but they can also penetrate the growth cone peripheral domain and interact with F-actin (Fig. 1.8A).

Growth cones can be observed in processes of cultured neurons, including sensory ganglionic neuron explants, a few hours after plating. This occurs even in the absence of signals involved in dynamic behaviour, as a result of spontaneous electrical activity in the culture. Cheng & Mudge have observed that tetrodotoxin (TTX) affects growth cone dynamics by decreasing the percentage of growth cone collapse in sensory explants (personal communication). TTX blocks action potentials in nerves by binding to the pores of the voltage-gated sodium channels in nerve cell membranes. Growth cone behaviour can also be altered by pharmacological agents. For example, cytochalasin B causes depolymerisation of F-actin and retraction of filopodia, whereas colchicine induces disruption of microtubules (without affecting filopodia), which results in neurite retraction and induction of protrusions of new lamellipodia and filopodia along the axon. Of the mood stabilizers, high doses of lithium have been reported to increase the number of stable (detyrosinated) microtubules in sensory neuron growth cones and increase growth cone spread area (Goold *et al.*, 1999; Hall *et al.*, 2000; Lucas *et al.*, 1998; Owen & Gordon-Weeks, 2003); these effects were mimicked by potent GSK3 inhibitors (Fig. 1.8B). Lithium (20 mM) and GSK3 inhibitors (SB-216763 – 10 μM- and SB-415286 – 30 μM) were also shown to prevent the collapse induced by the repulsive guidance cue Sema3A (Luo *et al.*, 1993), which activates GSK3 at the leading edge of growth cones (Eickholt *et al.*, 2002). Sema3A is known to bind Neuropilin-1 receptor and to interact with the signalling co-receptor Plexin to subsequently activate GSK3. Another study has shown that Sema3A suppresses PI3K signalling concomitant with the activation of GSK3, which depends on the phosphatase activity of PTEN. Interestingly, application of the PI3K inhibitor LY294002 (10 μM) induced a very fast collapse (within minutes) in DRG neurons (Chadborn *et al.*, 2006). Another study showed that addition of LY294002 to DRG neurons induced apoptosis and prevented neurite outgrowth and when added to newly formed neurites it caused neurite retraction (Virdee *et al.*, 1999).

These data suggested that GSK3, via PI3K, may be a key signalling player in regulating growth cone morphology and other cellular processes, such as cell survival.

Another study using sensory neuron explants showed a common effect of lithium, VPA and CBZ on the growth cone dynamics (Williams *et al.*, 2002). Each of the drugs increased the growth cone spread area and decreased the percentage of collapsed growth cones.

Interestingly, this common effect was reversed by addition of exogenous *myo*-inositol, thereby implicating the PIns pathway as the common pathway regulated by the drugs.

The key signalling players in regulating growth cone dynamics and vesicle trafficking in both neuronal and non-neuronal cell types are the Rho family of GTPases. This family includes RhoA, Rac1 and Cdc42 that are regulated by guanine nucleotide exchange factors (GEFs), which promote their activation, and by GTPase-activating proteins (GAPs), which attenuate the function and retain the inactive GDP-bound state. Small GTPases shuttle between a GDP- (inactive) and a GTP- (active) bound state. When bound to GTP they interact with a variety of effectors. Among these, $PI(4,5)P_2$ is a key signalling molecule, which in cooperation with Cdc42, binds N-WASP and triggers a conformational change that allows activation of the ARP2/3 complex, a potent actin assembly nucleator (Pollard & Borisy, 2003; Rohatgi *et al.*, 2000). $PI(4,5)P_2$ facilitates actin filament elongation by promoting the dissociation of capping proteins, such as gelsolin. In addition, $PI(4,5)P_2$, through its binding to profilin, promotes the association of actin-monomer-profilin complexes, thus making G-actin available.

Interestingly, Rho and Rac associate with PIP5-kinase, which catalyses the formation of $PI(4,5)P_2$ (Ren & Schwartz, 1998; Tolias *et al.*, 1998; Chong *et al.*, 1994) Rho proteins affect actin polymerisation by regulating cofilin, an actin filament-severing and actin-depolymerising factor. The Rho target ROCK in turn phosphorylates and activates LIM kinases, which directly phosphorylate cofilin and, therefore, inactivate it, leading to an increase in polymerised actin (Ridley, 2006).

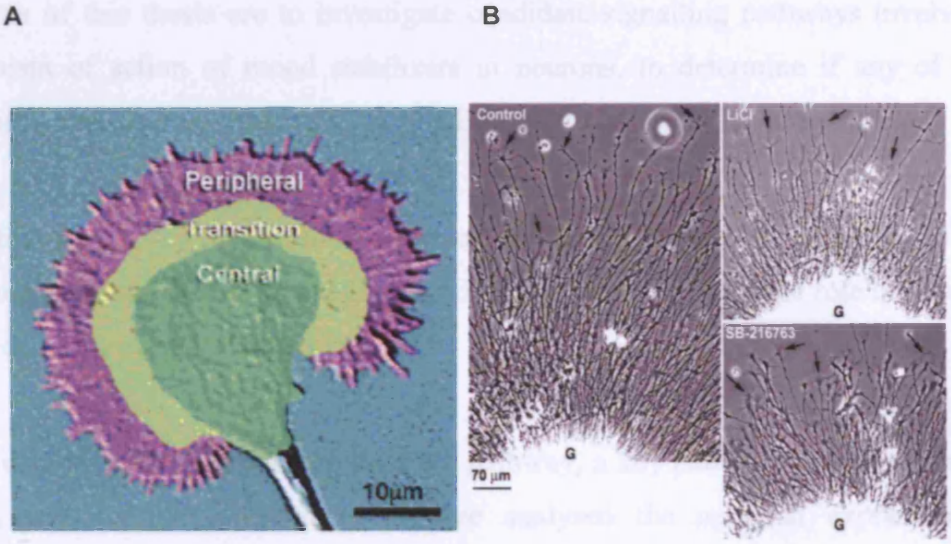

Fig. 1.8 Examples of growth cone morphology.
A Example of a large paused cortical growth cone imaged in differential interference contrast microscopy. The central, transition and peripheral regions of the growth cone are indicated in green, yellow and pink, respectively. Source: (Dent & Kalil, 2001)
B Low-power, phase-contrast images of chicken embryonic DRG explant cultures grown for 24 h *in vitro* in control conditions (Control) or in the presence of either 10 mM LiCl or 10 µM SB-216763. In control cultures, there is a profuse, radial outgrowth of axons tipped with growth cones (arrows). In drug-treated cultures, outgrowth is also profuse, but axons are shorter in length than controls and have larger growth cones (arrows). Ganglia are marked with G. Source: (Owen & Gordon-Weeks, 2003).

AIMS OF THE THESIS

The aims of this thesis are to investigate candidate signalling pathways involved in the mechanism of action of mood stabilizers in neurons, to determine if any of these are commonly regulated by lithium, VPA or CBZ, and to identify new drug targets.

In the first part of my thesis I have focussed on the signalling component GSK3 and used biochemical assays as well as the growth cone assay to investigate the role of this kinase in the action of mood-stabilizing drugs.

Subsequently, I have focussed on the PIns pathway, a key pathway implicated in synaptic activity and cellular morphology. I have analysed the neuronal expression of key components of this pathway, including the inositol transporters HMIT, SMIT1 and SMIT2 and the enzyme MIP-synthase and showed that HMIT only is expressed in neurons and it can, therefore, contribute to the action of the mood stabilizers. Moreover, the effects of each of the mood stabilizers examined in the growth cone assay seem to be dependent on inositol.

Furthermore, I have extensively analysed the enzyme PO, which has been reported to modulate the PIns pathway and has been implicated in the mechanism of action of the drugs. I have used a PO null-mutant mouse, viral delivery technology and the results of Y2H assay to shed light on the role of this enzyme in the action of mood stabilizers.

CHAPTER 2
Materials and Methods

2.1 Reagents

VPA, LiCl, CBZ, trychostatin A (TSA), *myo*-inositol, gabapentin (GPT) and dimethyl sulfoxide (DMSO) were purchased from Sigma Aldrich; SB-415286, SB-216763 and the PO inhibitor S-17092 were synthesised at GlaxoSmithKline; phenytoin (PTN) was from Calbiochem; Z-Pro-Pro-aldehyde-dimethyl acetal was from Bachem. All chemicals used for buffer preparation were purchased from Sigma Aldrich, unless otherwise stated.

2.2 Cell culture

2.2.1 Cell lines

Human embryonic kidney cells, HEK-MRSII, HEK293 and HEK293T (obtained from GlaxoSmithKline) were cultured in MEM (Invitrogen), 10% (v/v) fetal bovine serum (FBS), 1% (v/v) MEM non-essential amino acids (Invitrogen) and 2 mM L-glutamine. The Chinese hamster ovary cells, CHO_K1, (obtained from GlaxoSmithKline) were cultured in Ham's F12 medium (Invitrogen) with 10% (v/v) FBS.

2.2.2 Rat primary cortical, hippocampal and striatal neurons

Cortical, striatal and hippocampal neurons were prepared from embryonic day 18 (E18) Sprague Dawley rat brains (Charles River). Animals were euthanased in accordance with the 1986 Animals (Scientific Procedures) Act. The cortex (or striatum or hippocampus) was carefully dissected, placed into ice-cold Hank's Balanced Salt Solution (HBSS) (Invitrogen) with 1 mM sodium pyruvate (no Ca^{2-} or Mg^{2-}) (Invitrogen), 100 U penicillin/50 µg streptomycin/ml (Invitrogen), 10 mM N-2-hydroxyethylpiperazine-N'-2-ethanesulfonic acid (HEPES) pH 7.4 (Invitrogen), 0.035% (v/v) $NaHCO_3$ (Invitrogen), and dissociated with 0.5% (v/v) trypsin/ethylenediaminetetraacetic acid (EDTA) (Invitrogen) for 5 min at 37°C (or for hippocampal neurons with 0.1% (v/v) trypsin/EDTA for 30 min at 37°C). Trypsin was neutralised by adding an equal volume of Neurobasal Medium (Invitrogen) with 10% (v/v) FBS, and cells were dissociated using fire-polished Pasteur pipettes of decreasing size. Cells were centrifuged for 5 min at 100xg and resuspended in Neurobasal Medium (*myo*-inositol concentration of 7.2 mg/l) (Brewer *et al.*, 1993) containing 1 mM sodium pyruvate, 100 U penicillin/50 µg streptomycin/ml, 2% B27 supplement with antioxidants (Invitrogen), 0.025 mM L-glutamate (Sigma) and 1 mM L-glutamine. For Western blotting analysis, neurons were seeded at 500,000 cells/well in poly-D-lysine (molecular weight (MW) >300,000, Sigma) coated 6-well plates. For mRNA analysis, neurons were seeded at 500,000 cells/well in poly-D-lysine coated 6-well plates and lysed after 5, 7, or 9 days in culture (dic). For growth cone morphological studies,

neurons were plated at 12,500 cells/well on poly-D-lysine coated coverslips in 24-well plates and treated with drugs 20 h after plating for 4 days.

2.2.3 Mouse primary neurons

Cortical neurons were dissociated from embryonic day 15 (E15) mouse brains in accordance with the 1986 Animals (Scientific Procedures) Act. The papain dissociation kit from Lorne Laboratories was used following the manufacturer's instructions. Briefly, cortices were carefully dissected, placed into ice-cold HBSS with 1 mM sodium pyruvate (no Ca^{2+} or Mg^{2+}), 100 U penicillin/50 µg streptomycin/ml, 10 mM HEPES pH 7.4, and 0.035% (v/v) $NaHCO_3$. Cortices were subsequently incubated with 5 ml of a solution made with 0.005% DNAse, 20 units/ml papain, 1 mM L-cysteine and 0.5 mM EDTA for 10 min at 37°C. After trituration, the cell suspension was filtered through a 70 µm strainer (Falcon) and centrifuged for 5 min at 150xg. The pellet was then re-suspended in a solution made by 2.7 ml EBSS and 300 µl of 10 mg/ml ovomucoid protease inhibitor in EBSS, 10 mg/ml bovine serum albumin and 150 µl of DNAse solution (2,000 units/ml). The cell suspension was applied gently on the top of 5 ml EBSS solution with 10 mg/ml albumin and 10 mg/ml ovomucoid inhibitor solution and centrifuged for 5 min at 70xg. The pellet was then resuspended in Neurobasal medium containing 1 mM sodium pyruvate, 100 U penicillin/50 µg streptomycin/ml, 2% (v/v) B27 supplement with antioxidants, 0.025 mM L-glutamate, 1 mM L-glutamine and neurons were plated at 100,000 cells/well in a 24-well plate for immunocytochemistry.

2.2.4 Rat and mouse dorsal root ganglia explants

Dorsal root ganglia (DRG) from P0-P2 rats (Charles River) or P0-P1 mice (Deltagen and GlaxoSmithKline) were dissected in L15 medium with 100 U penicillin/50 µg streptomycin/ml (Invitrogen) and cultured as explants on coverslips. Coverslips were coated with 500 µl of 10 µg/µl poly-D-lysine (MW >300,000, Sigma) overnight at 37°C, washed three times with distilled water, air-dried for ~30 min and subsequently coated with laminin (50 µg/ml, Sigma - note that this is 5x concentration when compared with that used for culture of other cell types) for 4h at 37°C. The following plating medium was used: DMEM/F12 with Glutamax (Invitrogen; it contains 12.60 mg/l of *myo*-inositol), nerve growth factor (50 ng/ml, Invitrogen, stored at -20°C), insulin (5 µg/ml, Sigma, stored at -80°C), and SATO medium, as previously described (Cheng & Mudge, 1996; Williams *et al.*, 2002; Cheng *et al.*, 2005). A X10 solution of the following components (SATO) was made and stored at -20°C (Bottenstein & Sato, 1979): 500 ml DMEM/F12 with Glutamax, transferrin (1 mg/ml, Sigma), BSA (1 mg/ml, Sigma), putrescine (160 mg/ml, Sigma), sodium selenite (390 ng/ml, Sigma), L-thyroxine (T4: 500 ng/ml, Sigma), and 3,3,5-triiodo-L-thyronine (T3: 500 ng/ml, Sigma). Drugs were added after 20 h in culture and explants were cultured for at least a further 24 h (or as indicated) before loading the neurons with calcein AM dye (1 µg/ml, Molecular Probes) and proceeding with fixation.

2.2.5 Transient transfection of cell lines

Many parameters influence transfection efficiency, including cell culture conditions, vector characteristics and quality, and the transfection technology used. Cells should have a low passage number (<50 passage numbers) and be sub-cultured around 24 h before transfection. This ensures normal cell metabolism and increases the likelihood of nucleic acid uptake. On transient transfection, many copies of the DNA are present in the cell following transfection, but the introduced DNA does not integrate into the chromosomes. Transient transfection often results in high levels of expression of the introduced gene, but only for a few days following transfection. Cationic liposomes typically contain a mixture of cationic and neutral lipids organised into lipid bilayer structures. Transfection-complex formation is based on the interaction of the positively charged liposome with the negatively charged phosphate groups of the nucleic acid. The uptake of the liposome – DNA complexes may be mediated by endocytosis. Compared to other methods, liposomes often offer higher transfection efficiency and better reproducibility. Serum often lowers the transfection efficiency, and it is therefore usually omitted. Cells were plated one day before transfection at 500,000 cells/well in a 6-well plate and they were ~80% confluent at the time of transfection. Transfection mix was prepared by adding DNA to DMEM with no serum followed by Fugene-6 (Roche) (Fugene-DNA ratio = 3:1). The mix was incubated for 15 min at room temperature and then added dropwise to the cells.

2.3 Cell assays

2.3.1 Analysis of sensory and cortical neuron growth cone area

Random fields of calcein- or GAP43-labelled axons at the perimeter of the axonal halo that grew out from the explant cell bodies were scored using a X40 objective and Olympus BX51 microscope equipped with epifluorescence optics. The perimeter of labelled growth cones was traced with a light pen and the area was calculated using Image-Pro Plus software. Images of cortical neurons were acquired from 10 random fields with a X20 objective. For each drug treatment at least 100 growth cones were measured. The experiment was repeated as described in the figure legends.

2.3.2 PO enzyme activity assay

Brains were removed from mice or rats, weighed and homogenised in 5X volume of cold PBS. Cells from 10 cm dishes were washed with cold PBS and subsequently sonicated in 500 µl of cold PBS. Homogenates were centrifuged at 16,000g for 5 min at 4°C and supernatants analysed for PO activity. Duplicate reactions were prepared for each sample consisting of 20 µl supernatant (neat or diluted), 160 µl PBS and 20 µl of substrate N-benzyloxycarbonyl-glycyl-7-amino-4-methylcoumarin (Z-Gly-Pro-AMC, 30 µM final, Bachem) according to a modification of the method by (Venalainen *et al.*, 2002) (Fig. 2.1). Z-Gly-Pro-AMC was dissolved in 60% (v/v) methanol, as this solvent has been reported to minimally affect PO activity.

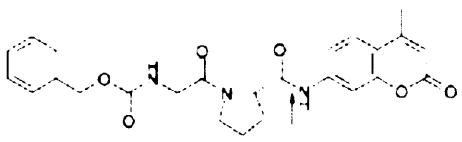

Z-Gly-Pro-AMC

Fig. 2.1 Chemical structure of Z-Gly-Pro-AMC.
The arrow indicates the peptide bond cleaved by PO.

The reaction was performed at room temperature for the time indicated and terminated by addition of 400 µl of 1.5 M acetic acid. A blank for each reaction was also included, consisting of no addition of enzyme or substrate, or a zero incubation time, which was subtracted from the results. 200 µl from each reaction were transferred into 2 wells of a 96-well plate with white base and sides (total four replicates). Measurement of the fluorescent AMC liberated by PO cleavage of the prolyl bond was quantified spectrofluorometrically using a FlexStation plate reader, with excitation and emission wavelengths set at 355 nm and 460 nm, respectively. Values were normalised to protein concentrations for cell lysates or protein weight for tissues.

2.4 Biochemical techniques

2.4.1 Determination of protein concentration

Protein concentration was determined using a standard BCA™ protein assay kit (Pierce). Bovine serum albumin was used as standard, prepared according to the manufacturer's instructions. Sample protein levels were quantified by colorimetric detection using a SpectraMax 340PC plate reader after 30 min incubation at 37°C. Several dilutions of the unknown samples were prepared in order to obtain values within the standard curve range.

2.4.2 Western blotting

Cells were washed with cold PBS and lysed in sample buffer consisting of 2% (w/v) sodium dodecyl sulphate (SDS), 10% (v/v) glycerol, 25 mM TRIS pH 6.8, 1% (w/v) bromophenol blue, 1% (v/v) β-mercaptoethanol. For β-catenin extraction, a detergent-free, hypotonic buffer was used (Cross *et al.*, 2001). Equal amounts of protein lysates were resolved by SDS polyacrylamide gel electrophoresis (SDS-PAGE) using 4-20% Tris-Glycine gels (Novex) and TGS buffer (25 mM Tris pH 8.6, 192 mM Glycine, 0.1% (w/v) SDS, Bio-Rad). Wet immunoblotting was performed using TG buffer (25 mM Tris pH 8.3, 192 mM Glycine and 20% (v/v) methanol, Bio-Rad) and 20V overnight in order to transfer the proteins to the nitrocellulose membrane (Amersham). Precision Plus Dual Colour marker was from Bio-Rad. Transfer quality was assessed by Ponceau S (Sigma) staining. After 1 h blocking with 10% (w/v) non-fat dry milk in TBST (Tris buffered saline containing: 150 mM NaCl, 50 mM Tris-HCl pH 7.5/0.1% (v/v) Tween 20) the blots were probed with the primary antibody in 5% (w/v) non-fat dry milk TBST overnight.

Primary antibodies used were: rabbit polyclonal anti-mitogen-activated protein kinase (ERK1/2) (Upstate, used at 1:10,000), monoclonal anti-tau de-phosphorylated on Ser 189/207 (clone Tau-1, Chemicon, used at 1:1,000), monoclonal anti-tau phosphorylated on Ser 202 (clone AT8, Autogen Bioclear, used at 1:1,000), monoclonal anti-β-catenin (Chemicon, used at 1:1,000), monoclonal anti-phospho-glycogen synthase (generated and

validated at GlaxoSmithKline, used at 1:500), rabbit polyclonal anti-PO #1216 (Cambridge Research Biochemicals, used at 1:1,000), rabbit polyclonal anti-GAP43 (Abcam, used at 1:3,000), rabbit polyclonal anti-P-GAP43 (Zymed, used at 1:3,000). The blots were then washed with TBST for 45 min, changing the buffer every 15 min, incubated with goat anti-rabbit IgG or goat anti-mouse IgG HRP-conjugated secondary antibodies (Santa Cruz, used at 1:10,000) in 5% (w/v) non-fat dry milk TBST and developed using the SuperSignal West Pico Chemiluminescent Substrate (Pierce). Protein levels were normalised to ERK1/2 and expressed as fold-induction relative to control. Quantitation was performed using GeneTools software from Syngene. Single sample *t* test was used for statistical analysis.

2.4.3 Immunoprecipitation and co-immunoprecipitation

Cells were lysed in a mild lysis buffer consisting of 50 mM Tris-HCl pH 7.5, 150 mM NaCl, 0.5% (v/v) Triton X-100, 1 mM EDTA. Protease and phosphatase inhibitors (Sigma protease inhibitor cocktail, used at 1:200, Sigma phosphatase inhibitor cocktail II, used at 1:100) were added just before use. In order to allow formation of the antibody-antigen complex, 500 µl of cell lysates were used for each immunoprecipitation reaction and aliquoted into pre-chilled tubes. The specific antibody directed against target protein or epitope-tag was added to the lysate (1-5 µg of antibody per sample). Samples were incubated at 4°C on a rotating wheel overnight. 25 µl bed volume of Protein G Sepharose (Sigma) was used per sample, washed 3 times in TBS, followed by 3 washes with lysis buffer. Beads were finally resuspended in lysis buffer to give a 50% solution. 25 µl bed volume protein G Sepharose was added per sample and incubated on the rotating wheel at 4°C for 1-3 h. The complex was briefly spun and the supernatant was carefully removed and discarded. Three washes with suitable wash buffer were performed, twice with protein lysis buffer followed by one wash with 1x TBS. After the last wash, all traces of liquid were carefully removed with a fine pipette tip. In order to elute proteins from Protein G Sepharose, 35 µl of 2x protein sample buffer (4% (w/v) SDS, 20% (v/v) glycerol, 50 mM TRIS pH 6.8, 2% (w/v) bromophenol blue, 2% (v/v) β-mercaptoethanol) were added to the Protein G Sepharose pellet and boiled for 5 min at 100°C, spun briefly, and the supernatant run on a SDS-gel.

2.4.4 PO antibody generation

The typical peptide length for good antibody production is in the range of 15-20 residues. Peptide sequences of this length should contain at least one epitope, should be easy to synthesise, be relatively soluble in aqueous solutions and should adopt a limited number of conformations.

PO peptide sequences were selected based on the crystal structure and the following criteria:

1. Hydrophilic pattern: it is important to determine which parts of the protein are exposed and thus available for reaction;

2. Content of charged residues: the selected peptides should be neutral. It is also best to avoid multiple amino acid repeats;

3. Peptide solubility: it is preferable to avoid hydrophobic residues, such as tryptophan, valine, leucine, isoleucine and phenylalanine, as well as glutamine, which can form hydrogen bonds between peptide chains;

4. Post-translational modifications: some sites within a protein may be modified e.g. by glycosylation. These sites must be avoided.

A Blast search was performed to eliminate any sequences with significant homology with other proteins. Considering the high PO sequence homology among species, antibodies were expected to recognise PO protein from rat, mouse and human, amongst other species (Fig. 2.2). The following peptides (or whole protein) were used:

LSFQYPDVYRDET (N-terminal sequence) (rabbits #1216, #1217)

YPQQDGKSDGTETSTNLH (internal sequence) (rabbits #9635, #9636)

IVGRSRKQSNPLLIH (close to C-terminal) (rabbits #1422, #1423)

Full-length recombinant PO (made at GlaxoSmithKline, C-terminal His-tagged)

(rabbits #1890, #1891)

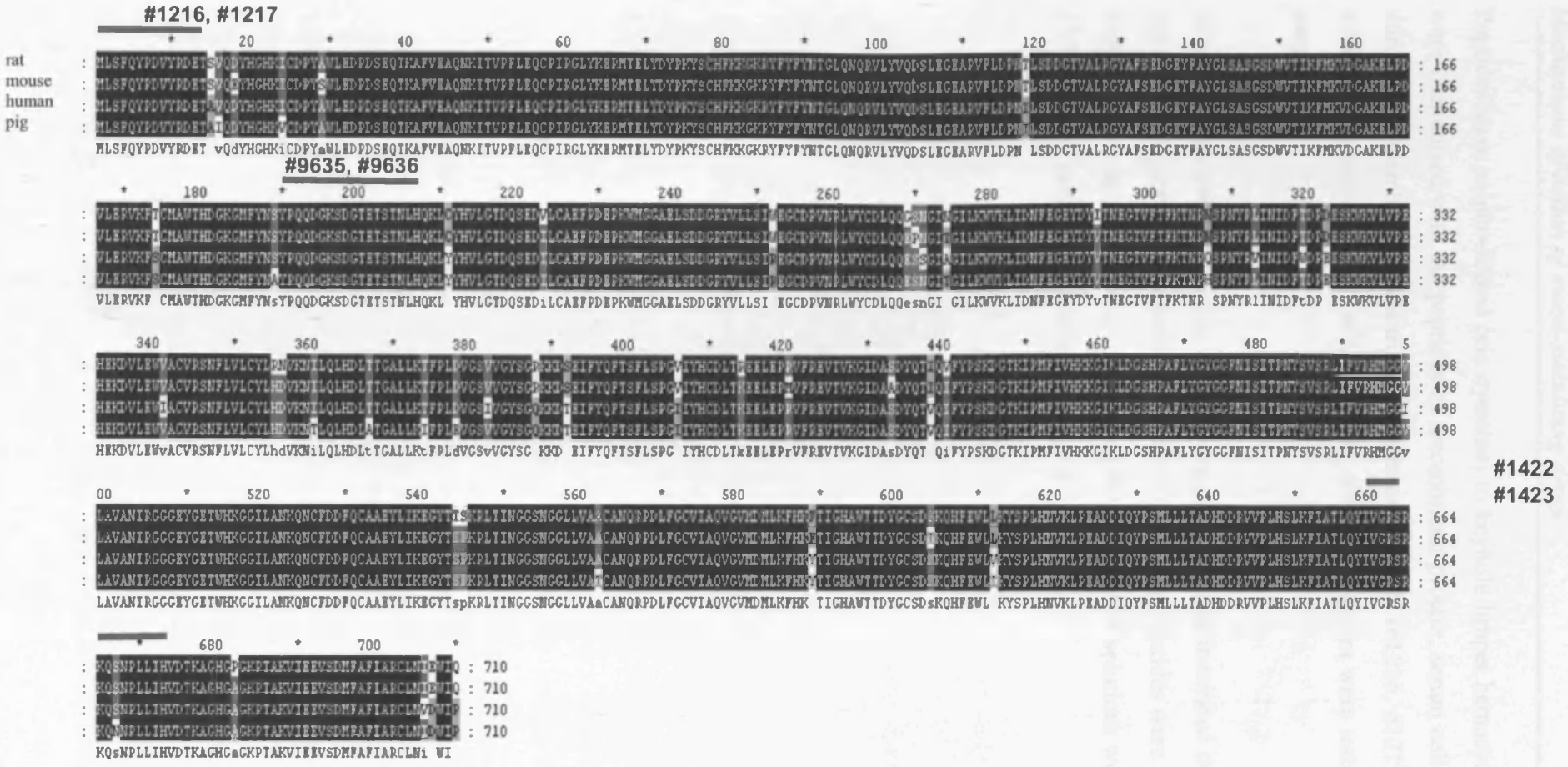

Fig. 2.2 Alignment of PO protein sequence from rat, mouse, human and pig.
Conserved residues are indicated in dark blue, white residues represent amino acids that are not conserved amongst species, light blue are residues that are partially conserved. Peptides that have been selected for antibody generation are highlighted with a red bar together with the rabbit identification number (#).

Peptides were sulpho-linked (via cysteine) to keyhole limpet hemacyanin (KLH). Rabbits were immunised with the peptides or recombinant protein, serum collected and antibodies purified by Cambridge Research Biochemicals (CRB) (#1216, #1217, #1890, #1891) or Research Genetics (#1422, #1423, #9635, #9636). Antisera were tested by ELISA by the suppliers.

In peptide competition studies, the primary antibody was incubated overnight at 4°C with the respective peptide (re-suspended in distilled water). Peptides were used in excess of ten fold (in μg) over the antibody. Peptide or antibody alone solutions were also incubated at 4°C using the same experimental conditions.

2.4.5 Immunocytochemistry

Primary neurons and cell lines: Cells were fixed with 4% (v/v) paraformaldehyde (PFA) for 15 min, washed three times with PBS and permeabilised with 0.3% (v/v) Triton X-100 for 5 min. Cells were then blocked with 5% (v/v) normal goat serum (Chemicon) in PBS for 1 h, followed by incubation with primary antibody for 1-3 h at room temperature or overnight at 4°C in PBS with 5% (v/v) normal goat serum. A secondary Alexa-conjugated goat anti-rabbit or mouse IgG antibody (Molecular Probes, used at 1:400) was added after 3 washes with PBS for 1 h. Coverslips were mounted with ProLong Gold antifade reagent, with or without the nuclear marker DAPI (Molecular Probes).

Sensory neurons: Explants were loaded with the fluorescent dye calcein for 30 min at 37°C and then fixed with 4% (v/v) PFA and 0.2% (v/v) glutaraldehyde (Sigma) in PBS for 30 min. Coverslips were labelled with primary and secondary antibodies as above and mounted.

2.4.6 Immunohistochemistry

Rats or mice (wild-type and PO null-mutant) were perfused with 4% PFA (v/v) (Laboratory Animal Support group, GlaxoSmithKline). Brains were removed, immersed in the same fixative for ~24 h and then transferred into 30% (w/v) sucrose solution for 1-2 days. Brains were cut as 30-40 μm sections free-floating in PBS. Sections were subsequently incubated for ~30 min in 20% (v/v) methanol, 1.5% (v/v) hydrogen peroxide in PBS followed by a 10 min wash in PBS. Sections were incubated for 30-45 min in blocking solution made of PBS with 3% (v/v) normal goat serum, 2 g/l bovine serum albumin, 0.1% (v/v) Triton X-100 followed by incubation with the primary anti-PO #1216 antibody in blocking solution for 24 h at 4°C with gentle shaking. Three 10 min washes with 0.3% (v/v) Triton X-100 in PBS were performed and sections incubated for 1 h at room temperature, with gentle shaking, with biotinylated goat anti-rabbit or anti-mouse antibody (Vector, used at 1:200) in blocking solution. Three 10 min washes with 0.3% (v/v) Triton X-100 in PBS were performed and sections were then incubated for 1 h at room temperature with gentle shaking in Avidin/Biotin reagent (Vector, following manufacturer's instructions) followed by three 10 min washes with 0.3% (v/v) Triton X-

100 in PBS. Sections were transferred into TBS and incubated with diaminobenzidine tetrahydrochloride (DAB) substrate (Vector) following the manufacturer's instructions until suitable staining developed. The reaction was stopped by transferring sections into distilled water. Sections were mounted onto slides and allowed to air dry thoroughly before mounting them with coverlips using DPX (Sigma).

2.5 Molecular protocols

2.5.1 RNA extraction

Freshly dissected cortices from wild-type and PO null-mutant mice were lysed with 500 µl of RLT buffer (Qiagen) containing 1% (v/v) β-mercaptoethanol. Similarly, primary neurons were washed with PBS and lysed with 500 µl of RLT buffer containing 1% (v/v) β-mercaptoethanol. Samples were homogenised using the Mixer Mill MM 300 (Retsch) 2 x 2 min at 30 Hz. RNA extraction was performed using Qiagen RNeasy Mini Kit following the manufacturer's instructions, including the DNase digestion step. RNA from rat cortex and kidney (postnatal day 21) was obtained by the same procedure. RNA quality was determined by measuring absorbance at 260 nm and 280 nm. To ensure significance, A260 should be higher than 0.15. An absorbance of 1 unit at 260 nm corresponds to 40 µg of RNA per ml at neutral pH. All samples were considered of good quality and purity if the 260/280 ratio was >1.8. The concentration of RNA can be calculated using the following equation: [RNA] in µg/µl = (A260 x 40 x D)/1000, where 1 optical density unit is equivalent to 40 µg/ml single stranded RNA and D is the dilution factor. Occasionally, the RNA quality was checked on a 1% (w/v) agarose gel.

2.5.2 Reverse transcription reaction

In order to reverse transcribe (RT) RNA to cDNA, two mastermixes were prepared (+ RT and – RT), triplicates for the +RT reaction and one reaction for the -RT. 8 µl of mastermix were added in each well (2 µl of 10x buffer RT, 2 µl of dNTP mix (5 mM each), 2 µl of Oligo-(dT) 12-18 primer (Invitrogen) (0.5 µg/µl, diluted 1:10 with dH20), 1 µl of RNase out inhibitor (Invitrogen) (40 units/µl, diluted 1:4 with 1x RT buffer), 1 µl of Omniscript Reverse Transcriptase (Qiagen) (or water in the negative reaction). RNA (50 ng-2 µg) and water were added to bring the reaction volume to 20 µl. Samples were incubated for 60 min at 37°C in a PCR machine (MJ Research). 60 µl of dH_20 were added to each well (total volume 80 µl) and aliquoted at 4 µl/well with an Hydra machine (Matrix) into 96-well optic plates.

2.5.3 Taqman RT-PCR

RT-PCR analysis was performed using an Applied Biosystems ABI 7700 PE machine (or ABI 7900 in more recent studies) following the manufacturer's instructions. The mastermix used was Excite 2x probe mastermix (GeneSys), primers were synthesised by Invitrogen and probes by Operon Biotechnology or ABI. Rat or mouse genomic DNA (BD Biosciences) was used to generate the standard curve. Analysis was performed following Medhurst *et al.* and Harrison *et al.* (Harrison *et al.*, 2000; Medhurst *et al.*, 2000). The following primer and probe sequences were used (Table 2.1):

Gene/Species/Accession n°	Forward primer	Reverse primer	Taqman probe
Cyclophilin/ Rat and Human/ M19533	5'-TGTGCCAGGGTGGTGACTT	5'-TCAAATTTCTCTCCGTAGATGGACT	5'-CCACCAGTGCCATTATGGCGTGT-3
β-actin/ Rat/ NM_031144	5'-TCTGTGTGGATTGGTGGCT 3'	5'-CTGCTTGCTGATCCACATCTG-3'	5'-CCTGGCCTCACTGTCCACCTTCC-3
β-actin/ Mouse/ NM_031144	5'-TCTGTGTGGATTGGTGGCT 3'	5'-CTGCTTGCTGATCCACATCTG-3'	5'-CCTGGCCTCACTGTCCACCTTCC-3
PO/ Rat and Mouse/ NM_031324	5'-AGGCTCACGATCAATGGAG	5'-GTGGAACTTCAACATGTCCATCAC-	5'-TCCAATGGCGGCCTCTTAGTGGC-3
PO/ Human/ NM_002726	5'-TCCATGACCTGACTACTGG 3'	5'-GACCGCTGTACCCTACAATGCT-3'	5'-CTTAAGACCTTCCCGCTCGATGTC(
SMIT1/ Rat/ NM_053715	5'-ATGAAGACGTCCCATGGCC	5'-CCCTCTGCACGATGACTTGG-3'	5'-ATTCATTCTTGGGCAGACCCCAGC(3'
HMIT/ Rat/ NM_133611	5'-TCGAATCGCTCTTCGACCA(	5'-CCTTCACGCGGATGTACTCG-3'	5'-CGGACTCGGACGAGGGCAGGTAC/
SMIT2/ Rat/ Prediction XM_574554.1	5'-TCCTGTGGCTCTGTGGGAT	5'-TGCACACAATGCAGTTGACG-3'	5'-CCCCAAGCAAAGTGGAGCCTGTCAT/
MIP synthase/ Rat/ NM_001013880	5'-AAGATGGAGCGCCCTTTCC	5'-AGCTCTGGTGTTGGTGCCTG-3'	5'-CCACTGCCTTGCAAGAAAGAGTCC 3'
GAP43/ Rat/ M88356	5'-TCCTCCAAGGCCGAAGATG -3'	5'-TCAGTGACAGCAGCAGGCAC-3'	5'-CCAAGGAGGAGCCTAAACAAGCCC

Table 2.1 Taqman primers and probe sequences.
Primers and probes have been designed at the 3'-prime end of the sequence.

2.5.4 Transformation of bacteria

One to 5 ng of DNA were added to TOP10 competent cells (Invitrogen) and incubated on ice for 30 min. Cells were subjected to heat shock at 42°C for 30 s and then placed immediately on ice. 250 µl of pre-warmed SOC medium (Invitrogen) were added and incubated at 37°C for 1 h with moderate shaking. 20 to 200 µl of transformation mix were spread on Luria-Bertani (LB) agar plates (made by dissolving 10 g Bacto Tryptone, 5 g yeast extract, 10 g NaCl, 15 g Bacto Agar in 1 l water, pH 7.5 and including the appropriate antibiotic, e.g. 50 – 100 µg/ml ampicillin), and incubated at 37°C overnight.

2.5.5 DNA purification

Qiagen plasmid purification kits are based on a modified alkaline lysis procedure followed by binding of plasmid DNA to anion-exchange resins under appropriate low-salt and pH conditions. Plasmid DNA is eluted in a high-salt buffer and then concentrated and desalted by isopropanol precipitation. A single colony was picked from a freshly streaked plate and inoculated into 5 ml LB medium (made by dissolving 10 g Bacto Tryptone, 5 g yeast extract, 10 g NaCl in 1 l water, pH 7.5 and including the appropriate antibiotic, i.e 50 - 100 µg/ml ampicillin), for ~8 h at 37°C with vigorous shaking. This starter culture was diluted 1:500 into selective LB medium and grown at 37°C for 12-16 h with vigorous shaking at 37°C. The bacterial cells were harvested by centrifugation for 20 min at 4°C and the Qiagen protocol was followed. DNA was re-suspended in TE buffer or water, the concentration measured spectrophotometrically and purity checked by 260/280 ratio (DNA was considered of good quality if 260/280 ratio was between 1.7-2.0).

2.5.6 PO sub-cloning

Rat PO was amplified from pcDNA3.1D/V5-His-TOPO (Fig. 2.3) (generated at GlaxoSmithKline, stop codon not removed) by PCR and subcloned into pcDNA4/V5-His (Invitrogen) (Fig. 2.4) using the following primers:

Rat PO_Fw 5'-CC**GGTACC**ATGCTGTCCTTCCAGTACC-3'

Rat PO_Rev 5'-CC**CTCGAG**CTGGATCCACTCGATGTTC-3'

Where **GGTACC** is a KpnI site and **CTCGAG** is a XhoI site. CC were added at the 5'-primed end to improve the PCR amplification. The PO stop codon was removed in order to obtain a His-V5 tagged clone.

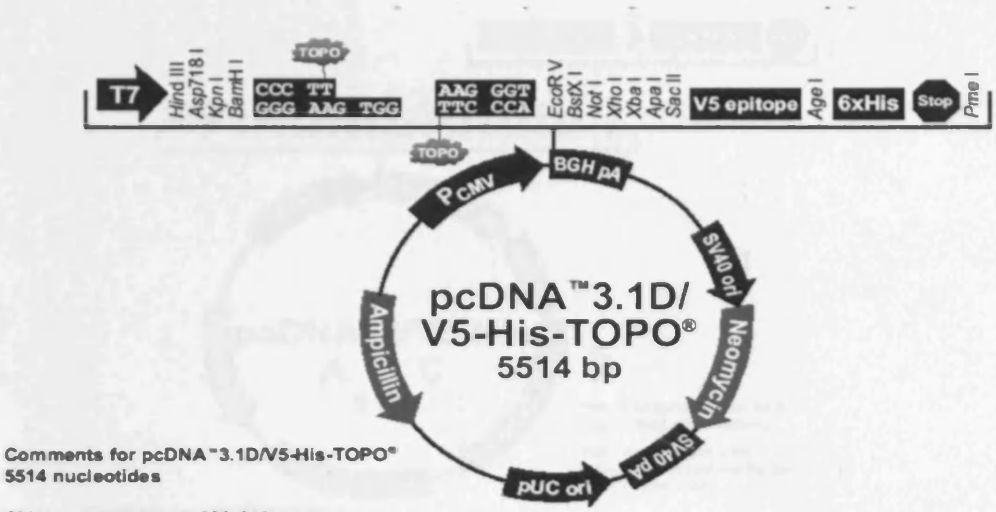

Comments for pcDNA™3.1D/V5-His-TOPO®
5514 nucleotides

CMV promoter: bases 232-819
T7 promoter/priming site: bases 863-882
TOPO® recognition site 1: bases 930-934
Overhang sequence (complementary strand): bases 935-938
TOPO® recognition site 2: bases 939-943
V5 epitope: bases 1011-1052
Polyhistidine (6xHis) tag: bases 1062-1079
BGH reverse priming site: bases 1102-1119
BGH polyadenylation signal: bases 1108-1332
SV40 early promoter and origin: bases 1833-2142
Neomycin resistance gene: bases 2217-3011
SV40 early polyadenylation signal: bases 3189-3319
pUC origin: bases 3700-4373 (complementary strand)
Ampicillin (*bla*) resistance gene: bases 4518-5378 (complementary strand)
bla promoter: bases 5379-5477 (complementary strand)

Fig. 2.3 pcDNA3.1D/V5-His-TOPO plasmid map from Invitrogen.

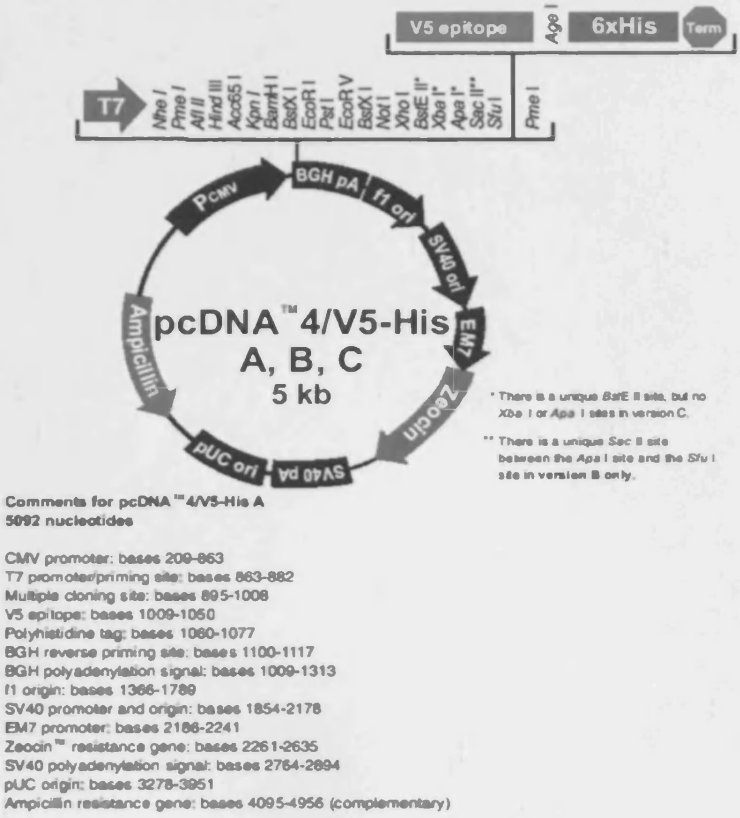

Fig. 2.4 pcDNA4/V5-His plasmid map from Invitrogen.

100 ng of DNA template and the Expand High Fidelity PCR System (Roche) were used to amplify PO. The following PCR conditions were applied: (i) 2 min at 94°C, (ii) 15 s at 94°C, 30 s at 55°C, 90 s at 72°C, (iii) step ii repeated 10x, (iv) 15 s at 94°C, 30 s at 55°C, 90 s at 72°C, (v) step iv repeated 10x, (vi) 5 min at 72°C. 10 µl of PCR product were run on a 0.8% (w/v) agarose gel (1 kb DNA marker, Invitrogen). Agarose (ultra pure, electrophoresis grade) was dissolved in boiling 1x Tris-acetate-EDTA (TAE) buffer (50x: 40 mM Tris-acetate, 1 mM EDTA pH 8.0) with the addition of ethidium bromide (0.5 µg/ml). The gel was cast on a gel bed with a suitable comb using a horizontal gel apparatus and placed in an electrophoresis tank containing 1x TAE buffer to a level just above the gel surface. The DNA sample containing DNA loading buffer (10x: 50% (v/v) glycerol, 0.25% (w/v) bromophenol blue in TAE) was loaded into the sample wells and run at 2-10 V/cm. Gels were placed in a UV transilluminator (λ= 302 nm) and DNA visualised. A 2.1 kb product was observed (Fig. 2.5).

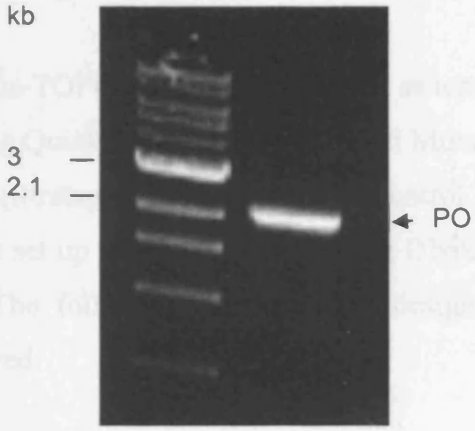

Fig. 2.5 Rat PO cloning.
PO was amplified by PCR from pcDNA3.1D/V5-His-TOPO. A ~ 2.1 kb band was observed. 10 µl of 1 kb DNA marker and reaction product were loaded.

The product was purified using the PCR purification kit following the manufacturer's instructions (Qiagen) and eluted in 30 µl water. Enzyme digestion was performed for 2 h at 37°C (30 µl DNA + 3 µl KpnI (10 u/µl) + 1.5 µl XhoI (20 u/µl) (both NEB), using buffer 1 (100% KpnI activity and 75% XhoI activity). 3 µg of the vector pcDNA4/V5-His were also cut using the same conditions, treated with alkaline phosphatase (Roche) for 10 min at 37°C, followed by 15 min at 65°C to inactivate it. A preparative 0.8% (w/v) agarose gel was made, all the digestion products loaded and bands were excised with a clean scalpel. The Quiaex II purification kit was used following the manufacturer's instructions (Qiagen) and DNA eluted in 40 µl water. Products were run on a 0.8% (w/v) agarose gel (10 µl) and concentration determined based on the band intensity observed: for PO: ~ 150 ng/µl, for the vector: ~10 ng/µl. Ligation was performed using T4 ligase (NEB) overnight at 4°C using different amounts of DNAs (200 ng total/8 µl reaction). Maximum efficiency TOP10 cells were transformed with 5 µl DNA as described in section 2.5.4. 2 to 3 colonies were counted in vector only transformed bacteria (negative control) and 24 in plates with the ligation product. All 24 colonies were picked, grown overnight at 37°C and DNA extracted using the Miniprep kit following the manufacturer's instructions (Qiagen). DNA sequence was confirmed by the Sequencing group at GlaxoSmithKline, using primers that I have designed every ~ 500 base pairs.

2.5.7 Generation of catalytically-dead PO

Rat PO in pcDNA3.1D/V5-His-TOPO (untagged) was used as template. **T**CC was mutated to **G**CC (Ser 554 to Ala) using Quickchange II Site-Directed Mutagenesis kit following the manufacturer's instructions (Stratagene). The positive control from the kit was also included. Four reactions were set up using 10-20-50-100 ng DNA. A 5 min extension time and 12 cycles were used. The following primers were designed, both containing the mutation highlighted in bold red:

Fw 5'-GGCTCACGATCAATGGAGGC**G**CCAATGGCGGCCTCTTAGTGGC-3'
Rev 5'-GCCACTAAGAGGCCGCCATTGGC**G**CCTCCATTGATCGTGAGCC-3'

After transformation, ~100 blue colonies were observed in the positive control plate and 22 colonies were counted in the plates containing the catalytically-dead PO. These colonies were picked, grown overnight at 37°C and DNA extracted using the Miniprep kit from Qiagen. Five colonies were judged to be of bad DNA quality (260/280 ratio < 1.6) while the remaining 17 colonies had a 260/280 ratio > 1.8. The latter were sequenced with the same primers used in the PCR reaction in order to check for the mutation (Sequencing group, GlaxoSmithKline). DNA from 11 colonies contained the desired mutation. Two were chosen (clones #1 and #17) and fully sequenced using 5 primer sets that were designed every ~300 bp of the PO gene. No other mutations were observed in both clones.

2.5.8 PO-null mutant mouse generation

PO null-mutant mice were generated by Deltagen by targeting a LacZ-Neo cassette to exon 2 and part of exon 3 of the PO mouse gene (Accession N°: BC012869). The deleted sequence is shown in bold red (Fig. 2.6). Genomic DNA isolated from ES lines was digested with restriction enzymes chosen to cut outside of the construct arms and the DNA was analysed by Southern hybridization (performed by Deltagen). ES cells derived from the 129/OlaHsd mouse substrain were used to generate chimaeric mice. F1 mice were generated by breeding with C57BL/6 females. F2 homozygous mutant mice were produced by intercrossing F1 heterozygous males and females (Laboratory Animal support team, GlaxoSmithKline). Experiments were performed on mice fully backcrossed to C57Bl/6 (N = 5 or greater). Mice were made homozygous in order to simplify analysis of embryos and early post-natal mice. Mouse genotyping was performed at GlaxoSmithKline.

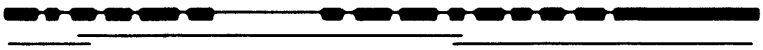

Exons: *1 2 3 4 5 6 7 8 9 10 11 12 13 14 15*

ATGCTGTCCTTCCAGTACCCCGACGTGTACCGCGACGAGACCTCCGTGCAGGAGTATCATGGACATAAAATTTGTGACCCGTATTCTTGGC
TTGAAGACCCAGACAGCGAGCAGACTAAGGCTTTCGTGGAGGCACAAAACAAGATTACTGTGCCATTTCTTGAGCAATGTCCAATCAGAGG
TTTATACAAGGAGAGAATGACTGAGCTGTACGACTACCCCAAGTACAGCTGCCACTTCAAGAAAGGAAAGCGGTACTTTTATTTTTACAAT
ACAGGTTTGCAGAACCAACGCGTGTTATATGTGCAAGACTCCTTAGAGGGGGAGGCCAGAGTGTTCCTGGACCCCAACACACTGTCGGATG
ATGGTACAGTGGCACTCCGAGGTTATGCCTTCAGTGAAGATGGCGAATACTTTGCCTATGGTCTGAGCGCCAGCGGCTCCGACTGGGTGAC
GATCAAGTTCATGAAGGTCGATGGTGCCAAAGAGCTCCCGGATGTGCTGGAGAGAGTCAAGTTCACCTGCATGGCCTGGACGCATGACGGG
AAGGGAATGTTCTATAACTCATACCCGCAGCAGGACGGGAAGAGCGATGGCACAGAGACATCCACCAATCTCCACCAAAAGCTCTGCTACC
ACGTCTTGGGGACGGATCAGTCAGAAGATATTTTGTGTGCTGAGTTCCCCGATGAGCCTAAATGGATGGGAGGAGCTGAGCTATCCGACGA
TGGCCGGTACGTCTTGTTATCCATCTGGGAGGGATGTGATCCAGTAAACCGACTGTGGTACTGTGACCTCCAGCAAGAACCCAATGGTATC
ACCGGAATCCTGAAGTGGGTAAAACTGATAGACAACTTTGAAGGAGAATACGACTACGTAACCAACGAGGGCACAGTGTTCACATTCAAGA
CGAACCGCAATTCTCCCAATTATCGGCTGATCAATATCGACTTCACGGACCCTGACGAGTCCAAGTGGAAAGTGCTCGTACCGGAGCACGA
GAAGGATGTCTTAGAATGGGTGGCTTGTGTCAGGTCCAACTTCCTGGTCTTGTGCTACCTCCATGACGTGAAGAACATTCTACAGCTTCAC
GACCTGACGACTGGTGCTCTCCTCAAGACCTTCCCCCTGGATGTGGGCAGCGTGGTGGGCTACAGTGGGCGCAAGAAGGACTCTGAGATCT
TCTACCAGTTCACATCCTTCCTATCTCCAGGTGTCATTTACCACTGCGATCTTACCAAAGAGGAACTGGAGCCCATGGTTTTCCGAGAGGT
GACGGTGAAGGGAATCGATGCTGCTGATTACCAGACAATCCAGATTTTCTACCCTAGCAAGGATGGCACCAAGATTCCCATGTTTATTGTG
CATAAAAAAGGCATAAAGCTGGATGGCTCACACCCTGCTTTCTTATATGGCTACGGGGGCTTCAACATCTCCATTACACCCAACTACAGCG
TGTCCAGGCTCATTTTTGTGAGACATATGGGCGGCGTCCTCGCGGTGGCTAACATCAGAGGCGGCGGTGAATACGGAGAGACGTGGCACAA
AGGTGGTATCTTGGCCAACAAACAGAACTGTTTTGATGACTTCCAGTGTGCTGCTGAGTACCTCATCAAGGAAGGTTACACATCTCCCAAG
AGGCTCACGATCAACGGAGGCTCCAACGGCGGCCTCTTAGTAGCTGCTTGCGCAAATCAGCGTCCAGACCTCTTCGGCTGTGTTATTGCCC
AGGTTGGAGTGATGGACATGTTGAAGTTCCACAAATTTACTATCGGCCATGCATGGACCACTGATTACGGGTGCTCCGACACTAAACAACA
CTTTGAATGGCTTCTCAAATACTCGCCACTACACAATGTGAAGCTTCCGGAGGCAGACGACATCCAGTACCCGTCCATGCTTCTCCTCACG
GCTGACCACGACGACCGCGTGGTCCCGCTGCACTCACTGAAGTTCATTGCCACCCTTCAGTACATCGTGGGCCGCAGCCGGAAGCAGAGCA
ACCCCCTGCTCATCCACGTGGACACCAAGGCCGGCCACGGGGCCGGGAAACCCACCGCCAAAGTGATAGAAGAAGTCTCGGATATGTTTGC
GTTCATAGCACGGTGCCTGAACATCGAGTGGATCCAGTAA

Fig. 2.6 PO mouse sequence.
PO consists of 15 exons (black boxes). The PO β-propeller domain is encoded by exons 3-10 (black line), whereas the catalytic domain is encoded by exons 1-3 and 10-15 (blue line) (Kimura *et al.*, 1999). Highlighted in bold red is exon 2 and part of exon 3 of the PO gene, which was replaced in the PO-null mutant mice with a LacZ-Neo cassette.

2.6 Statistical analysis

Statistical analysis was performed using Statistica v6. Results were considered significant at $p<0.05$ (*). Briefly, separate one-way ANOVAs were performed on the data from the growth cone studies. Comparison of treatment groups was made using Fisher's LSD test. Single sample *t* test was used to analyse results from Western blotting.

CHAPTER 3
Analysis of the effects of mood stabilizers on GSK3 vs PIns pathways

The results presented in this chapter have been published (Di Daniel *et al.*, 2006). Much of the content is taken from the published work, which was written together with Professor Anne Mudge.

3.1 Introduction

The three most-frequently prescribed mood stabilizers – lithium, VPA and CBZ – have a common effect on the dynamic behaviour of rat sensory neurons: all three drugs inhibit the collapse and increase the spread area of growth cones (Williams *et al.*, 2002). Moreover, these effects are reversed by inositol, suggesting that all three mood-stabilizing drugs inhibit recycling of PIns. The commonality of the drug effects on PIns signalling suggests that this pathway may be the therapeutic target for the mood stabilizers and furthermore, that defects in the regulation of PIns signalling may underlie BD (Kim *et al.*, 2005b).

Lithium directly inhibits two key enzymes involved in PIns recycling: IMPase and IPPase. Berridge *et al.* (Berridge *et al.*, 1989) and later Batty and Downes (Batty & Downes, 1995) suggested that these inhibitory effects on the PIns cycle may partly explain the therapeutic action of lithium. In contrast, lithium's inhibition of GSK3 has led to the suggestion that this kinase may be the therapeutically-relevant target for lithium in mood stabilization rather than PIns signalling (Klein & Melton, 1996; O'Brien *et al.*, 2004; Phiel & Klein, 2001). There are several reports that VPA also inhibits GSK3 either directly or indirectly (Chen *et al.*, 1999a; Hall *et al.*, 2002; Werstuck *et al.*, 2004), although these observations are disputed by other studies (De Sarno *et al.*, 2002; Jin *et al.*, 2005; Phiel & Klein, 2001; Williams *et al.*, 2002).

Inhibition of GSK3 with potent but non-selective inhibitors induces changes in growth cone morphology. Owen and Gordon-Weeks reported that the GSK3 inhibitor SB-216763 and 10 mM lithium increased the growth cone spread area of chicken sensory neurons (Owen & Gordon-Weeks, 2003). Therefore, confusion exists as to whether the effects of lithium and VPA are mediated by GSK3 or inositol. While studying the effects of Wnt signalling on neural development, Salinas and colleagues found that both lithium and VPA increased the spread area of growth cones of rat cerebellar mossy and granule neurons and these drug effects were not inhibited by inositol (Hall *et al.*, 2000; Hall *et al.*, 2002; Lucas & Salinas, 1997). Guidance molecules, such as Sema3A, provide cues that are involved in directing axons to or away from particular targets and induce a dramatic 'collapse' of growth cones and axon retraction. This Sema3A-induced 'collapse and retraction'

behaviour is dependent on activation of a highly localised pool of inactive GSK3 at the leading edge of the growth cone, which was elegantly demonstrated by Eickholt *et al.* using the GSK3 inhibitors SB-216763 and SB-415286, as well as 20 mM lithium (Eickholt *et al.*, 2002). In discussing whether the relevant therapeutic target of lithium in the treatment of BD is either inhibition of GSK3 or inhibition of PIns signalling, O'Brien *et al.* make no distinction between semaphorin-induced 'collapse and retraction' and the cycles of dynamic 'collapse and spread' described in Williams *et al.* (O'Brien *et al.*, 2004; Williams *et al.*, 2002). In addition, Klein and colleagues comment that there may be additional functions of inositol other than the known effect on PIns recycling, because addition of inositol can reverse the developmental defects induced by dominant negative GSK3β in *Xenopus* (Hedgepeth *et al.*, 1997).

The study of Williams *et al.* is the only example demonstrating a common effect of all three mood stabilizers – lithium, VPA, and CBZ – on a intracellular signalling pathway in neurons (Williams *et al.*, 2002). Given the importance of determining the therapeutically relevant targets of these drugs, we sought to clarify the effects of mood stabilizers on growth cone dynamics and to further characterise this assay.

3.2 Results

3.2.1 Characterisation of rat sensory neuron growth cones

Growth cones from rat DRG explants were characterised in terms of tubulin expression, using an antibody specific to the post-translational acetylated form, which is a marker of stable microtubules (Bianchi *et al.*, 2005; Dent & Kalil, 2001) Stable microtubules do not usually extend into the growth cone in control cultures (Fig. 3.1A). Treatment with 10 mM LiCl, however, alters microtubule dynamics by inducing coiled structures, which penetrate the growth cone in a small percentage of neurons (Fig. 3.1B). Because this effect was observed with 10 mM LiCl only and not with a more therapeutically-relevant LiCl concentration or with VPA or CBZ - it is likely that this effect may not derive from modulation of the pathway commonly regulated by the drugs.

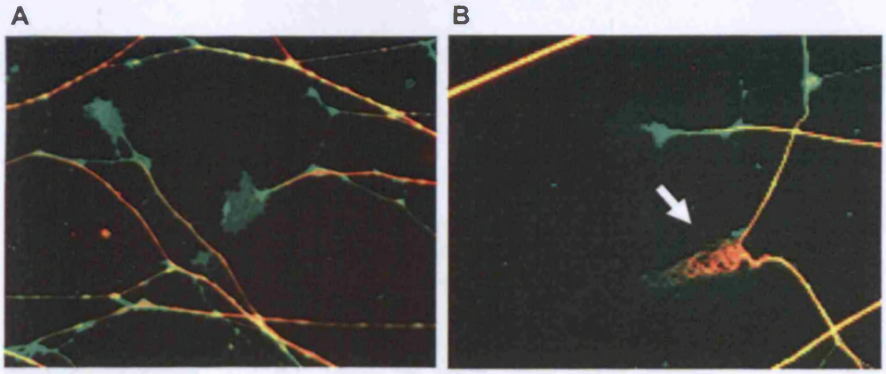

Fig. 3.1 Expression of acetylated tubulin in rat sensory neurons.
Neurons were treated with LiCl for 24 h and labelled with anti-acetylated tubulin (Sigma, 1:3,000) (red) and anti-GAP43 (Abcam, 1:5,000) (green) antibodies. **A** control cultures **B** LiCl 10 mM-treated neurons. The arrow shows abnormal microtubules penetrating the growth cone area.

3.2.2 Effect of PTN and GPT on sensory neuron growth cones

In order to test whether the growth cone assay is a useful model for mood-stabilizing drug action, growth cones were labelled and scored as collapsed or spread as illustrated in Fig. 3.2A. Using this assay we confirmed previous findings by Williams *et al.* that lithium inhibits the frequency of collapse and that this effect is reversed by the addition of 1 mM inositol to the culture medium (Fig. 3.2B) (Williams *et al.*, 2002). To determine the specificity of this morphological assay, we then tested GPT (50 μM) and PTN (50 μM), two anticonvulsants with no mood-stabilizing properties (Yatham *et al.*, 2002). There was no effect of either drug on collapse (Fig. 3.2C). These results show that two anticonvulsants that are not effective as anti-manic drugs do not induce inositol-reversible effects on sensory neuron growth cones and, therefore, do not mimic the effects of the mood stabilizers lithium, VPA, or CBZ.

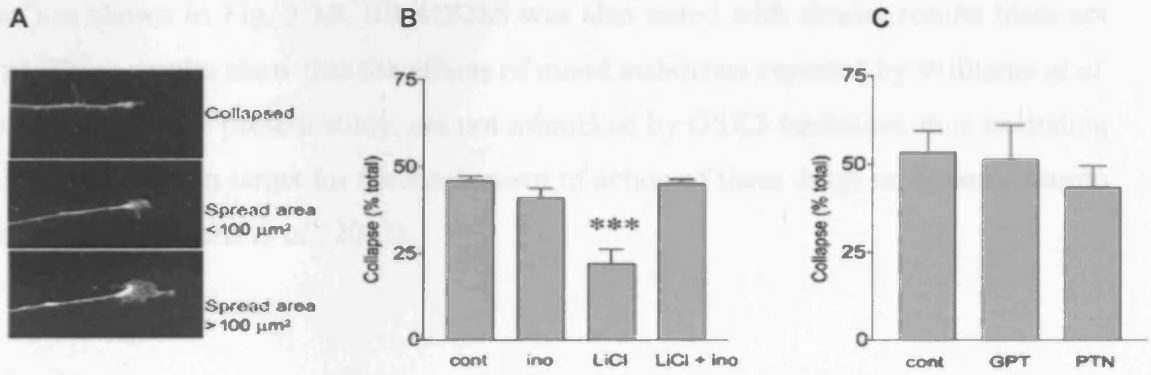

Fig. 3.2 Drug effects on sensory neuron growth cones.
A Micrographs showing a collapsed growth cone (top) and spread growth cones (middle and low panels). Sensory explants were labelled with calcein and fluorescent images acquired with a X40 objective using an Olympus BX51 microscope.
B The histogram shows the effect of LiCl (3 mM) with/without inositol (1 mM) on the number of growth cones collapsed expressed as a percentage of total. Data are presented as mean ± sem. Significant change from control is indicated (one-way ANOVA and Fisher's LSD test, *** $p<0.001$ in LiCl-treated explants). Results shown are from two independent experiments each in duplicate ($n = 4$). **C** The histogram shows the percentage of growth cones collapsed in cultures treated with GPT 50 μM or PTN 50 μM. Results are from one representative experiment ($n = 3$ explants). This experiment was repeated three times with similar results.

3.2.3 Effect of SB-216763 on sensory neuron growth cones

To determine whether GSK3-mediated effects on growth cones are sensitive to inositol levels as suggested by Klein and colleagues from studies in *Xenopus* (Hedgepeth *et al.*, 1997; O'Brien *et al.*, 2004), sensory neuron explants were treated with the GSK3 inhibitor SB-216763 (10 μM), with or without addition of extracellular inositol (1 mM). SB-216763 treatment did not change the percentage of collapsed growth cones (Fig. 3.3A), but it did increase the percentage of large growth cones with area >100 μm^2 (control: 6 ± 3%, SB-216763-treated: 20 ± 5%; mean ± sem). There was no difference when inositol was added with the inhibitor (SB-216763 plus inositol-treated: 17 ± 5%) (Fig. 3.3A). There was an increase in the mean spread area of growth cones; for those with areas <100 μm^2 or >100 μm^2, the increases in drug-treated explants were ~40% and ~75%, respectively (Fig. 3.3B). The mean spread area of all growth cones in control was 53 ± 4 μm^2 and this area doubled in the presence of SB-216763. Importantly, the addition of 1 mM inositol together with the GSK3 inhibitor did not change significantly the mean growth cone area (96 ± 18 vs. 89 ± 17 μm^2) as shown in Fig. 3.3B. SB-415286 was also tested with similar results (data not shown). These results show that the effects of mood stabilizers reported by Williams *et al.* and of lithium, in the present study, are not mimicked by GSK3 inhibitors, thus excluding GSK3 as the common target for the mechanism of action of these drugs on sensory neuron growth cones (Williams *et al.*, 2002).

A

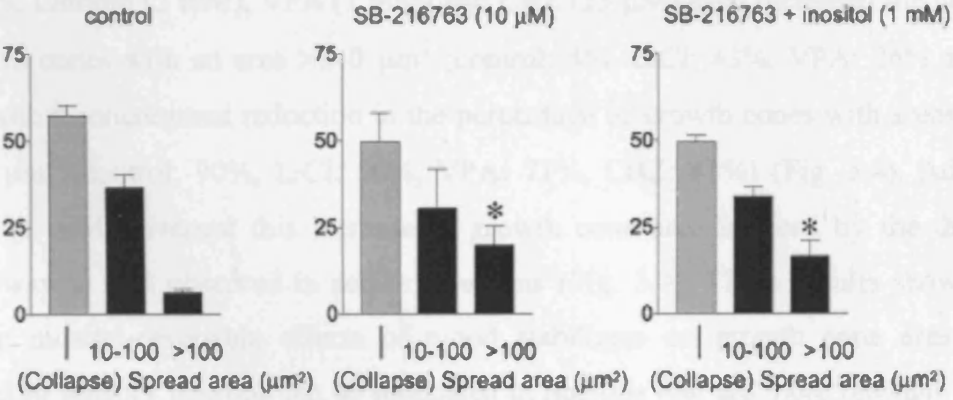

B

	Collapse (% total)	Mean area (μm² ± sem) <100	>100	all
control	57 ± 3	41 ± 2	131 ± 8	53 ± 4
SB-216763	50 ± 11	58 ± 6	229 ± 41	96 ± 18
SB-216763 + inositol	50 ± 2	52 ± 3	182 ± 17	89 ± 17

Fig. 3.3 Effect of SB-216763 on sensory neuron growth cones.
A SB-216763 (10 μM) increases sensory neuron growth cone area and inositol does not reverse the effect. Histograms show the percentage of sensory neuron growth cones that were collapsed or had spread areas between 10-100 μm^2 or >100 μm^2 in control or SB-216763-treated cultures with/without inositol (1 mM), as indicated. *$p<0.05$ in SB-216763-treated cultures in the population of growth cones with area >100 μm^2 when compared with control (ANOVA and Fisher's LSD test). Results were pooled from three independent experiments (n = 3 explants each). The total number of growth cones scored in each bar was ~300.
B SB-216763 increases the growth cone spread area values when compared with control. The table shows the percentage of collapse and growth cone area values for control or SB-216763-treated cultures with/without inositol (mean ± sem). Data are from the same experiment shown in Fig. 3.3A.

3.2.4 Effect of mood stabilizers on cortical neuron growth cone area

We next analysed the effect of mood stabilizers on rat primary neurons derived from the cerebral cortex, a brain region that has been implicated in the pathophysiology of mood disorders. Lithium (2 mM), VPA (1 mM) and CBZ (25 μM) each increased the percentage of growth cones with an area >140 μm^2 (control: 4%, LiCl: 43%, VPA: 26% and CBZ: 67%), with a concomitant reduction in the percentage of growth cones with areas between 20-140 μm^2 (control: 90%, LiCl: 56%, VPA: 71%, CBZ: 41%) (Fig. 3.4). Addition of inositol (1 mM) reversed this increase in growth cone area induced by the drugs in a similar way to that observed in sensory neurons (Fig. 3.4). These results show that the common inositol-reversible effects of mood stabilizers on growth cone area that we observed in sensory neurons can be replicated in neurons that are more relevant for mood disorders.

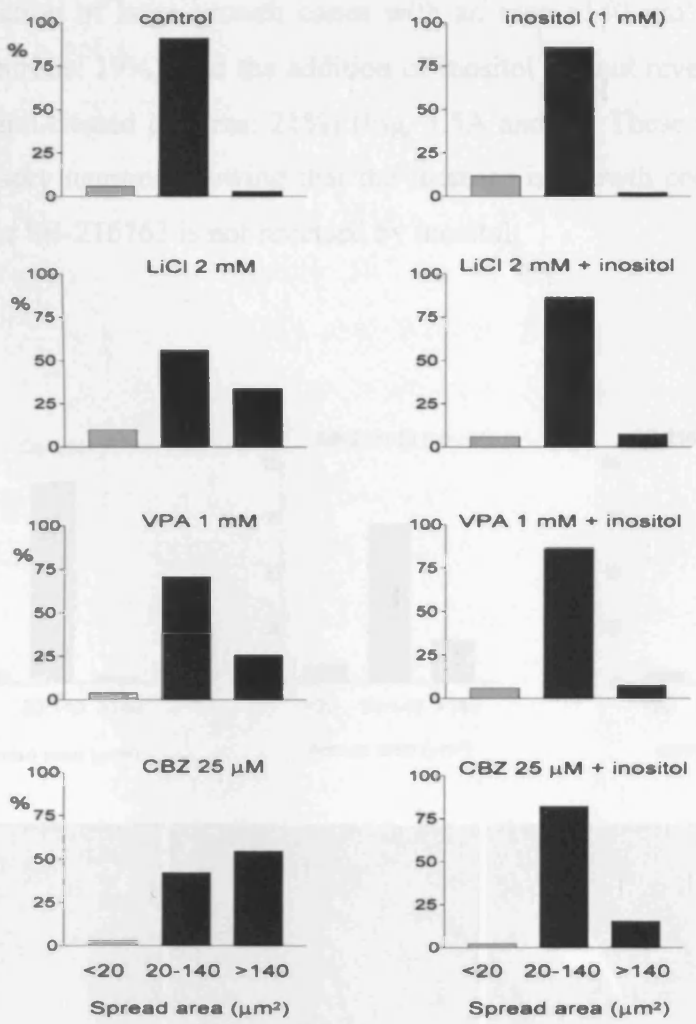

Fig. 3.4 Effect of mood stabilizers on growth cone area in cortical neurons.
Histograms show the percentage of spread growth cones after treatment with drugs with/without the addition of inositol, as indicated. LiCl, VPA and CBZ at the concentrations indicated each induced a shift to larger areas and addition of inositol completely or partially (CBZ) reversed the drug effects. Data are from one experiment (n = 3 coverslips, pooled data) and the total number of growth cones scored in each bar was ~100-150. The experiment was repeated with similar results. Note that cortical neurons do not have a cycle of complete collapse and so the first bar shows small growth cones with area <20 μm^2.

3.2.5 Effect of SB-216763 on cortical neuron growth cones

We then analysed the effect of SB-216763 on cortical neurons. This GSK3 inhibitor induced the formation of large growth cones with an area >140 μm^2 (control: 3%, SB-216763-treated neurons: 19%), and the addition of inositol did not reverse this effect (SB-216763 plus inositol-treated cultures: 21%) (Fig. 3.5A and B). These results confirm our findings with sensory neurons showing that the increase in growth cone area induced by the GSK3 inhibitor SB-216763 is not reversed by inositol.

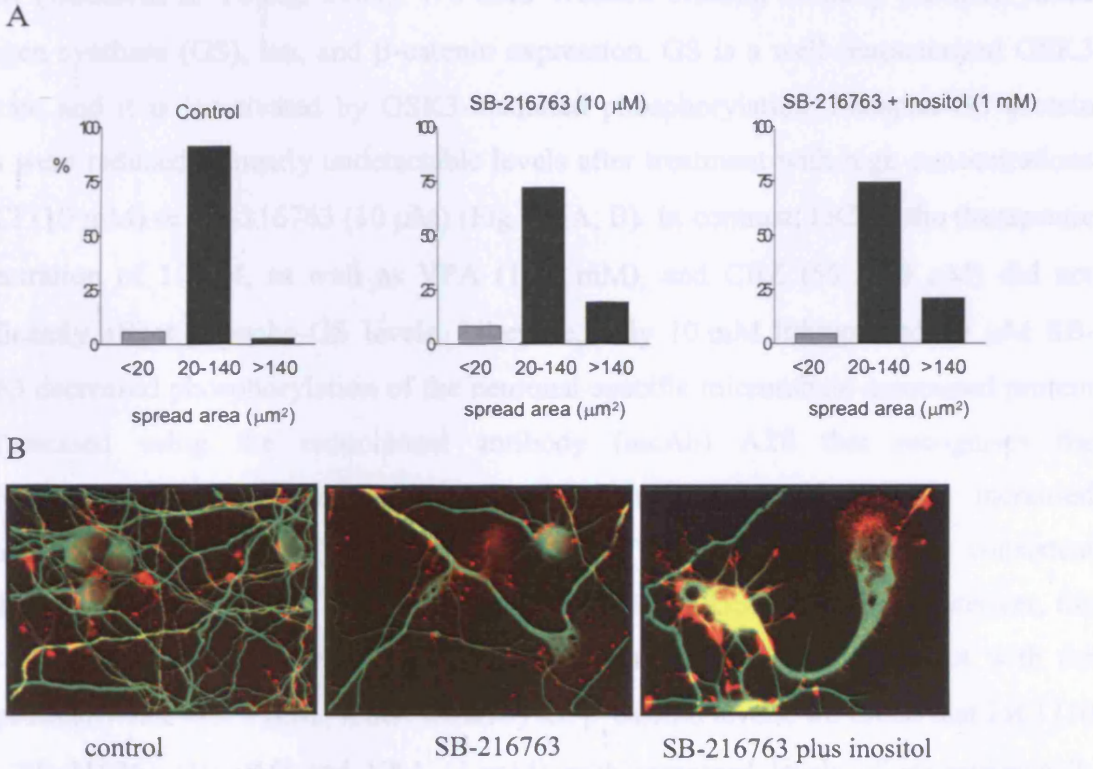

Fig. 3.5 Effect of SB-216763 on cortical neuron growth cones.
A SB-216763 (10 μM) increases cortical neuron growth cone spread area and inositol does not reverse the effect. Histograms show the percentage of different size cortical neuron growth cones treated with SB-216763 with/without inositol. Data are from one experiment (n = 3 coverslips pooled data). The total number of growth cones scored in each bar was ~100-150. The experiment was repeated with similar results.
B Representative images of cortical neurons untreated or treated with SB-216763 (10 μM) with or without inositol (1 mM) labelled with an anti-GAP43 (red) and anti-acetylated tubulin (green) antibodies. Images were acquired with a X60 oil lens.

3.2.6 Effect of mood stabilizers on GSK3 downstream targets

To clarify further the involvement of GSK3 as the common mechanism of action of mood stabilizers, the drug effects on intracellular proteins activated/inhibited by GSK3-dependent phosphorylation were analysed. Cortical neurons were treated at 5 days in culture with two different concentrations of mood stabilizers for 6 h (1 and 10 mM LiCl, 1 and 2 mM VPA, 50 and 100 μM CBZ; in each case, the lower concentration is close to the therapeutic range for blood levels of the drugs). The therapeutic concentrations for the mood stabilizers analysed in this study are: LiCl 0.6-1.5 mM, VPA 0.3-0.6 mM, CBZ 20-50 μM (Goodwin & Young, 2003). We used Western blotting to study phosphorylated glycogen synthase (GS), tau, and β-catenin expression. GS is a well-characterised GSK3 substrate and it is inactivated by GSK3-mediated phosphorylation. Phospho-GS protein levels were reduced to nearly undetectable levels after treatment with high concentrations of LiCl (10 mM) or SB-216763 (10 μM) (Fig. 3.6A, B). In contrast, LiCl at the therapeutic concentration of 1 mM, as well as VPA (1, 2 mM), and CBZ (50, 100 μM) did not significantly affect phospho-GS levels. Likewise, only 10 mM lithium and 10 μM SB-216763 decreased phosphorylation of the neuronal-specific microtubule-associated protein tau (assessed using the monoclonal antibody (mcAb) AT8 that recognises the tau/phosphoserine$_{202}$ epitope), whilst both lithium and SB-216763 increased dephosphorylated tau levels (assessed using mcAb Tau-1). These results are consistent with lithium (but not VPA or CBZ) inhibiting endogenous GSK3 activity; moreover, the effect of LiCl was only seen with the high concentration of 10 mM and not with the therapeutically-relevant 1 mM. When we analysed β-catenin levels, we found that LiCl (10 mM), SB-216763 (10 μM) and VPA (2 mM) each increased levels of cytoplasmic β-catenin. The HDAC inhibitor TSA also induced a 3-fold increase in β-catenin levels (data not shown), suggesting that the effects of VPA on β-catenin levels are likely due to HDAC inhibition. Our results strongly suggest that only lithium (and not VPA or CBZ) inhibits GSK3 either directly or indirectly. Similar conclusions were drawn in a recent study where only lithium decreased tau phosphorylation (mcAb AT270 was also used) (Ryves *et al.*, 2005). In the latter study, however, neither lithium nor VPA changed β-catenin levels, whereas we saw an increase in β-catenin levels in response to LiCl, VPA and TSA, confirming a previous report (Phiel *et al.*, 2001). The lack of effect of VPA on β-catenin in Ryves *et al.* may be due to differences in extraction procedure as they used a detergent-

based extraction buffer that is reported to solubilise membranes as well, therefore masking the drug effect on the cytosolic pool of β-catenin (Ryves *et al.*, 2005). Our data, together with the growth cone results presented above, strongly support the idea that the common effects of mood stabilizers on both sensory and cortical neuron growth cones are mediated by inhibition of PIns signalling rather than by inhibition of GSK3 signalling.

A

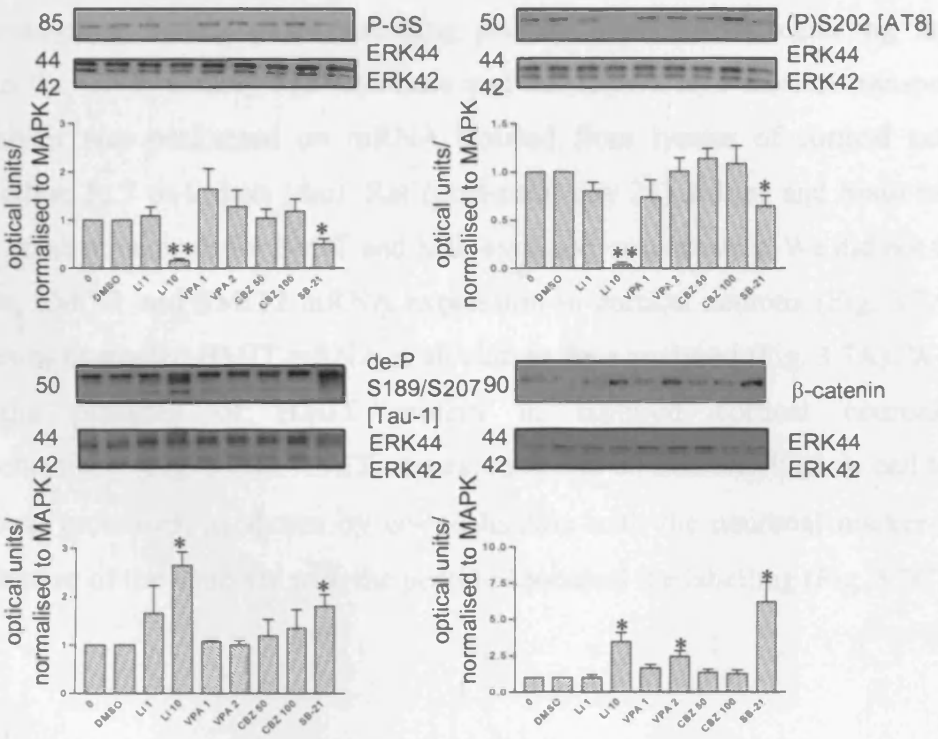

B

	P-GS	AT8	TAU-1	β-catenin
LiCl (10 mM)	↓ 0.15 ± 0.04 (**p < 0.01)	↓ 0.04 ± 0.02 (**p < 0.01)	↑ 2.64 ± 0.29 (**p < 0.01)	↑ 3.47 ± 0.62 (*p < 0.05)
VPA (2 mM)	No Change	No Change	No Change	↑ 2.44 ± 0.41 (*p < 0.05)
CBZ (100 μM)	No Change	No Change	No Change	No Change
SB-216763	↓ 0.50 ± 0.11 (*p < 0.05)	↓ 0.65 ± 0.11 (*p < 0.05)	↑ 1.80 ± 0.25 (*p < 0.05)	↑ 6.25 ± 1.34 (*p < 0.05)

Fig. 3.6 Effect of mood stabilizers on GSK3 downstream targets.
A Lithium inhibits GSK3 activity in cortical neurons. Western blotting analysis of cortical neurons treated with drugs for 6 h. A representative blot is shown.
B Quantitative changes of GSK3 downstream target expression after treatment with mood stabilizers or with the GSK3 inhibitor SB-216763. Data were quantified from at least three independent experiments and normalised to ERK/MAPK for sample loading. Increase in protein expression when compared with control is indicated with ↑ and decrease with ↓. Mean ± sem are shown. Single sample *t* test was used in the analysis and the p value is given when the effect was statistically significant (*p<0.05).

3.2.7 SMIT, MIP-synthase and HMIT expression in cortical neurons

We then investigated several genes encoding proteins involved in regulating inositol availability in the CNS, namely MIP-synthase and the known *myo*-inositol transporters. RT-PCR analysis was performed on mRNA isolated from lysates of cortical neurons cultured for either 5, 7 or 9 days (dic). Rat (post-natal day 21) kidney and brain mRNA were used as positive controls for SMIT and MIP-synthase, respectively. We did not detect MIP-synthase, SMIT1 and SMIT2 mRNA expression in cortical neurons (Fig. 3.7A). In contrast, neurons expressed HMIT mRNA at all culture days analysed (Fig. 3.7A). We also confirmed the presence of HMIT protein in cultured cortical neurons by immunocytochemistry (Fig. 3.7B). HMIT was expressed in all neurons, both in cell bodies and in neuronal processes, as shown by co-localisation with the neuronal marker β-III-tubulin. Incubation of the antibody with the peptide abolished the labelling (Fig. 3.7C).

A

MIP-synthase	SMIT1	SMIT2	HMIT	
-	-	-	+	mRNA measured in cortical neuron lysates

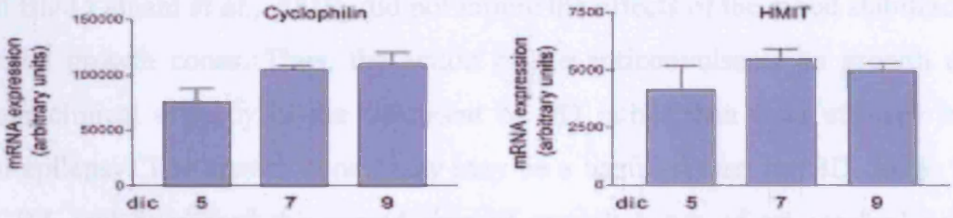

B

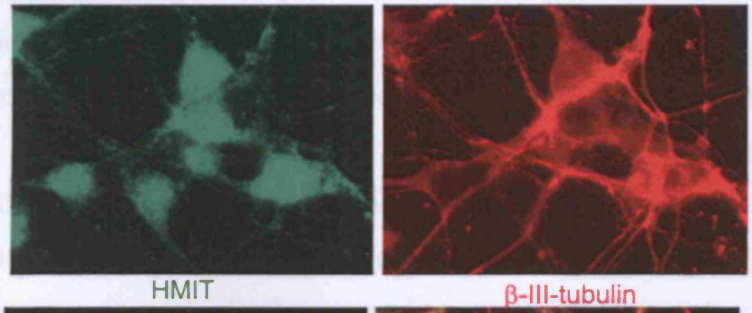

C

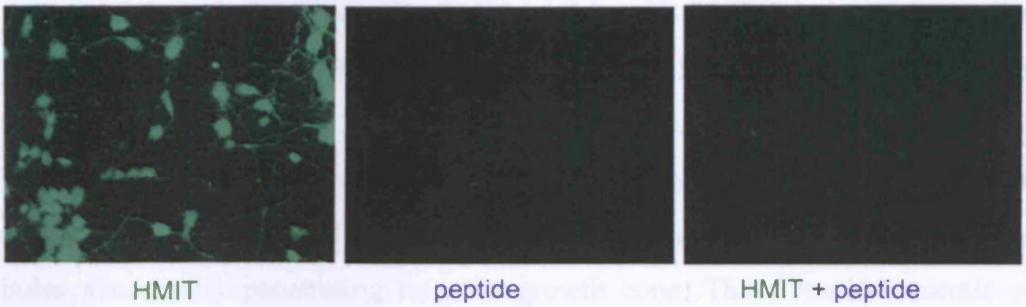

Fig. 3.7 Expression of HMIT, SMIT1, SMIT2 and MIP-synthase in primary neurons.
A Cortical neuron mRNA analysis. Taqman RT-PCR analysis of primary cortical neurons at 5, 7 and 9 days in culture shows expression of HMIT mRNA at all culture times examined. Cyclophilin was used as housekeeper control gene.
B Cortical neurons express HMIT protein. Fluorescent micrographs show HMIT immunolabelling in cell soma and neurites (green). HMIT colocalises with the neuronal marker β-III-tubulin (red). Cell nuclei are labelled with DAPI. Images were acquired with an epifluorescence microscope using a X100 oil objective.
C HMIT peptide competition performed on dic 5 cortical neurons. HMIT antibody was used at 10 μg/ml and peptide used at 100 μg/ml. Images were acquired with a X40 oil objective using the same exposure time.

3.3 Discussion

In this chapter some controversial issues about the growth cone assay were addressed and the role of the PIns signalling pathway in the common action of LiCl, VPA, and CBZ on neurons has been further investigated. GPT and PTN, anticonvulsant drugs not commonly used to treat BD (Yatham *et al.*, 2002), did not mimic the effects of the mood stabilizers on sensory neuron growth cones. Thus, the action of the anticonvulsants on growth cones parallels their clinical efficacy in the treatment of BD rather than their efficacy in the treatment of epilepsy. The growth cone assay may be a useful screen for BD drugs. LiCl, VPA and CBZ each increased the spread area of growth cones of rat cerebral cortical neurons and these effects are inositol-dependent. These are important results as they suggest that signalling pathways present in sensory explants may be common to the CNS and, therefore, effects observed with the drugs in sensory explants may be also extrapolated to CNS neurons. Whilst it is important that the drugs work in a similar fashion on neurons from a brain region known to be involved in mood control, sensory neurons offer several advantages over cortical neurons for assay. In fact, growth cones from DRG explants show directionality, are well-separated and can be easily scored as collapsed or spread, whereas dissociated cortical neurons form an intricate network where it is more difficult to identify the nerve endings. Moreover, DRG growth cones present cycles of complete 'collapse' as they continue to grow, which can be easily scored as a percent of total growth cones. This results in reduced bias in area measurements.

In both sensory and cortical neurons, the GSK3 inhibitor SB-216763 induced a population of very large growth cones (>100 μm^2), some of which had microtubules abnormally penetrating into the growth cone. Addition of inositol did not change the number of large growth cones, nor did inositol reverse the increase in average growth cone area of 20-100 μm^2 induced by the inhibitor. The latter population generally did not contain stable microtubules abnormally penetrating into the growth cone. These results contrast with Hedgepeth *et al.*, who reported that inositol reversed the effect of GSK3 ablation in developing *Xenopus* (Hedgepeth *et al.*, 1997). Since inositol-reversibility was used to argue that the common effect of the mood stabilizers on growth cones was mediated by inhibition of PIns signalling (Williams *et al.*, 2002), the fact that inositol did not reverse the effects of GSK3 inhibition on growth cones adds further support to the previous conclusions by Williams *et al.*

In the sensory neuron study by Williams *et al.* the authors commented that there was a small population (2%) of very large growth cones with penetrating microtubules in the presence of 10 mM, but not 3 mM, lithium, but these did not contribute significantly to the growth cone data presented (Williams *et al.*, 2002). In contrast, Owen & Gordon-Weeks describe many more abnormal growth cones in 10 mM LiCl-treated chicken embryonic day 8-neurons (Owen & Gordon-Weeks, 2003). These chicken embryonic neurons would still be at the stage where axons are using guidance cues such as semaphorin to navigate to their targets, whereas the postnatal rat neurons used would have reached their peripheral targets prior to explanting, so axon growth would be of a regenerative nature where axons use laminin in Schwann cell basement membranes to navigate. Because Sema3A action uses an active pool of GSK3 in the growth cone, a difference in the levels of GSK3 present in embryonic vs postnatal neurons could explain the extent to which lithium produces GSK3-dependent effects on growth cone spreading.

Chicken sensory neurons have larger growth cone areas under control conditions than do postnatal rat neurons (~ 150 vs 100 μm^2). The cerebellar neurons (both mossy and granule) used by Salinas and colleagues to study Wnt (Hall *et al.*, 2000; Hall *et al.*, 2002; Lucas & Salinas, 1997) were also large (~200 μm^2) compared with both the rat sensory and cortical neurons used here. Sensory neurons provide a convenient morphological readout of intracellular signalling events, while growth cone function is probably better studied using neurons with large growth cones that do not collapse spontaneously and where the effects of GSK3 inhibition may be greater.

Interestingly, biochemical analysis of some GSK3 downstream targets has shown that 10 mM LiCl inhibits GSK3 at higher levels compared with the GSK3 inhibitor SB-216763. These findings do not correlate with growth cone morphological observations, as SB-216763 only induced a pronounced increase in the percentage of very large growth cones. Possible reasons for this discrepancy are different effects of lithium and SB-216763 on different targets, which may be localised into different intracellular compartments or expressed at different levels in the cell body and neurites. It would be interesting to perform a lithium concentration-response in primary neurons in order to determine the concentration at which expression levels of GSK3 targets start to change. It has been reported that a low concentration of lithium, which can partially inhibit GSK3, favours the

extension of neurites from developing neurons, whereas a high concentration of the drug impaired neurite growth (Munoz-Montano *et al.*, 1999). Similar effects were observed with the GSK3 inhibitor 6-bromoindirubin-3-acetoxime in DRG and hippocampal neurons. Interestingly, the differential regulation of primed versus all GSK3 substrates is associated with a specific morphological outcome (see CRMP2 versus MAP1B) (Kim *et al.*, 2006). In our study, we have used the antibody clones AT8 and TAU1, which recognise unprimed sites of tau (Cho & Johnson, 2003) and an anti-GS and anti-β-catenin antibodies, which recognise primed substrates. It is, therefore, not unexpected that the effect of GSK3 inhibitors on these substrates may be different.

Lithium inhibition of GSK3 directly led Klein and colleagues to suggest that GSK3 may be the therapeutically-relevant target for lithium in mood stabilization rather than PIns signalling (Klein and Melton, 1996; O'Brien et al., 2004; Phiel and Klein, 2001). Moreover, there is much controversy regarding the question of whether VPA inhibits GSK3, either directly or indirectly. We have shown here that LiCl at non therapeutic concentrations, but not VPA affects phosphorylation of known GSK3 targets in cortical neurons in agreement with others (De Sarno *et al.*, 2002; Jin *et al.*, 2005; Phiel *et al.*, 2001; Williams *et al.*, 2002). In contrast to Williams *et al.* and Ryves *et al.*, both VPA and lithium increased the levels of β-catenin (Ryves *et al.*, 2005; Williams *et al.*, 2002); the VPA effect was mimicked by TSA suggesting that VPA increased β-catenin levels by inhibiting HDAC in cortical neurons, as predicted by earlier work (Phiel *et al.*, 2001). VPA inhibition of HDAC is probably responsible for the teratogenic effects of VPA (Gurvich *et al.*, 2005).

MIP-synthase and the inositol transporters SMIT1 and SMIT2 have been suggested as therapeutically-relevant targets for the mood stabilizers. Given that cortical neurons in culture do not express these proteins, they are not expected to play a part in the inositol-dependent effects of the drugs on cortical neurons. The location of MIP-synthase in brain endothelial cells and the high levels of SMIT1 in the choroid plexus make it likely, however, that both are involved in regulating the level of inositol in the brain, which is ~ 10-fold higher than in blood (Fisher *et al.*, 2002). Cortical neurons express HMIT, but not SMIT1 or SMIT2. HMIT is expressed predominantly in the brain, suggesting that it has a unique role in regulating brain inositol metabolism (Uldry *et al.*, 2001). The cellular

location of HMIT is regulated by neuronal activity, which may link the supply of inositol to activity of the PIns cycle (Uldry *et al.*, 2004). HMIT is present in subsets of neurons in the cerebral cortex, an area implicated in mood control (Uldry *et al.*, 2001; Uldry *et al.*, 2004). Our results show that HMIT is expressed in cultured cortical neurons, whereas SMITs and MIP-synthase are not, suggesting that HMIT plays a crucial role in regulating the supply of inositol for PIns synthesis. It is, however, not clear whether HMIT is expressed at the plasma membrane in neurons either in resting or in activated state.

In summary, the present results confirm and extend previous conclusions that the common effects of the three mood stabilizers on neurons are mediated by inhibition of PIns signalling and that these inositol-reversible effects do not involve GSK3 inhibition. Moreover, the growth cone assay should prove useful for identifying drugs that mimic the common effect of lithium, VPA, and CBZ on inositol-reversible signalling in neurons that is independent of drug effects on GSK3, SMIT or MIP-synthase. Our results also raise intriguing questions about how cortical neurons regulate their levels of intracellular inositol, which is crucial for PIns synthesis and thus PIns signalling pathway function.

CHAPTER 4
PO interaction with GAP43

4.1 Introduction

PO protein comprises a seven-bladed β-propeller domain and a peptidase domain with an α/β hydrolase fold (Fulop *et al.*, 1998). The catalytic domain is split, with the first 72 amino acids in the N-terminus of the protein and the remaining approximately 300 residues at the C-terminus, as shown below highlighted in red (Fig. 4.1). The three amino acids from the catalytic triad are highlighted and underlined in green (Ser554, Asp641 and His680 in the PO human enzyme).

MLSLQYPDVY RDETAVQDYH GHKICDPYAW LEDPDSEQTK AFVEAQNKIT VPFLEQCPIR
GLYKERMTEL YDYPKYSCHF KKGKRYFYFY NTGLQNQRVL YVQDSLEGEA RVFLDPNILS
DDGTVALRGY AFSEDGEYFA YGLSASGSDW VTIKFMKVDG AKELPDVLER VKFSCMAWTH
DGKGMFYNSY PQQDGKSDGT ETSTNLHQKL YYHVLGTDQS EDILCAEFPD EPKWMGGAEL
SDDGRYVLLS IREGCDPVNR LWYCDLQQES SGIAGILKWV KLIDNFEGEY DYVTNEGTVF
TFKTNRQSPN YRVINIDFRD PEESKWKVLV PEHEKDVLEW IACVRSNFLV LCYLHDVKNI
LQLHDLTTGA LLKTFPLDVG SIVGYSGQKK DTEIFYQFTS FLSPGIIYHC DLTKEELEPR
VFREVTVKGI DASDYQTVQI FYPSKDGTKI PMFIVHKKGI KLDGSHPAFL YGYGGFNISI
TPNYSVSRLI FVRHMGGILA VANIRGGGEY GETWHKGGIL ANKQNCFDDF QCAAEYLIKE
GYTSPKRLTI NGGSNGGLLV AACANQRPDL FGCVIAQVGV MDMLKFHKYT IGHAWTTDYG
CSDSKQHFEW LVKYSPLHNV KLPEADDIQY PSMLLLTADH DDRVVPLHSL KFIATLQYIV
GRSRKQSNPL LIHVDTKAGH GAGKPTAKVI EEVSDMFAFI ARCLNVDWIP

Fig. 4.1 Amino acid sequence of human PO enzyme.
The catalytic domain is indicated in red and the β-propeller in blue. PO source: NP 002717.

The PO crystal structure has revealed a cylindrical shape of 60 Å height and 50 Å diameter (Fig. 4.2). The peptidase domain consists of a central eight-stranded β sheet with all strands except the second one aligned in parallel. The β sheet is twisted and it is flanked by two helices on one side and six helices on the other (Goossens *et al.*, 1995). The propeller is based on a seven-fold repeat of four antiparallel β sheets. The sheets are twisted and radially arranged around a central tunnel. There are only hydrophobic interactions between the first and the last blade, instead of a Cys-Cys bond more commonly found in β-propeller structures. One of the catalytic residues, Ser 554, is found at the tip of a very sharp turn, referred to as nucleophile elbow. It was hypothesised that the narrow entrance of the propeller (4 Å) might be enlarged by spatial separation of the unclosed blades 1 and 7. Interestingly, Szeltner *et al.* showed that the propeller domain increases the catalytic capability of the peptidase domain and, in particular, Cys 255 (in the 4th blade of the

propeller domain) seems to contribute to catalysis (Szeltner *et al.*, 2000). It has been proposed that the β-propeller provides a tunnel that allows only small peptides to access the active site, and introduction of a disulphide bond between blades 1 and 7 of the β-propeller results in loss of enzymatic activity (Fulop *et al.*, 1998). More recent studies have shown, however, that the propeller domain is rigid and does not permit the substrate to approach the active site through this domain (Juhasz *et al.*, 2005; Fuxreiter *et al.*, 2005). Instead, a smaller tunnel at the inter-domain region comprising the highly flexible N-terminal segment of the peptidase domain facing the hydrophilic loop from the propeller (AA 192-205) was identified as the only likely pathway for the substrate to access the catalytic site.

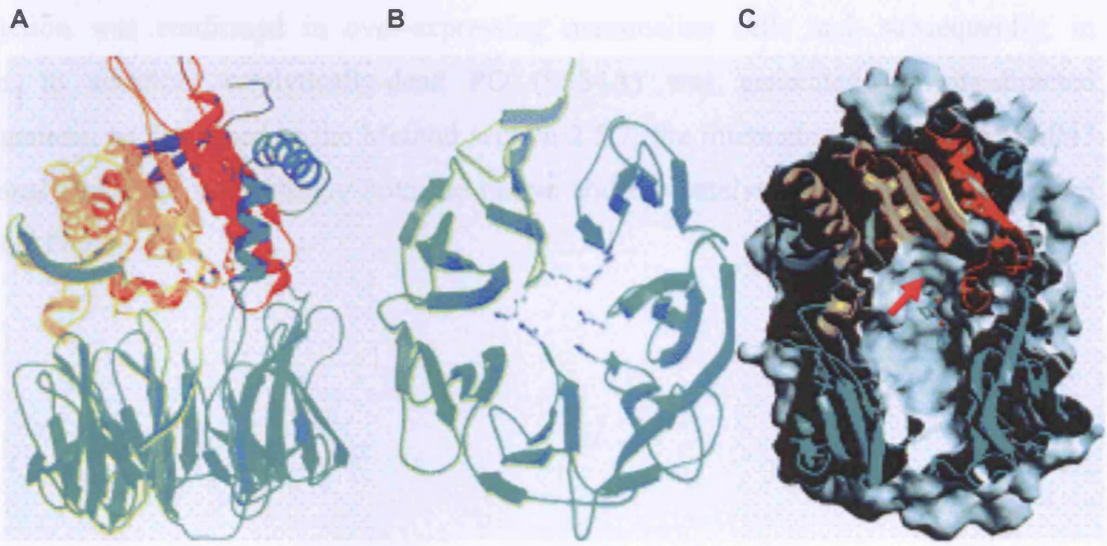

Fig. 4.2 Porcine PO crystal structure.
A Stereorepresentation of PO enzyme with the propeller domain in green/blue and the catalytic domain in red and orange on the top.
B Perpendicular representation of the propeller domain only with the first and seventh blades non-covalently bound.
C Cut-through view of the enzyme as in A, where binding of the inhibitor Z-Gly-Pro-prolinal to the catalytic site can be observed at the top right indicated with a red arrow.
Source: (Fulop *et al.*, 1998).

The PO enzyme is structurally intriguing since each domain appears to modulate the function of the other. Moreover, PO is functionally interesting as it is has been reported to play a role in cognition via its effect on neuropeptide cleavage. However, neuropeptides are secreted molecules and PO does not appear to be secreted, at least in mammals, therefore suggesting that PO may exert other unknown intracellular functions within the cell, and in particular, in neurons. PO has recently been linked to the mechanism of action

of mood-stabilizing drugs via possible modulation of the PIns signalling pathway (Williams *et al.*, 2002). Importantly, amongst mood stabilizers, VPA inhibits recombinant PO directly (Cheng *et al.*, 2005).

The aim of this study was to shed light on the PO intracellular functions by analysing PO protein interactors. PO antibodies were not commercially available at the beginning of this thesis. Antibodies were therefore generated and extensively characterised using biochemical techniques. Moreover, a PO null-mutant mouse was acquired from Deltagen and characterised. A yeast-two-hybrid analysis (Y2H) (performed at GlaxoSmithKline) revealed several potential protein interactors, including GAP43, which is of interest due to its involvement in growth cone plasticity. This hit was chosen for further investigation and interaction was confirmed in over-expressing mammalian cells and, subsequently, in tissue. In addition, catalytically-dead PO (S554A) was generated by site-directed mutagenesis, as described in the Method section 2.5.7; the interaction of PO with GAP43 was analysed, and, interestingly both the native and the catalytically-dead PO interacted with GAP43.

4.2 Results

4.2.1 Characterisation of a PO null-mutant mouse

In order to characterise the PO null-mutant mouse generated by Deltagen, brains were removed and analysed for PO mRNA expression. No PO mRNA was detected by Taqman RT-PCR in PO null-mutant cortices (as well as in other brain areas – data not shown), whereas PO was highly expressed in wild-type samples, with intermediate levels in the heterozygotes (~60% compared with wild-type) (Fig 4.3A). Further confirmation of the PO null-mutant mouse was obtained by analysing LacZ expression in brain lysates. Only PO null-mutant brain extracts showed β-galactosidase expression (band > 100 kDa), confirming insertion of the LacZ cassette in the PO null-mutant mouse (Fig. 4.3B).

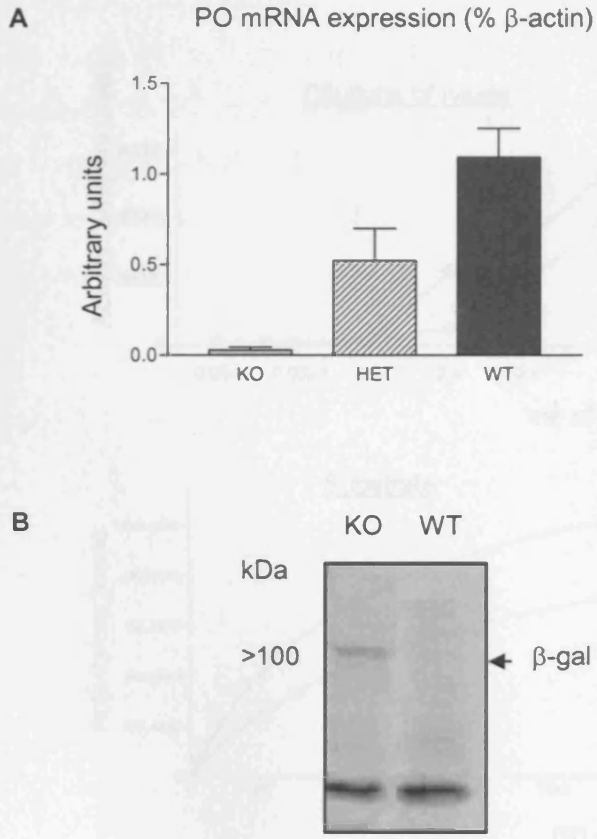

Fig. 4.3 PO mRNA and LacZ expression in the PO null-mutant mouse.
A PO mRNA analysis was performed by TaqMan RT-PCR. No PO mRNA was detected in the cortices from PO null-mutant mice (KO), while intermediate levels were measured in heterozygotes (HET) when compared with wild-type mice (WT) (n = 5 mice, mean ± sem). Data are expressed as a percentage of β-actin.
B PO KO and WT brain extracts were analysed by Western blotting using a polyclonal anti-β-galactosidase antibody (Abcam, 1:5,000, overnight). A band >100 kDa, representing the expression of LacZ, can be observed in the PO KO extract only. The lower molecular weight band represents a cross-reactive protein.

In order to determine PO activity in the PO null-mutant mouse, an enzymatic assay for PO was established (see Materials and Methods section 2.3.2) and optimised in terms of concentration of brain homogenate, substrate, and incubation time (Fig. 4.4).

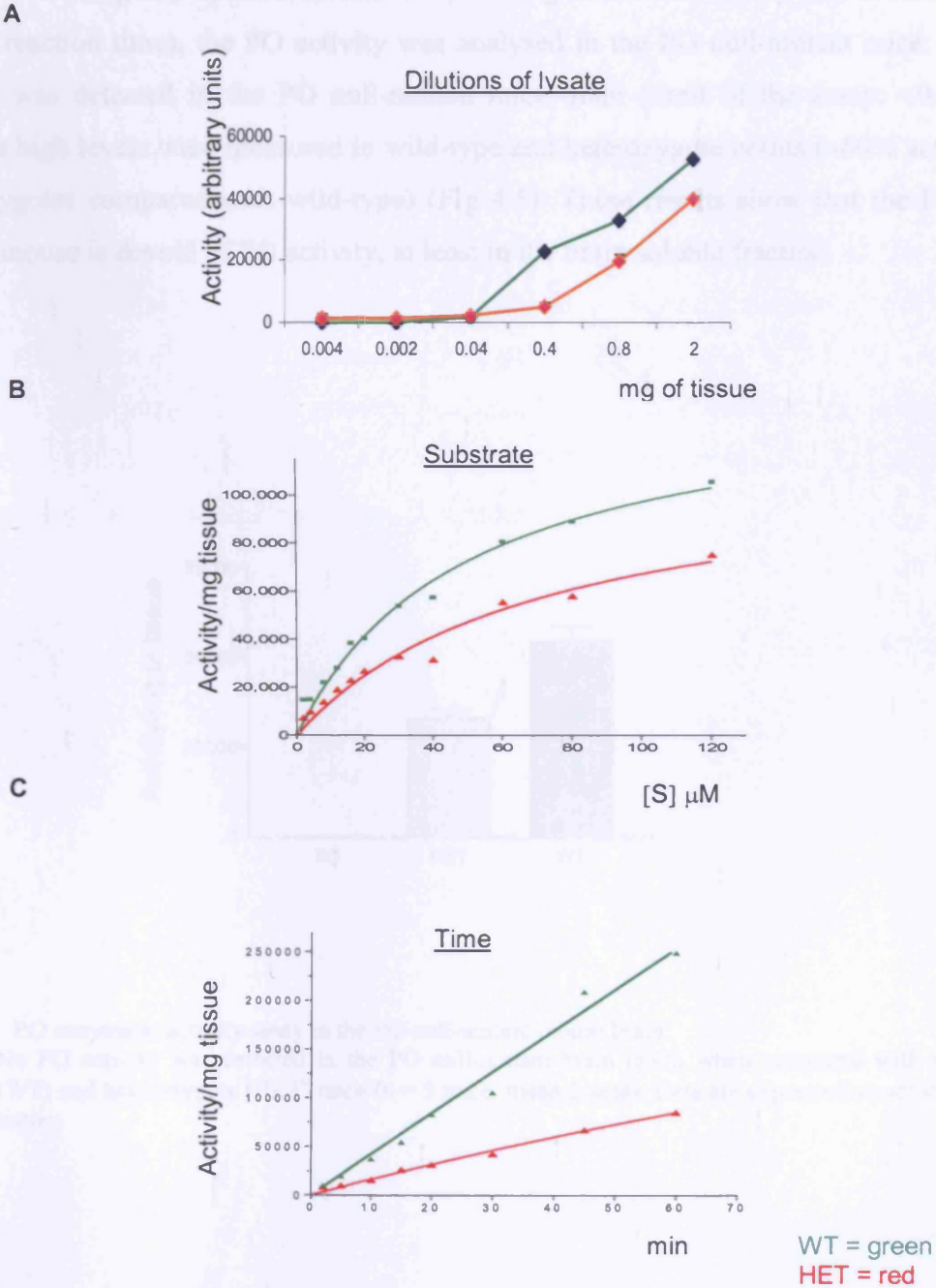

Fig. 4.4 Optimisation of the PO enzyme activity assay.
The PO enzyme activity assay was optimised for mouse brain homogenate by testing different concentrations of **(A)** brain lysate, **(B)** substrate and **(C)** reaction incubation time. Wild-type (WT) and PO heterozygote mice (HET) were analysed.

After establishing the optimal conditions (>0.4 mg brain tissue, ~30 μM substrate, 20-30 min reaction time), the PO activity was analysed in the PO null-mutant mice. No PO activity was detected in the PO null-mutant mice brain (limit of the assay: <0.003%), whereas high levels were measured in wild-type and heterozygote brains (~60% activity in heterozygotes compared with wild-type) (Fig 4.5). These results show that the PO null-mutant mouse is devoid of PO activity, at least in the brain soluble fraction.

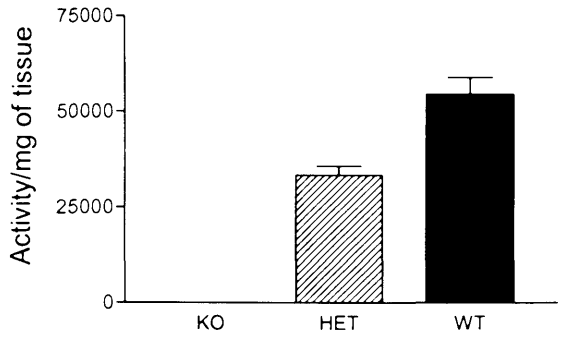

Fig. 4.5 PO enzymatic activity assay in the PO null-mutant mouse brain.
No PO activity was detected in the PO null-mutant brain (KO), when compared with wild-type (WT) and heterozygote (HET) mice (n = 5 mice, mean ± sem). Data are expressed as activity/mg of tissue.

4.2.2 PO expression studies

In order to study the functions and neuronal localisation of PO, it is critical to have selective antibodies. As there were no commercially available antibodies at the start of these studies, we chose peptide sequences specific to PO and antibodies were generated by Cambridge Research Biochemicals and Research Genetics, as described in the Method section 2.4.4. Before proceeding with the validation, I examined a number of cell lines for their endogenous mRNA PO expression by Taqman RT-PCR (Fig. 4.6A). PO expression was also analysed in rat primary neurons (cortical, hippocampal and striatal) cultured for 5, 7, 9, 12, 15, and 20 days (dic) (Fig. 4.6B). PO expression was detected in all cell lines and in primary neurons, independent of time in culture.

A

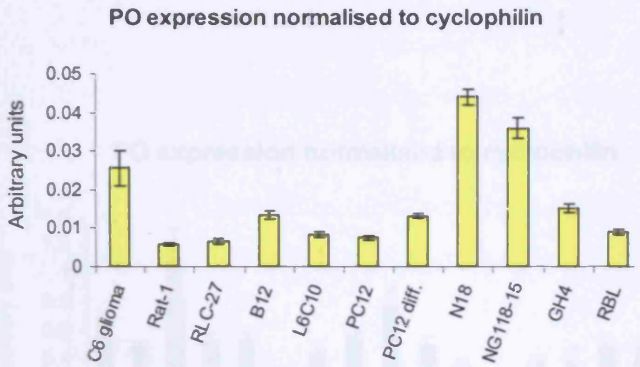

B

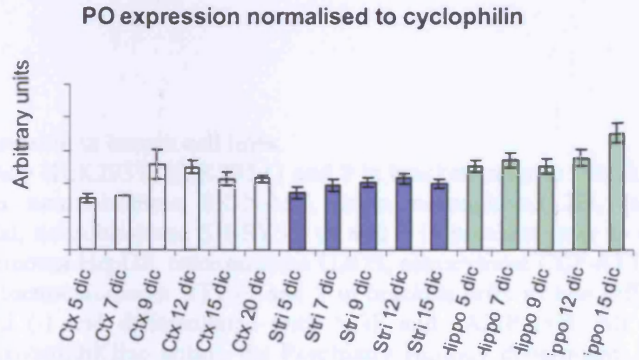

Fig. 4.6 Rat PO mRNA expression.
A PO mRNA expression in rat cell lines. RNA was analysed from glioma C6, fibroblast Rat-1, liver RLC-27, glial B12, skeletal muscle myoblast L6C10, adrenal pheochromocytoma PC12 (undifferentiated and differentiated with NGF), mouse neuroblastoma x rat glioma hybrid N18, mouse neuroblastoma x rat glioma hybrid NG118-15, pituitary tumour GH4, and basophilic leukaemia granulocytes RBL. All these cell lines were cultured at GlaxoSmithKline. PO expression was normalised to cyclophilin.
B PO mRNA expression in primary neurons. Cells were lysed at the times indicated. RNA was extracted and PO mRNA levels measured by Taqman RT-PCR.
Mean ± sem are from three + RT reactions (both A and B).

A number of human cell lines were also examined, all of which expressed PO (Fig. 4.7).

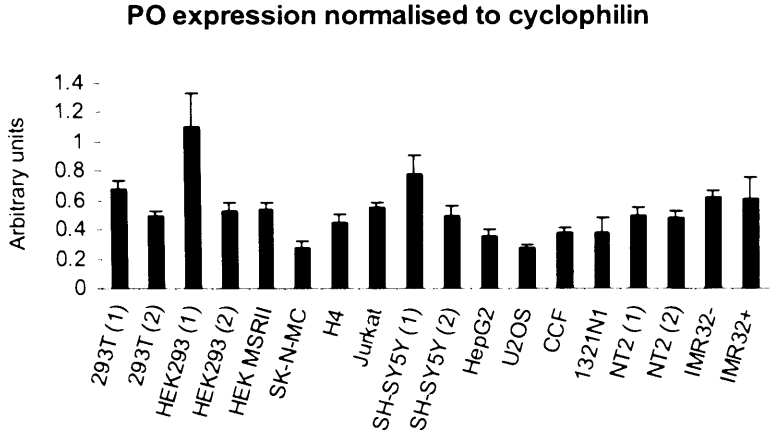

Fig. 4.7 PO mRNA expression in human cell lines.
Embryonic kidney HEK293T, HEK293 (1 and 2 in brackets refer to two different sources), HEK-MSRII, human neuroblastoma SK-N-MC, brain neuroglioma H4, peripheral blood-T-cell leukaemia Jurkat, neuroblastoma SH-SY5Y (1 and 2 in brackets refer to two different sources), hepatocyte carcinoma HepG2, osteosarcoma U2OS, astrocytoma CCF-STTG1, brain astrocytoma 1321N1, brain teratocarcinoma NT2 (1 and 2 in brackets refer to two different sources), IMR32 (undifferentiated (-) and differentiated with NGF and cAMP (+)). All these cell types were cultured at GlaxoSmithKline within the Psychiatry Biology department. Mean ± sem are from three + RT reactions.

In order to further analyse PO expression in the brain, different brain regions (hippocampus, cortex, hypothalamus, cerebellum, hindbrain and midbrain) were dissected from rats at different ages and analysed for PO mRNA expression. Values were normalised to the housekeeper gene cyclophilin (Fig. 4.8). PO was found to be expressed in all brain regions examined and the expression generally decreased with age from postnatal day 1 to 90 in all brain areas analysed. Subsequently, expression of the PO interactor GAP43 was analysed in the same samples. A very similar expression profile was observed for GAP43, which seemed to decrease with the age of the rats (Fig. 4.8B) in accordance with literature data (Neve *et al.*, 1987). Brain dissection and plate generation were performed at GlaxoSmithKline within the Psychiatry Biology Department.

A

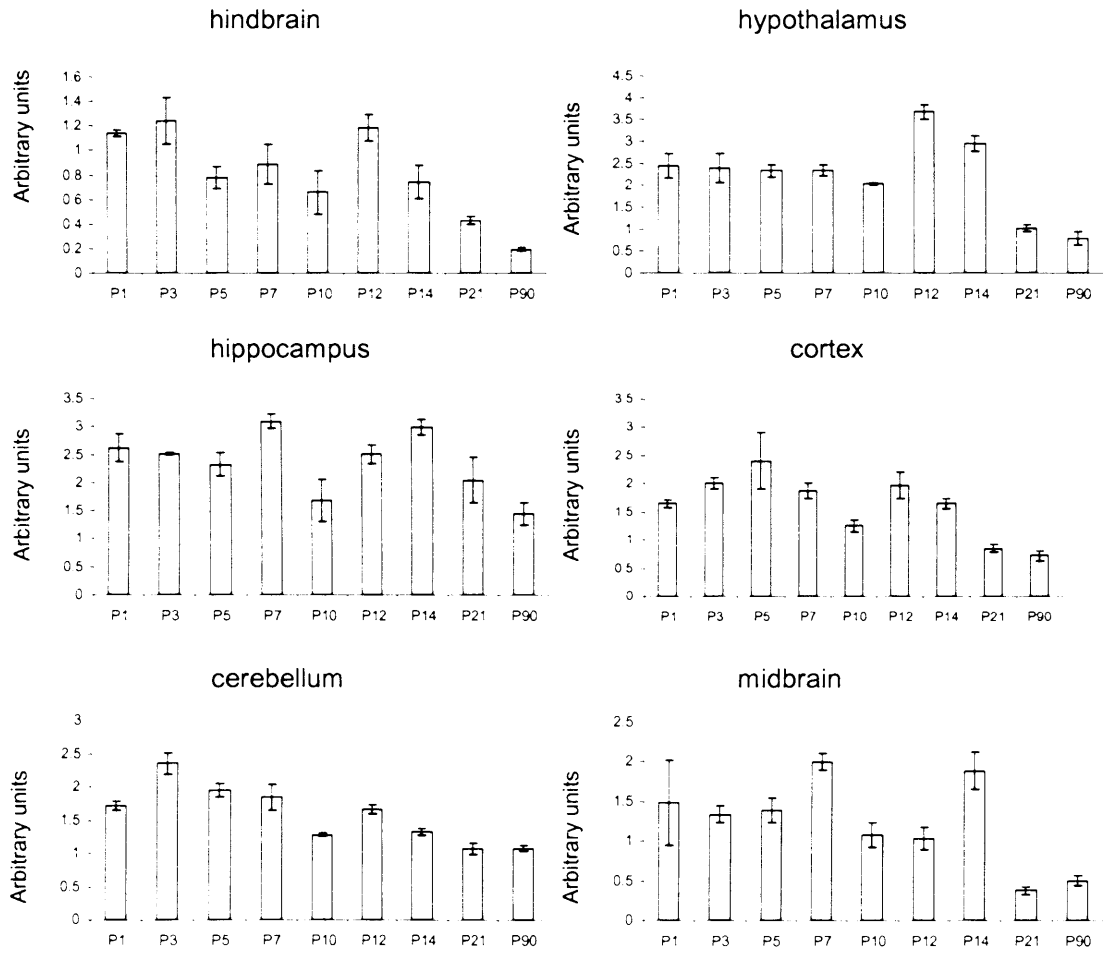
hindbrain
hypothalamus
hippocampus
cortex
cerebellum
midbrain
Arbitrary units
P1
P3
P5
P7
P10
P12
P14
P21
P90

B

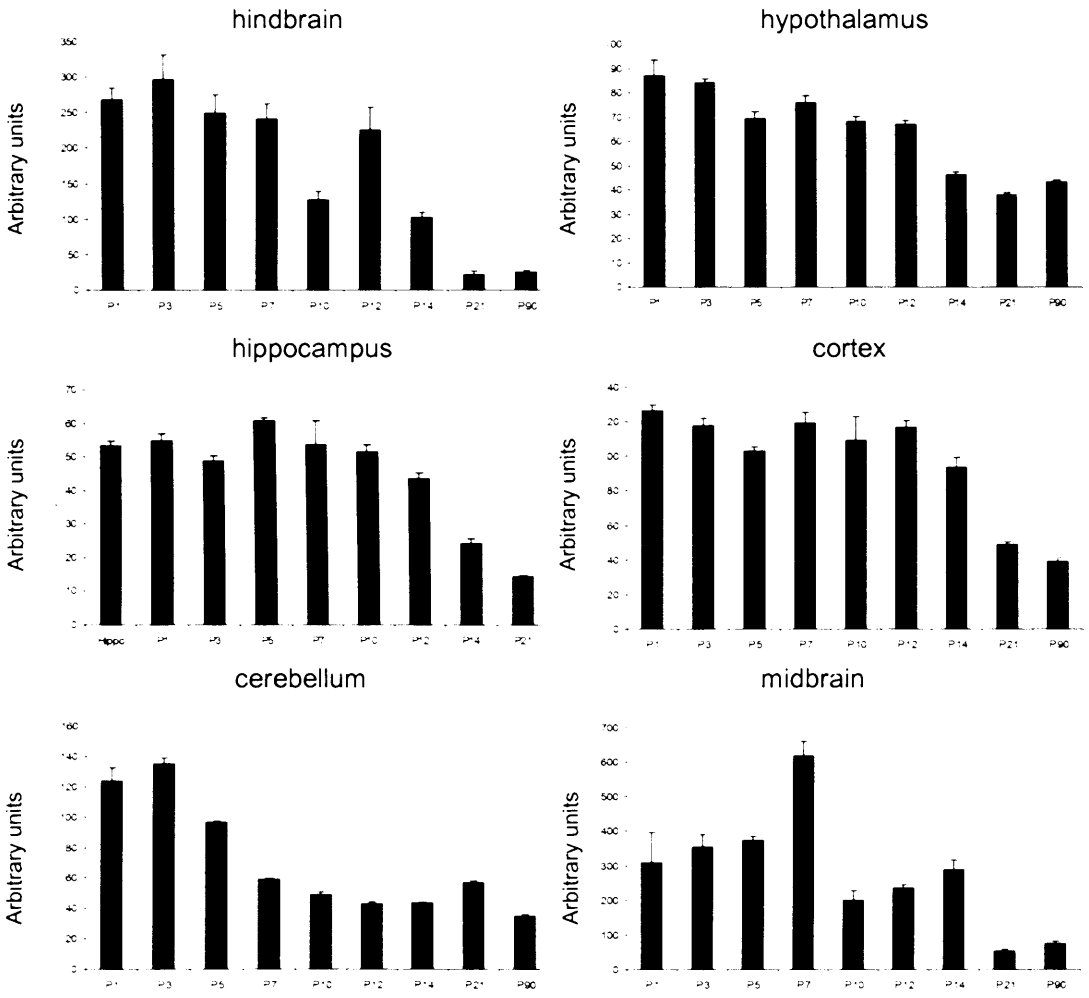

Fig. 4.8 PO and GAP43 mRNA expression during rat brain development.
A PO Taqman RT-PCR expression.
B GAP43 Taqman RT-PCR expression.
The following regions were dissected from postnatal day (P) rats (1-3-5-7-10-12-14-21-90): cortex, midbrain, hippocampus, hypothalamus, cerebellum and hindbrain. Brain regions from several animals were pooled in order to extract RNA. Data are mean ± sem of three + RT reactions (from the same sample) and are expressed as arbitrary units normalised to cyclophilin.

The very similar expression profile observed for PO and GAP43 during rat brain development suggests that these proteins may interact and exert similar functions in the brain. In this respect, GAP43 has been linked with neurite outgrowth and axonal remodelling, processes that occur in embryonic and early life and to a lesser extent in the adult brain.

4.2.3 Generation of V5-His-tagged PO cDNA

A useful method to validate antibodies is to use over-expressing cells. Rat PO was cloned at GlaxoSmithKline into pcDNA3.1D/V5-His-TOPO, without removing the stop codon. In order to obtain a V5-His-tagged enzyme, PO was sub-cloned into the expression vector pcDNA4/V5-His, in frame with the V5-His tags, as described in the Materials and Methods section 2.5.6.

4.2.4 PO antibody characterisation in HEK cells over-expressing PO

HEK cells (293T or MSRII depending on availability) were chosen for transfection studies. Cells were transfected with pcDNA4/V5-His-ratPO and then analysed two days later by Western blotting, immunoprecipitation and immunocytochemistry. A total of eight antibodies were initially tested in over-expression studies. Subsequently, we proceeded with the validation of antibody #1216 only, as this appeared to be the most specific antibody. I am, therefore, showing data for antibody #1216 only, as this has been extensively used in subsequent studies. A band of ~75 kDa was observed by Western blotting in untransfected HEK cells and the signal strongly increased in over-expressing cells (Fig. 4.9). An additional band of ~35 kDa was also observed in both samples.

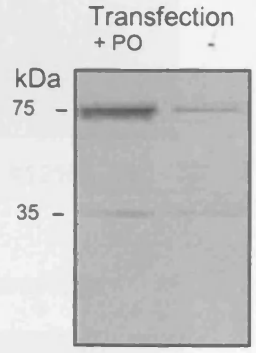

Fig. 4.9 Western blotting of PO over-expressing HEK cell lysates as well as of untransfected HEK. Anti-PO antibody #1216 (1:1,000, overnight) was used.

PO was immunoprecipitated from HEK-MSRII cell lysates using anti-PO or anti-V5 antibodies and Western blotting performed with the reciprocal antibody (Fig. 4.10). Antibody #1216 detected PO using immunoprecipitation, as well as Western blotting, and a band of ~ 75 kDa was observed (Fig. 4.10 A and B).

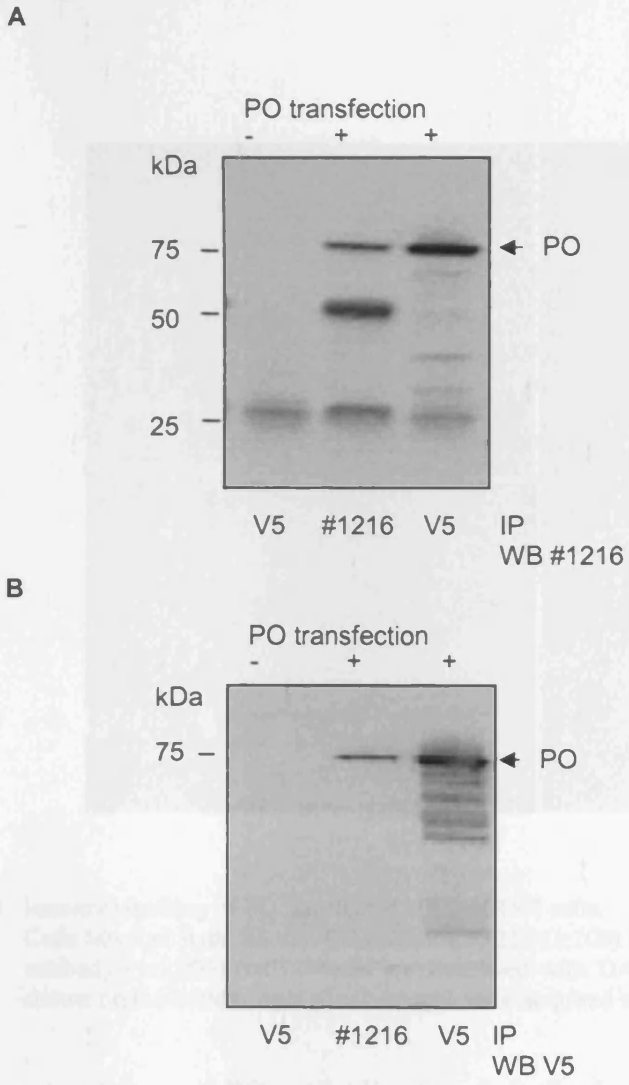

Fig. 4.10 Immunoprecipitation in PO over-expressing HEK-MSRII cells.
Immunoprecipitation was performed using the anti-PO #1216 or anti-V5 antibodies, as indicated, and Western blotting subsequently performed **(A)** with the anti-PO #1216 antibody (1:1,000 overnight) or **(B)** with an anti-V5 antibody (1:5,000 overnight), respectively. PO transfection is indicated by + and no transfection by -. The 25 and 50 kDa bands represent the light and heavy antibody chains, respectively, normally observed in immunoprecipitation experiments.

Immunocytochemistry was also performed on PO-transfected HEK cells. Fixed cells were incubated with the anti-PO polyclonal antibody #1216 together with an anti-V5 monoclonal antibody in order to confirm detection of PO. Several dilutions of the PO antibody were used (from 1:100 to 1:1,000). Fig. 4.11 shows that transfected cells, labelled with the anti-V5 antibody, are also labelled with the anti-PO antibody #1216, therefore showing that the anti-PO antibody is specific for this protein at the level of protein expression and antibody dilution analysed.

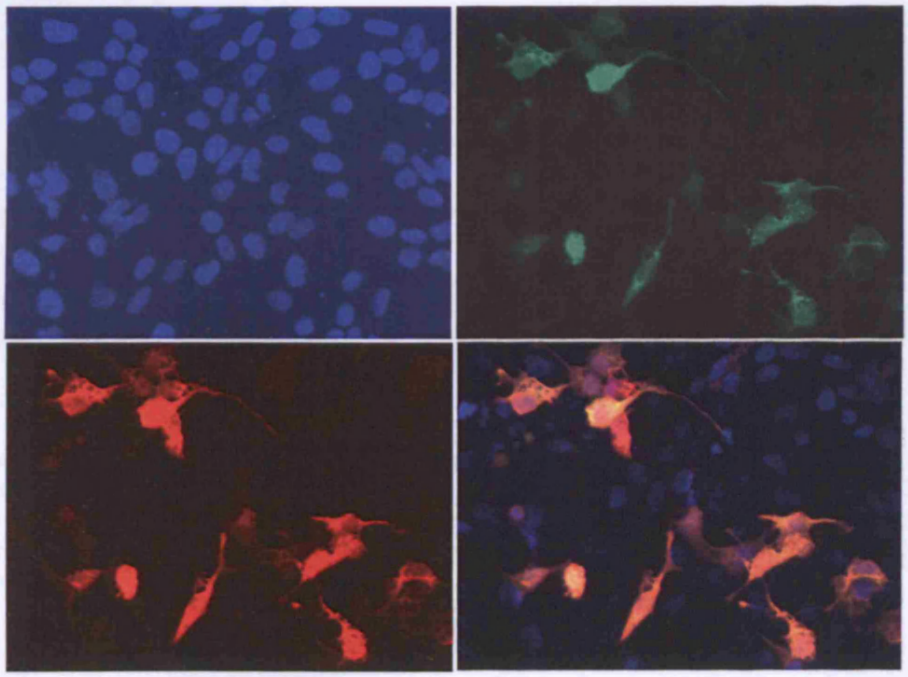

Fig. 4.11 Immunolabelling of PO transfected HEK-MRSII cells.
Cells labelled with the anti-PO antibody #1216 (1:100) (green) are also labelled with the anti-V5 antibody (1:5,000) (red). Nuclei are visualised with DAPI (blue). A merged microphotograph is shown on the bottom right panel. Images were acquired with a X 40 objective.

In summary, of the anti-PO antibodies tested, antibody #1216 was shown to recognise PO in over-expressing cells by Western blotting, immunoprecipitation and immunocytochemistry. Therefore, only this antibody was characterised further in neural tissue.

4.2.5 PO antibody characterisation in tissue

The antibody #1216 was tested in brain tissue by Western blotting. Cerebella and cortices from wild-type and PO null-mutant mice were analysed for PO expression. Antibody #1216 detected PO protein at ~ 75 kDa, as well as lower MW bands at ~65, ~35 and ~25 kDa. The latter were evident also in the PO null-mutant samples, whereas the 75 kDa band was not as it represented PO. When the peptide chosen for the immunisation was pre-incubated with the antibody, none of the bands were visible (Fig. 4.12).

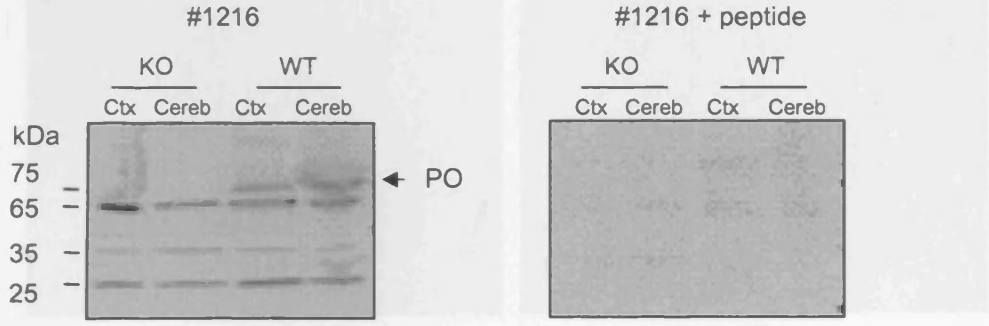

Fig. 4.12 Western blotting on PO null-mutant and wild-type brain lysates.
Western blotting was performed with antibody #1216 (1:1,000, overnight) on PO null-mutant (KO) or wild-type (WT) cortex (Ctx) and cerebellum (Cereb) lysates. The PO band is ~ 75 kDa. The panel on the right is a parallel blot where antibody #1216 was pre-incubated with the peptide and subsequently applied to the blot.

These results show that antibody #1216 recognises PO in the mouse brain and can be used by Western blotting. Other cross-reactive bands of smaller molecular weight were also observed both in PO null-mutant and wild-type samples suggesting that they are specific to the epitope used in the immunisation, but not specific to PO.

In order to understand better the PO intracellular localisation, it is critical to have an antibody that detects the protein in neurons and/or in brain slices. Antibody #1216 was therefore tested by immunocytochemistry on primary cortical neurons dissociated from E15 wild-type or PO null-mutant mice (Fig. 4.13). Neuronal cell bodies and processes were labelled with the antibody. There was, however, a strong signal in wild-type as well as in the PO null-mutant neurons. These findings were not unexpected, as several cross-reactive bands were previously observed by Western blotting.

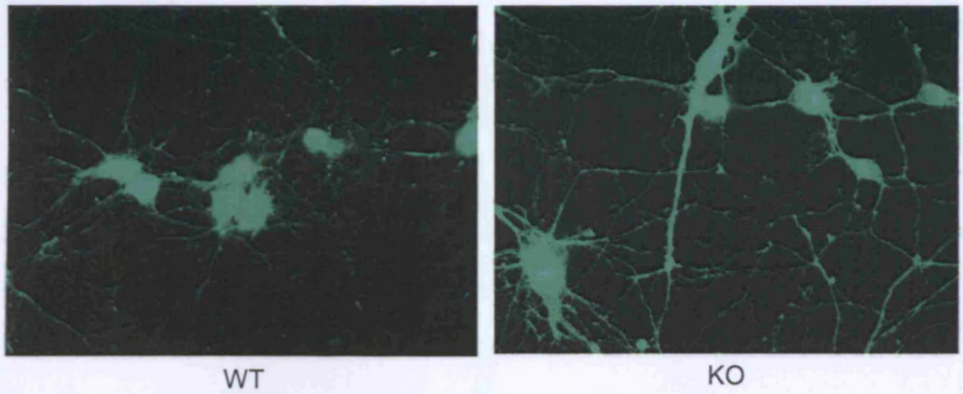

Fig. 4.13 Immunocytochemistry of wild-type and PO null-mutant cortical neurons.
PO labelling of processes and cell bodies showed similar intensities in WT and PO KO cultures. Images were acquired with a X 40 objective.

Similar results were also obtained when antibody #1216 was tested by immunohistochemistry on brain slices from wild-type and PO null-mutant (data not shown). In brain slices the PO immunoreactivity was widespread amongst brain areas and similar between the wild-type and PO null-mutant mouse. No decrease in labelling intensity was observed in the null-mutant brain, therefore indicating that the labelling is not specific for PO protein. For these reasons a detailed analysis of PO protein expression in the brain and at the subcellular level has not been performed in the course of my studies. Only very recently, protein expression data have been presented by Schulz *et al.* (Schulz *et al.*, 2005). During the course of my thesis, I have analysed a total of eight antibodies (3 peptides and the whole protein were injected into two rabbits each) and only two antibodies (#1216 and the whole protein – data not shown for the latter) specifically recognised PO protein. The reasons for this low success rate are at present unclear but are unexpected for a cytosolic protein such as PO.

In summary, these results indicate that antibody #1216 cannot be used for immunocytochemistry or immunohistochemistry to detect endogenous PO. The antibody #1216 can, however, be used for Western blotting and immunoprecipitation because with the latter techniques the 75 kDa PO protein band can be clearly identified, as crucially this band is missing from the PO null-mutant samples. Overall, antibody #1216 can be used for the purpose of our study, which focuses on the confirmation of the interaction, identified in an Y2H study, between PO and GAP43.

4.2.6 PO and GAP43 interaction

Y2H involves expression of a sequence of interest fused to the DNA binding domain of the transcription factor GAL4 (the bait = PO), and a library of target proteins fused to the GAL4 transcription activation domain (the prey). Association of the bait with the prey protein reconstitutes a functional transcription factor and this is detected by the expression of a reporter gene controlled by a promoter bearing the cognate DNA binding domain site, as schematically illustrated in Fig. 4.14. The most common detection system exploits the use of X-GAL (5-bromo-4-chloro-3-indolyl-β-D-galactopyranoside), which is hydrolysed by β-galactosidase, forming an intense blue precipitate.

In order to identify PO protein interactors, Y2H was performed (Helen Sanderson and Julia White at GlaxoSmithKline) using two baits: the rat full-length PO and the β-propeller domain only (73-437 AA) and human adult and foetal brain and rat brain libraries. A total of 135 interactors were revealed when the PO full-length bait was used (27 in human foetal brain, 39 in human adult brain, 69 in rat brain libraries), whereas 177 interactors were identified in the β-propeller screen (72 in human adult brain and 105 in human foetal brain libraries). Of these interactors, 16 confirmed in a 1:1 interaction assay in yeasts. Interestingly, when the propeller domain was used as a bait, stronger and a greater number of interactors were observed when compared with the full-length enzyme screening. This suggests that the catalytic domain may destabilise the protein. In fact, it was recently reported that the propeller domain could exist as a separate protein and it is stable in solution, in contrast to the catalytic domain, which has not been isolated as a separate protein (Juhasz *et al.*, 2005). Of the hits, we have selected GAP43 as the most interesting one in terms of biological functions and relevance to our study. In this respect, GAP43 is a cytosolic neuronal protein involved in growth cone morphology, axonal growth and synaptic plasticity and its putative interaction with PO appeared to be quite intriguing. The interaction between full-length PO and GAP43 was reported using a human adult brain library. Other interesting hits identified were α-synuclein, succinate dehydrogenase and cadherin 10 precursor, amongst others.

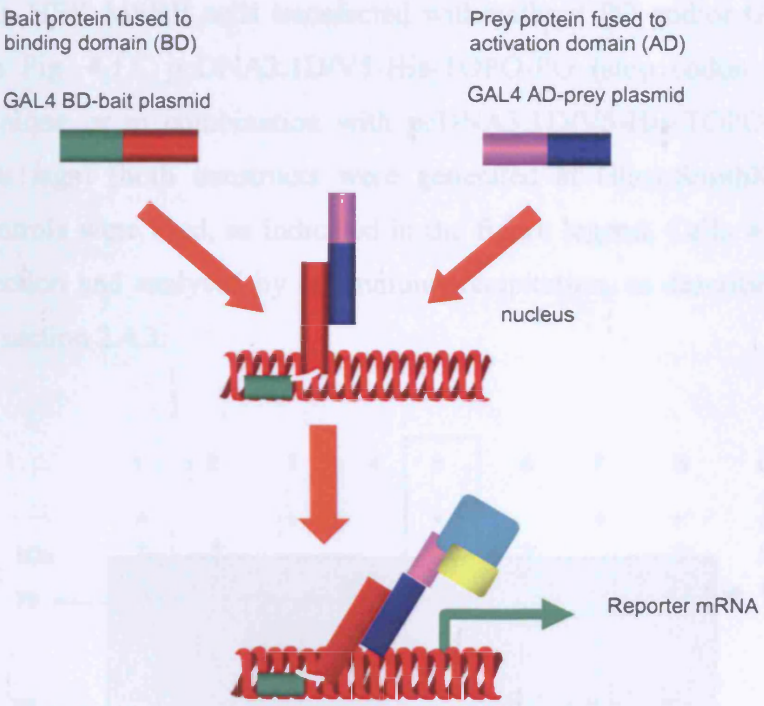

Fig. 4.14 Y2H schematic. Source: GlaxoSmithKline Y2H website.
The schematic shows the two plasmids used (GAL4 DNA-binding domain bait and the GAL4 activation domain prey). When co-expressed, they induce the formation of a functional transcription factor, which induces expression of the reporter β-galactosidase gene. Blue colonies are identified.

4.2.6.1 PO-GAP43 interaction in over-expressing cells: co-immunoprecipitation

In order to confirm the interaction in mammalian cells, co-immunoprecipitation was performed in HEK-MSRII cells transfected with/without PO and/or GAP43 plasmids, as indicated in Fig. 4.15. pcDNA3.1D/V5-His-TOPO-PO (stop codon not removed) was transfected alone or in combination with pcDNA3.1D/V5-His-TOPO-GAP43 (in frame with V5-His tags) (both constructs were generated at GlaxoSmithKline). Appropriate negative controls were used, as indicated in the figure legend. Cells were lysed two days after transfection and analysed by co-immunoprecipitation, as described in Materials and Methods in section 2.4.3.

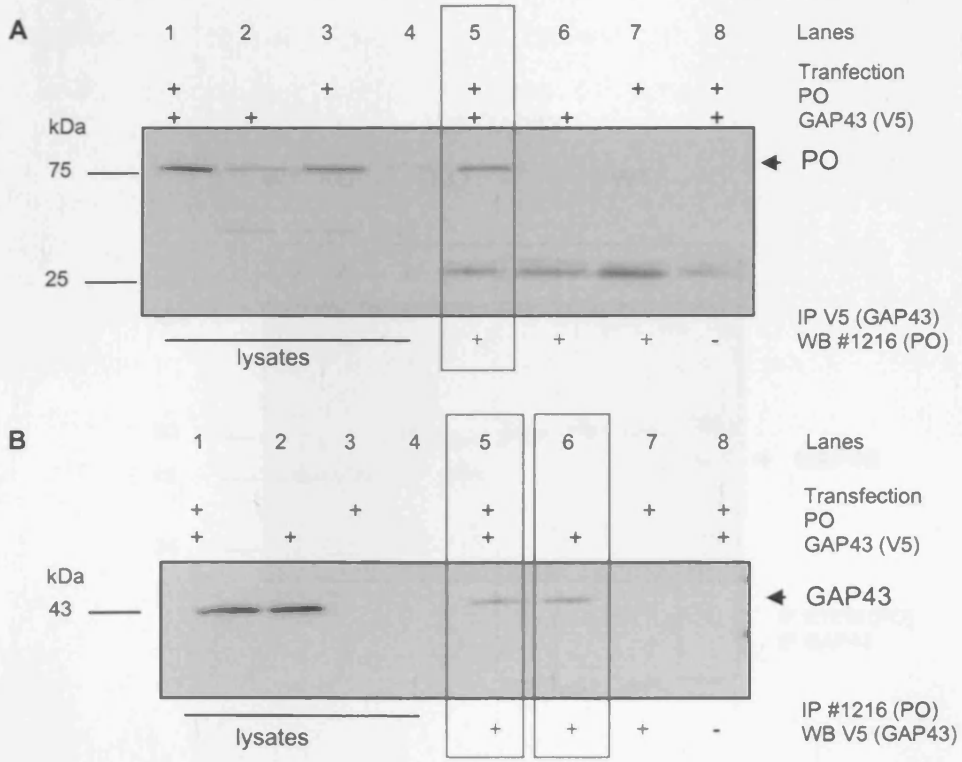

Fig. 4.15 PO and GAP43 co-immunoprecipitation in HEK-MSRII over-expressing cells.
A Immunoprecipitation (IP) was performed with the anti-V5 antibody (3 µl) (detects GAP43) and WB with the anti-PO antibody #1216 (1:1,000). PO is ~ 75 kDa. Lane 8 shows IP performed using an unrelated anti-mouse antibody in PO- and GAP43-transfected cells. Lane 5 shows that PO and GAP43 interact. No band at 75 kDa is observed in lanes 6 and 7 (negative controls). Cell lysates were also loaded on the gel. The 25 kDa band represents the antibody light chains.
B IP was performed with the anti-PO antibody #1216 (5 µl) and WB with the anti-V5 (1:5,000). GAP43 is ~43 kDa band. Lane 8 shows IP performed using an unrelated anti-rabbit antibody in PO- and GAP43-transfected cells. Lane 5 shows that PO and GAP43 interact. The band observed in lane 6 shows interaction between endogenous PO and transfected GAP43. No band is observed in lane 7 (negative control). The experiment was repeated at least three times. Representative blots are shown.

4.2.6.2 PO-GAP43 interaction in tissue: co-immunoprecipitation

In order to confirm that the above interaction occurs in neuronal tissue, wild-type and PO null-mutant brains (male, ~1 month old) were dissected and snap-frozen. Brain lysates were obtained following the same procedure used for cell lysates and co-immunoprecipitation performed using the anti-PO #1216 or the anti-GAP43 antibodies. Negative controls used were the PO null-mutant mouse lysates and immunoprecipitation with an unrelated anti-rabbit antibody (Fig. 4.16). Lane 8 shows that PO and GAP43 interact in endogenous tissue, whereas no interaction was observed in the PO null-mutant mouse (highlighted with a red box, lane 5), as expected due to the lack of PO.

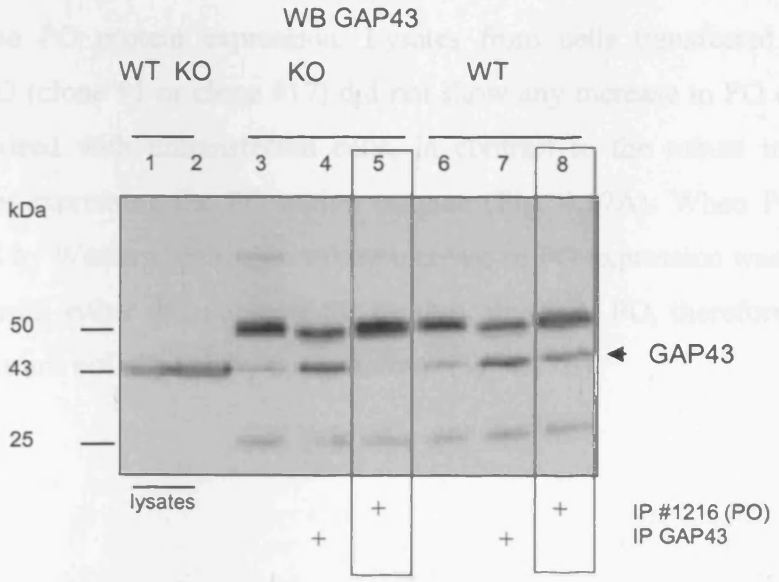

Fig. 4.16 PO and GAP43 co-immunoprecipitation in mouse brain.
IP was performed with the anti-PO antibody #1216 (5 µl) or GAP43 (3 µl) and Western blotting with an anti-GAP43 antibody (1:5,000). GAP43 is the 43 kDa band. Lanes 3 and 6 show IP with an unrelated anti-rabbit antibody in the PO null-mutant (KO) or wild-type (WT) brain, respectively. Brain lysates were also loaded on the gel (lanes 1 and 2). The band at ~25 kDa represents the antibody light chains.

4.2.6.3 Catalytically-dead PO-GAP43 interaction in over-expressing cells: co-immunoprecipitation

The literature suggests that the two domains (catalytic and β-propeller) of the PO protein modulate each other's functions and PO activity can be altered by the propeller domain (Szeltner *et al.*, 2000). We, therefore, asked if the PO enzymatic activity affects the PO interaction with its binding partner GAP43. A catalytically-dead PO was generated by site-directed mutagenesis, as described in the Materials and Methods section 2.5.7. Cells were transfected in parallel with either native PO or with the catalytically-dead PO plasmids (both in pcDNA3.1D/V5-His-TOPO, untagged as stop codon not removed) and lysed two days after transfection. Cell lysate from 1x10 cm dish was split into two tubes. In one tube, the lysate was sonicated and analysed for PO enzymatic activity, whereas the other sample was used to analyse PO protein expression. Lysates from cells transfected with the catalytically-dead PO (clone #1 or clone #17) did not show any increase in PO enzymatic activity when compared with untransfected cells, in contrast to the robust increase in activity in cells over-expressing the PO native enzyme (Fig. 4.17A). When PO protein levels were analysed by Western blotting, a strong increase in PO expression was observed in cells transfected with either the native or the catalytically-dead PO, therefore showing that PO protein levels are not affected by the mutation (Fig. 4.17B).

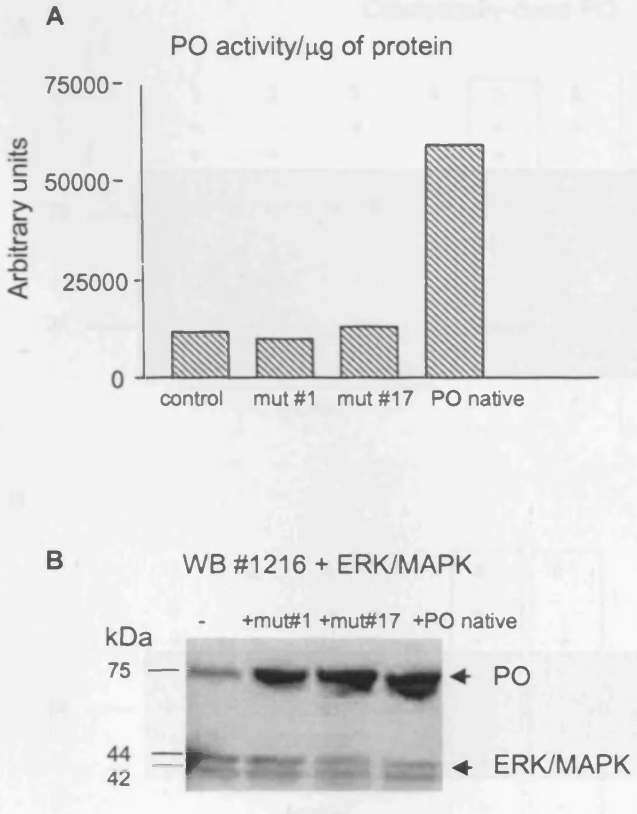

Fig. 4.17 Validation of catalytically-dead PO.
A CHO_K1 cells were transfected using Fugene with pcDNA3.1D/V5-His-TOPO-PO native or catalytically-dead (S554A) plasmids and lysed two days later. PO activity was measured and expressed per μg of protein. The experiment was repeated with similar results (n = 2 experiments, n = 2 reactions/experiment).
B Lysates from PO transfected cells were analysed by Western blotting with the anti-PO antibody #1216 (1:1,000) and ERK/MAPK (loading control) (1:10,000). Lane 1: untransfected CHO_K1; lane 2: cells transfected with catalytically-dead PO clone #1; lane 3: cells transfected with catalytically-dead PO clone #17; lane 4: cells transfected with native PO plasmid.

In order to determine if the PO enzymatic activity affects the interaction between PO and GAP43, the catalytically-dead PO (S554A) was transfected into HEK-MSRII cells and co-immunoprecipitation performed, as previously described (Fig. 4.18).

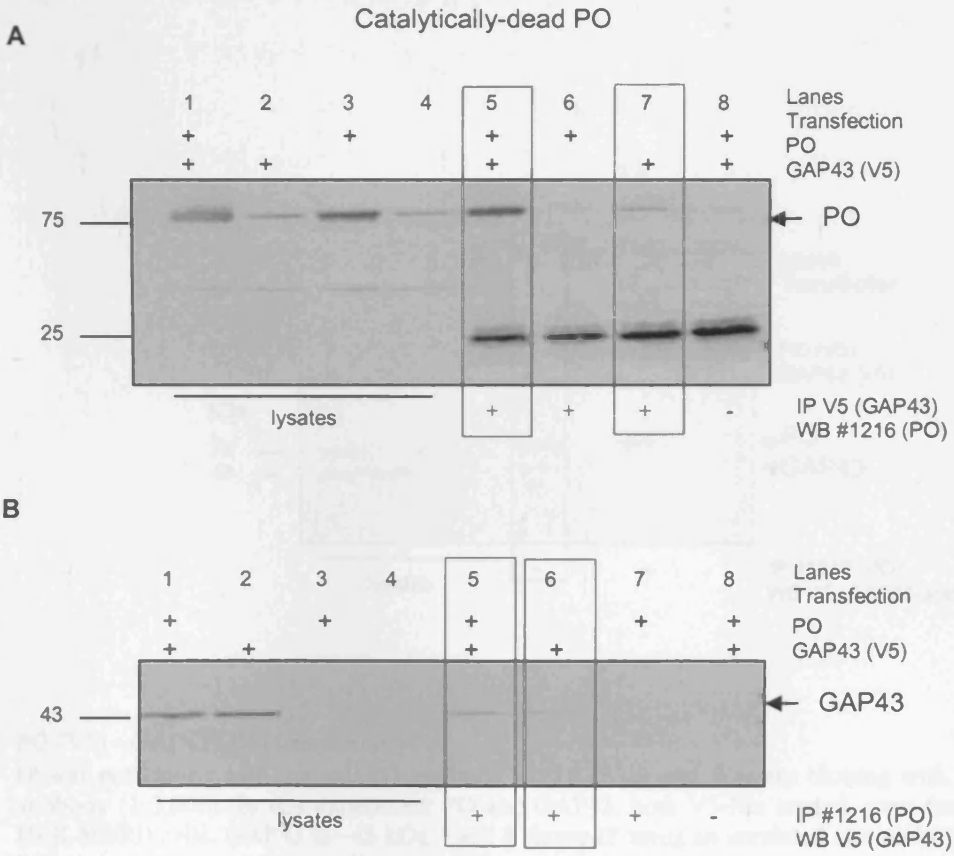

Fig. 4.18 Catalytically-dead PO and GAP43 co-immunoprecipitate in HEK-MSRII over-expressing cells.
A IP was performed with the anti-V5 antibody (3 µl) (recognises GAP43) and Western blotting with the anti-PO antibody #1216 (1:1,000). PO is the ~ 75 kDa band. Lane 8 shows IP performed using an unrelated anti-mouse antibody in PO and GAP43 transfected cells. Lane 5 shows that PO and GAP43 interact. Lane 7 shows interaction between endogenous PO and transfected GAP43. Cell lysates were also loaded on the gel (lanes 1, 2, 3, 4). The 25 kDa band represents the antibody light chain.
B IP was performed with the anti-PO antibody #1216 (5 µl) and Western blotting with the anti-V5 (1:5,000). GAP43 is ~ 43 kDa band. Lane 8 shows IP using an unrelated anti-rabbit antibody in PO and GAP43 transfected cells. Lane 5 shows that PO and GAP43 interact. The band observed in lane 6 shows interaction between endogenous PO and transfected GAP43. No band is observed in lane 7 (negative control).

These results show that catalytically-dead PO also interacts with GAP43, therefore indicating that lack of enzymatic activity is not sufficient to disrupt the interaction with GAP43 and that the enzyme is probably folded correctly.

Furthermore, in order to determine if the small V5-His tags, which may affect PO enzymatic activity, have a detrimental effect on PO interaction with GAP43, co-immunoprecipitation was performed in cells transfected with PO and GAP43 plasmids, both in frame with the V5-His tags. Results shown below indicate that the V5-His tags do not affect the PO-GAP43 interaction (Fig. 4.19).

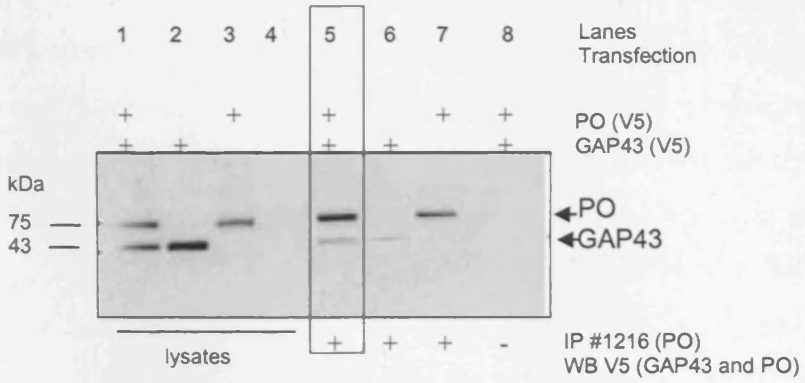

Fig. 4.19 PO (V5) - GAP43 (V5) interaction.
IP was performed with the anti-PO antibody #1216 (5 µl) and Western blotting with an anti-V5 antibody (1:5,000). In this experiment PO and GAP43, both V5-His tagged, were transfected in HEK-MSRII cells. GAP43 is ~43 kDa. Lane 8 shows IP using an unrelated anti-rabbit antibody in PO- and GAP43-transfected cells. Lane 5 shows that PO and GAP43 interact, but in this case two bands are observed. The faint band in lane 6 shows interaction between endogenous PO and transfected GAP43. Cell lysates were loaded on the same gel (lanes 1, 2, 3, 4).

In summary, we have shown that the interaction observed in Y2H between PO and GAP43 also occurs in mammalian cells. Firstly, the interaction was confirmed using an over-expression strategy and, subsequently, in mouse brain tissue. The validation in brain tissue is important as it confirms the interaction at native levels of cellular expression. Appropriate controls were used in the experiments as described in detail, which include immunoprecipitation using unrelated primary antibodies and the use of the PO null-mutant mouse. Interestingly, we have shown that mutation of one of the catalytic residues, which abolishes the PO enzymatic activity, does not affect the interaction with the binding partner GAP43. Moreover, when the PO-V5-His tagged plasmid was used in the experiments, it gave similar results to the untagged contruct, therefore suggesting that addition of these

small tags do not affect the conformation of the enzyme in such a way as to disrupt its interactions with other proteins, specifically GAP43.

Furthermore, the PO-GAP43 interaction was also analysed in terms of intracellular localisation, but the results were inconclusive as both proteins are highly abundant in the cytosol and therefore their co-localisation at the subcellular level cannot be assessed even with the use of the confocal microscopy. HEK-MSRII cells transfected with pcDNA3.1D/V5-His-TOPO-GAP43 assumed a neuronal-like morphology with long processes and growth cone-like structures, in accordance with literature data (Verhaagen *et al.*, 1994).

4.3 Discussion

The study described here is one of the few that explores the biological functions of PO, with particular focus on its intracellular binding partners. In order to analyse the results from Y2H, we generated/validated several tools e.g. plasmids expressing PO, Taqman primers and probes and antibodies. These tools also allowed us to increase understanding of PO expression in the rat brain and in cell lines.

Using Taqman RT-PCR, we showed that PO mRNA is widely distributed amongst a variety of human and rat cell lines. All cell types analysed by Schulz *et al.* also expressed PO, suggesting that PO exerts critical cellular functions (Schulz *et al.*, 2005). Other studies have looked at PO activity during brain development. Agirregoitia *et al.* reported that PO activity in cortex, striatum, cerebellum and hypothalamus decrease during rat development (Agirregoitia *et al.*, 2003). The temporal profile was area specific and differences between the soluble and particulate forms were observed. This study on PO mRNA expression in the rat brain seems to parallel those findings on PO activity, as we observed a decrease in PO expression with age in several brain areas (cortex, cerebellum, hippocampus, hypothalamus, hindbrain and midbrain). Interestingly, a similar expression profile has been observed for GAP43 during post-natal development. The decrease in GAP43 expression with age is in accordance with its role in synaptic plasticity and neurite outgrowth, processes that occur predominantly in embryonic and early post-natal life. Considering that PO interacts with GAP43 and that its mRNA expression decreases after birth, these data suggest putative critical roles of PO in the same processes affected by GAP43. In contrast, other studies have reported an increase in PO expression in aged mice, in particular in the hippocampus, which correlated with a decline in cognitive performance (Rossner *et al.*, 2005).

At present there is very little information on PO protein expression, and reliable antibodies are not commercially available. The PO antibodies generated, and in particular #1216, were extensively characterised by immunocytochemistry, Western blotting, immunoprecipitation and competition with peptide antigen. Antibody validation was further carried out by showing that the PO band of ~75 kDa was not detected in PO null-mutant brain lysates. However, several cross-reactive bands (65, 35, 25 kDa) were

observed both in wild-type and in PO null-mutant brain lysates. The identity of these bands, which are unrelated to PO, is at present unknown given that the PO null-mutant mouse did not show any PO enzymatic activity. The peptides chosen for immunisation were not expected to recognise any other proteins, as predicted from a Blast search. We showed that antibody #1216 is suitable for use by Western blotting and immunoprecipitation and it has proven a valuable tool to validate the interaction between PO and GAP43.

The interaction between PO and GAP43 is of particular interest as it suggests that PO may modulate intracellular events, such as growth cone morphology, secretion and trafficking, all regulated by GAP43, and possibly affected in BD and by mood stabilizers. A Y2H screening was also recently reported by Schulz *et al.* in a study where interaction with α-tubulin was shown, which suggested PO modulation of cytoskeletal dynamics (Schulz *et al.*, 2005). In the Y2H study performed at GlaxoSmithKline, however, tubulin was not identified as a binding partner, perhaps due to the different libraries used (HeLa cells vs brain in our study). In the study by Schulz *et al.*, the interaction in mammalian cells was shown only by immunofluorescence co-localisation of the two proteins and not by co-immunoprecipitation, which is the standard and most robust technique to confirm an interaction. Moreover, it is not clear how specific their anti-PO antibodies are. It is interesting to note that they have been designed to the N-terminal region of the protein (amino acids 10-15 of the human PO), similar to our antibody #1216 (amino acids 2-14). Another weak point in the Schulz *et al.* study is the fact that PO and α-tubulin are very abundant cytosolic proteins, and a conclusion of their co-localisation cannot be definitely made. In contrast, our data supporting the interaction between PO and GAP43 are robust, as the interaction was confirmed by co-immunoprecipitation in mammalian cells. We first analysed interaction in over-expressing cells and subsequently in brain tissue. Co-immunoprecipitation experiments are very labour intensive and often yield false positives or negatives, particularly using over-expressed proteins. A more reliable confirmation of interaction can be obtained by studying endogenous proteins and in these studies the PO null-mutant mouse was a valuable negative control due to the absence of the PO protein.

PO consists of a catalytic and a β-propeller domain, which seem to modulate each other's functions. It has been shown that besides selecting substrates by size, the β-propeller

domain remarkably contributes to catalysis of the peptidase domain via its Cys 255 (Szeltner *et al.*, 2000). We analysed whether loss of enzymatic activity affects the PO interaction with GAP43. Interestingly, loss of enzymatic activity obtained by mutating Ser554 to Ala did not disrupt PO-GAP43 interaction, therefore showing that mutation of one amino acid, although critical for activity, was not sufficient to disrupt the folding of the protein. Moreover, addition of two tags (V5-His) to the PO enzyme, which may alter the structure of the protein, did not prevent interaction with GAP43 either, therefore indicating that also in this case the interaction is stable.

GAP43 is a growth-associated phosphoprotein enriched in growth cones and in presynaptic terminals and its interaction with PO is very interesting in this context. The expression of the protein is restricted to neurons and is highest in the first week after birth, whereas in the adult brain, GAP43 is enriched in areas with high synaptic plasticity (Oestreicher & Gispen, 1986). Transgenic mice over-expressing GAP43 show spontaneous formation of new synapses and enhanced sprouting after injury (Aigner *et al.*, 1995). In contrast, GAP43 null-mutation disrupts axonal pathfinding and it is generally lethal shortly after birth (Maier *et al.*, 1999). Furthermore, chicken embryonic sensory neurons in culture fail to extend axons when treated with antisense oligonucleotides complementary to portions of GAP43 mRNA (Aigner & Caroni, 1993). Regulation of GAP43 gene expression occurs both at the transcriptional and post-transcriptional level by unknown mechanisms. Several post-translational modifications have been described: ADP-ribosylation and palmitoylation in the membrane binding domain, phosphorylation of Ser41 by PKC and casein kinase II, and dephosphorylation by several phosphatases. GAP43 is bound to the plasma membrane via palmitoylation of two cysteine residues and can undergo cytosol-to-membrane translocation upon activation (Skene & Virag, 1989). Interactions of GAP43 have been described with calmodulin, PIP kinase, F-actin, and phospholipids (He *et al.*, 1997). In particular, in growth cones, GAP43 is associated with the cytoskeletal proteins actin, α-actinin, and talin (Meiri & Gordon-Weeks, 1990; Moss *et al.*, 1990). Phosphorylation state and amount of calmodulin bound to GAP43 appear to regulate the rate of neurotransmitter release. Calmodulin binds to GAP43 but GAP43 phosphorylation on Ser41 prevents this interaction (Meiri & Gordon-Weeks, 1990). There is, therefore, the possibility that PO may form part of a protein complex and regulates several cellular processes. Interestingly, GAP43, and in particular the phosphorylated form, has been shown to modulate the PIns

pathway by inhibiting PIP kinase in the rat brain and in the nerve growth cone (Van Dongen *et al.*, 1985; Van Hooff *et al.*, 1988). A model has been proposed through which GAP43 mediates local sequestration of PIP_2 into lipid rafts and releases the inhibitory activity that PIns exerts on actin-regulating proteins, such as profilin, cofilin and gelsolin (Laux *et al.*, 2000). As a result, actin dynamics are increased, resulting in decreased cytoskeleton stability and growth cone elongation. The latter effects are reversed by GAP43 phosphorylation (Caroni, 2001; Laux *et al.*, 2000). The interaction between PO and GAP43, therefore, may be the key link between PO and the action of mood stabilizers on the PIns pathway. Thus, the interaction between PO and GAP43 is of particular interest in terms of growth cone and synaptic function.

CHAPTER 5
Characterisation of sensory neuron growth cones from PO null-mutant mice

5.1 Introduction

The first report of a common effect of the mood stabilizers - lithium, VPA and CBZ – showed that each drug inhibited collapse and increased growth cone spread area in rat sensory neurons (Williams *et al.*, 2002). These effects were reversed by addition of either extracellular *myo*-inositol or by PO inhibitors, therefore suggesting that PO modulates the action of mood stabilizers possibly via the PIns signalling pathway (Williams *et al.*, 2002). Interestingly, PO had previously been linked with the PIns pathway; an inverse correlation between PO and IP_3 levels was found in an astroglioma cell line using PO inhibitors and antisense technology. In fact, treatment with PO inhibitors induced an increase in intracellular IP_3 levels (Schulz *et al.*, 2002). Increased IP_3 levels were also observed in a *Dictyostelium discoideum* PO mutant, which also showed resistance to the effects of lithium and VPA on the mould morphology (Williams *et al.*, 1999). More recently, PO was reported to be inhibited directly by VPA (but not by lithium or CBZ), suggesting this enzyme to be a key modulator in mood regulation (Cheng *et al.*, 2005). The authors proposed that euthymic mood may be dependent on stable PIns signalling and that a mood stabilizer, like VPA, may limit mood swings to mania by decreasing PIns signalling and limit those to depression by enhancing PIns signalling, via PO inhibition. Further data point to regulation of the PIns pathway by PO: treatment of primary neurons with the PO inhibitor S-17092 reversed the effect of lithium on CDP-DAG accumulation, mimicking addition of *myo*-inositol (Thomas J. & Mudge A.W., personal communication).

A clinical study has shown lower PO activity in the plasma of depressed individuals and higher levels in manic subjects when compared with control; however, only limited numbers of individuals were analysed (Maes *et al.*, 1995). Intriguingly, depressed subjects treated with the antidepressant drug fluoxetine showed increased PO activity in plasma, while treatment of manic individuals with VPA decreased PO plasma activity. Neuroleptic treatments had no effect on PO levels (Maes *et al.*, 1995). Importantly, a second enzyme, called ZIP, is present in the blood, as described in the Introduction section 1.4.5, which can be a confounding factor for these observations. Moreover, these studies lack analysis of the drug effects on PO expression levels in control subjects.

In order to analyse the involvement of PO in the mechanism of action of mood stabilizers, we have analysed the cellular morphology of sensory neurons derived from a PO null-mutant mouse. We also compared the growth cone morphology of the PO null-mutant neurons with that of wild-type neurons treated with a selective PO inhibitor. Unexpectedly, PO null-mutant growth cones exhibited a phenotype that was different from wild-type neurons and resembled that observed in wild-type neurons treated with a mood stabilizer. Moreover, addition of a mood stabilizer did not alter the percentage of collapse any further. Phenotype rescue experiments were performed by transducing sensory neurons with an adenovirus expressing native or catalytically-dead PO. We also examined whether levels of GAP43 and its phosphorylated form were altered in the PO null-mutant mouse. GAP43, identified as a PO interactor in an Y2H screening, is involved in growth cone structure and alterations in levels of this protein may result in changes in growth cone area.

5.2 Results

5.2.1 Effect of the PO inhibitor S-17092 on PO activity

A potent and selective PO inhibitor, S-17092, developed by Servier as a potential therapeutic for memory impairment (Morain *et al.*, 2002), was synthesised at GlaxoSmithKline. S-17092 inhibited PO activity in rat brain homogenate, with an IC_{50} in the sub nM range (Fig. 5.1), in agreement with published data (Barelli *et al.*, 1999).

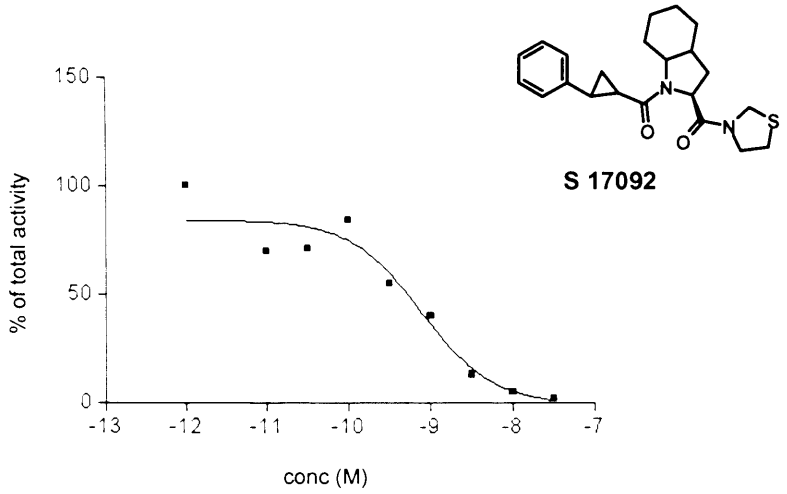

Fig. 5.1 PO inhibition by S-17092 and chemical structure.
Rat brain homogenate was processed as described in Materials and Methods and incubated with different concentrations of S-17092 for 30 min. Data are expressed as a percentage of total activity.

5.2.2 Growth cone analysis of mouse wild-type neurons treated with mood stabilizers: effect of S-17092

Sensory neuron ganglia were dissected from post-natal day 1 wild-type mice and treated with the PO inhibitor S-17092 over the concentration range of 1 nM - 10 μM. No changes in the percentage of growth cone collapse were observed at any concentration (Fig. 5.2A).

Explants were subsequently treated with VPA (1 mM), CBZ (50 μM) or LiCl (1 mM), with and without the PO inhibitor. Mouse wild-type sensory neurons responded to each of the mood stabilizers with a decrease in the percentage of collapse (Fig 5.2B) (from ~60% in control to ~30% in drug-treated explants (VPA: 34%; CBZ: 38%; LiCl: 35%), in agreement with previous findings in rat DRGs (chapter 4 of this thesis and (Williams *et al.*, 2002)). Moreover, when the PO inhibitor was added together with a mood stabilizer, the percentage of collapsed growth cones returned to control values (control: 66%, VPA + POi: 65%, CBZ + POi: 60%, LiCl + POi: 55%) (Fig. 5.2B).

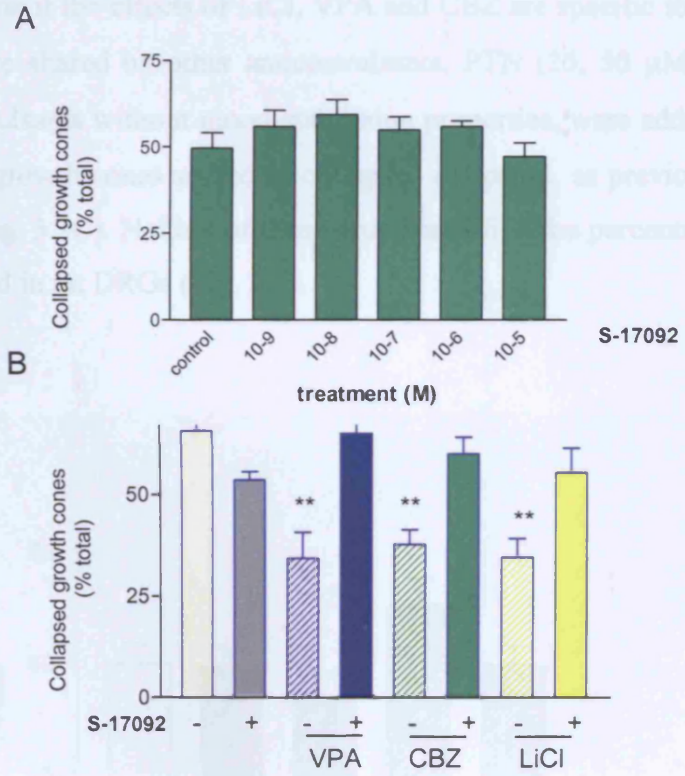

Fig. 5.2 Effect of mood stabilizers and of the PO inhibitor S-17092 on mouse wild-type growth cones.
A Concentration response effect of S-17092 on sensory neuron growth cone collapse. Growth cones were treated with 1 nM - 10 μM S-17092 and scored as collapsed or spread.
B Percentage of growth cone collapse in wild-type sensory neurons treated with the mood stabilizers LiCl (1 mM), VPA (1 mM) or CBZ (50 μM) with/without the PO inhibitor S-17092 (1 μM) (n = 6 independent experiments with at least two explants per experiment). Mean ± sem are indicated. P value <0.01 is indicated with ** (One-way ANOVA).

These results confirm previous findings with the three mood stabilizers in rat sensory neurons (Williams *et al.*, 2002) and extend the observations to mouse sensory neurons. Moreover, we showed that the potent and selective PO inhibitor, S-17092, produces similar effects to those described by Williams *et al.*, where two other potent compounds were used to inhibit PO (BOC-Glu (NHO-Bz)-Pyr and Z-Pro-Pro-aldehyde-dimethyl acetal).

5.2.3 Growth cone analysis of mouse wild-type neurons treated with PTN or GPT

In order to determine if the effects of LiCl, VPA and CBZ are specific for mood stabilizers or whether they are shared by other anticonvulsants, PTN (25, 50 μM) or GPT (25, 50 μM), two anticonvulsants without mood-stabilizing properties, were added to mouse wild-type explants and growth cones scored as collapsed or spread, as previously performed in rat explants (see Fig. 3.2C). Neither of these drugs modified the percentage of collapse, as previously observed in rat DRGs (Fig. 5.3).

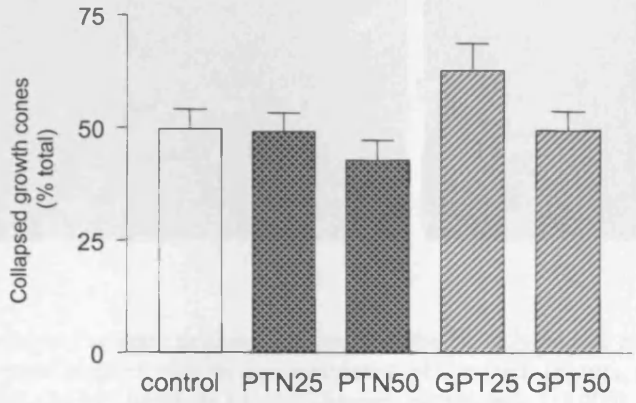

Fig. 5.3 Effects of PTN and GPT on mouse wild-type growth cones.
Explants were treated with drugs (25 or 50 μM) 24 h after plating and cultured for a further 20 h. Growth cones were scored as collapsed or spread and plotted as a percentage of the total number of growth cones examined (n = 3 explants, representative experiment, >100 growth cones scored). Mean ± sem are indicated. Similar results were obtained in a second experiment.

5.2.4 Growth cone analysis of mouse PO null-mutant neurons treated with mood stabilizers

Sensory neuron explants were immunolabelled for GAP43 in order to visualise the growth cone morphology, while an anti-acetylated tubulin antibody was used to visualise stable microtubules. Fig. 5.4 shows examples of a sensory ganglion explant (left, low magnification), and spread and collapsed growth cones (right panel, indicated with arrows).

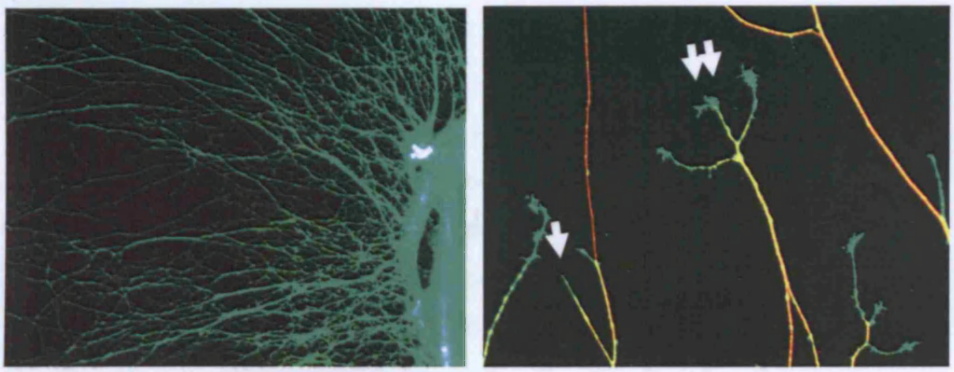

Fig. 5.4 Morphology of sensory neuron explants from the PO null-mutant mouse.
Explants were labelled with an anti-acetylated tubulin (red) (Sigma, monoclonal, 1:10,000) together with an anti-GAP43 antibody (green) (Abcam, polyclonal, 1:2,000). Goat anti-rabbit IgG Alexa488 and goat anti-mouse IgG Alexa594 secondary antibodies were used. Single arrow (right panel) shows a collapsed growth cone, and double arrows indicate a spread growth cone.

Growth cones of sensory neurons from PO null-mutant mouse displayed an unexpected morphology. Untreated explants showed a decreased percentage of collapsed growth cones (~30% of the total) when compared with wild-type explants; these values were similar to those obtained when wild-type neurons were treated with mood stabilizers (Fig. 5.5A). Addition of a mood stabilizer did not reduce further the percentage of collapse (Fig. 5.5A). Analysis of growth cone spread area revealed an increase in the percentage of growth cones with area >100 μm^2 and a decrease in the percentage of 'small' growth cones with area <20 μm^2 (Fig. 5.5B), with the mean area increasing from 33.55 ± 1.90 μm^2 in wild-type cultures to 56.94 ± 2.14 μm^2 in PO null-mutant neurons.

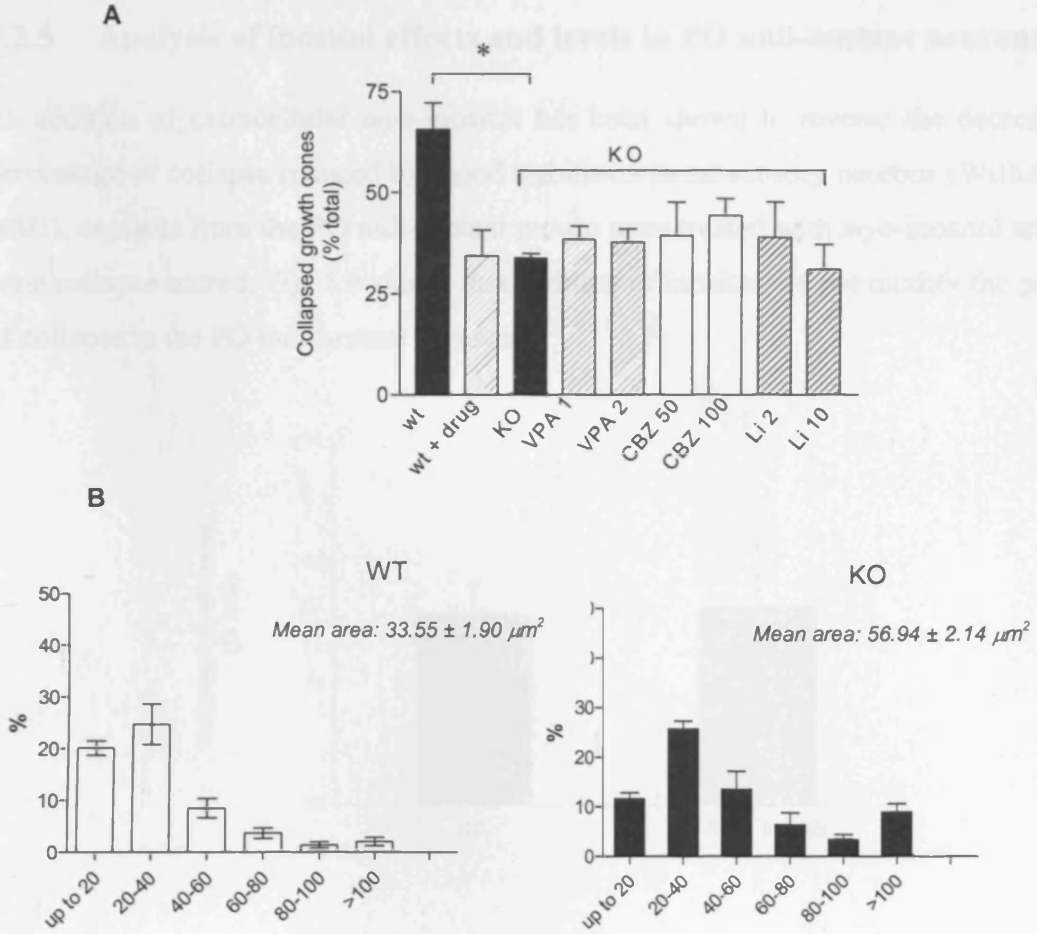

Fig. 5.5 Analysis of growth cones from the PO null-mutant mouse.

A Percentage of growth cone collapse in PO null-mutant sensory neurons (KO) with/without addition of a mood stabilizer (VPA: 1 and 2 mM; CBZ: 50 and 100 μM; LiCl: 2 and 10 mM). Control (WT) and LiCl-treated wild-type explants (WT + drug) are shown for comparison (n = 6 independent experiments with at least two explants per experiment, T-test, *P<0.05).

B Growth cone area distribution of WT and KO DRGs. Explants were labelled with an anti-GAP43 primary antibody followed by a goat anti-rabbit Alexa488 secondary antibody.

Mean ± sem are indicated (both A and B).

5.2.5 Analysis of inositol effects and levels in PO null-mutant neurons

As addition of extracellular *myo*-inositol has been shown to reverse the decrease in the percentage of collapse induced by mood stabilizers in rat sensory neurons (Williams *et al.*, 2002), explants from the PO null-mutant mouse were treated with *myo*-inositol and growth cone collapse scored. Fig. 5.6 shows that addition of inositol did not modify the percentage of collapse in the PO null-mutant explants.

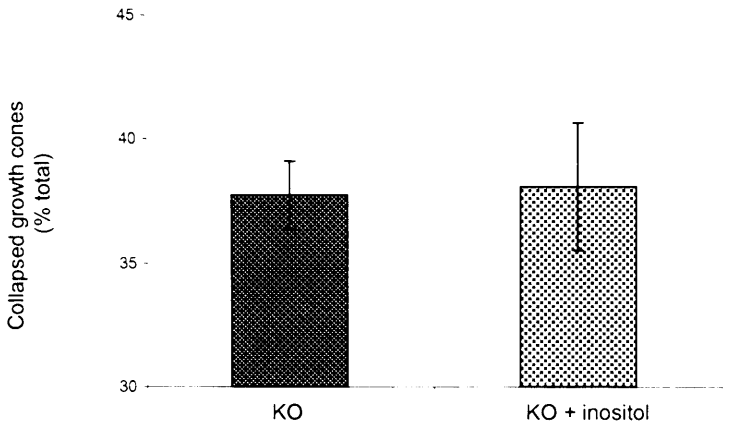

Fig. 5.6 PO null-mutant sensory explants treated with *myo*-inositol.
Explants were treated with 1 mM inositol, fixed after 24 h and growth cones were scored as collapsed or spread (n = 2 experiments, n > 100 growth cones/condition). Mean ± sem are indicated.

These data show that the reduction in the percentage of growth cone collapse observed in the PO null-mutant neurons when compared with wild-types is not altered by treatment with inositol. It can be hypothesised that inositol requires PO in order to exert any cellular effects.

In order to determine whether inositol levels are altered in the PO null-mutant mouse, measurements were performed in DRG extracts dissected from wild-type or PO null-mutant mice. No differences in inositol levels were observed between the PO null-mutant and wild-type extracts (Fig. 5.7).

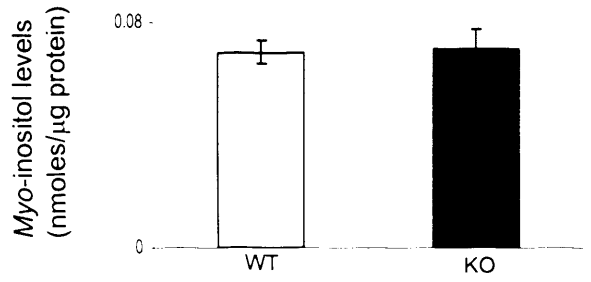

Fig. 5.7 Measurements of inositol levels in PO null-mutant DRGs.
Six DRGs were lysed in 100 µl of water and sonicated. Samples were analysed by Ajit Shah within the Neurochemistry Department at GlaxoSmithKline using liquid chromatography followed by tandem mass spectrometry (LC-MS/MS). Values are expressed as nmoles of inositol/µg of protein. Results are expressed as mean ± sem from six samples.

Overall, these data show that inositol levels are not altered in the PO null-mutant mouse neurons. Similar data were obtained when cortical and brain extracts were analysed. However, it is possible that other components of the pathway, such as PIP_2 or other inositol phosphates, are altered in the PO null-mutant mouse and it would be interesting to measure their levels/turnover.

5.2.6 GAP43 expression levels in the PO null-mutant mouse

In order to determine if the increase in growth cone spread area observed in the PO null-mutant neurons is associated with changes in expression levels of the PO interactor, GAP43, protein levels were analysed in brain and in sensory neuron extracts (data not shown for the latter) (Fig. 5.8A). Moreover, in order to determine if changes in the phosphorylation state of GAP43 protein occurred in the PO null-mutant mouse, parallel blots were probed with an anti-phospho(Ser41)-GAP43 antibody (Fig. 5.8B). The PO antibody was used to confirm PO null-mutant and wild-type samples. No differences in either GAP43 or in phospho-GAP43 were detected between the PO null-mutant and wild-type samples (Fig. 5.8C).

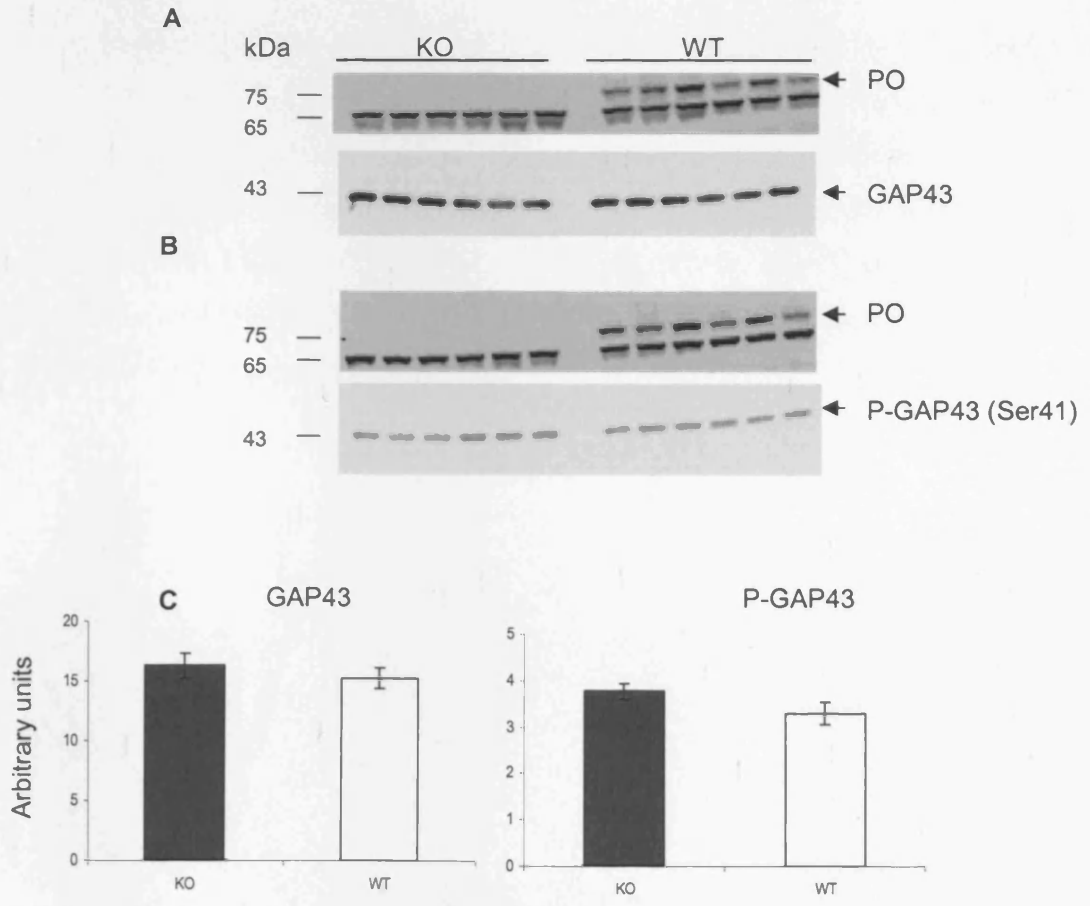

Fig. 5.8 GAP43 protein expression in PO null-mutant brain.
A GAP43 expression was analysed in the hippocampus from six WT and six PO KO mice. 20 μg of proteins were loaded per well. The blot was probed with an anti-GAP43 antibody (1:5,000) together with the anti-PO antibody #1216 (1:1,000). **B** P-GAP43 expression was analysed in the hippocampus from six WT and six PO KO mice. **C** GAP43 and P-GAP43 quantitation. Mean ± sem (n = 6). Quantitation was performed using Genetools from Syngene. T-test was performed to determine significance.

A similar analysis was performed using sensory neuron explant lysates and no differences in GAP43 expression were observed between wild-type and PO null-mutant samples. These data suggest that the increase in growth cone area observed in the PO null-mutant mice is not due to alterations in GAP43 protein. Furthermore, these changes are also not due to differences in phosphorylation levels of GAP43. It is possible that other post-translational modifications of GAP43 not analysed in this study e.g. palmitoylation, may be responsible for the changes in growth cone morphology. Another possibility is that analysis of steady-state levels does not allow detection of changes in dynamic interactions at the growth cone.

5.2.7 Viral transduction studies in sensory neurons: PO native enzyme

In order to determine if the null-mutant phenotype can be rescued by re-introduction of PO, an adenovirus expressing PO (untagged), as well as GFP (humanised form) (bicistronic construct) was made by Colin Glover at Bristol University (Ad.CMV.PO$_{IRES}$hrGFPII.WPRE). Several viral concentrations were tested on sensory explants (up to 10 µl of undiluted stock). Only weak GFP fluorescence was observed up to 5 days post-transduction and this was mainly confined to the explant cell bodies. The fluorescence was not strong enough to allow visualisation of neurites and measurements of growth cone area. An antibody approach could not be used due to the lack of specificity of the PO antibody #1216 by immunocytochemistry in tissue and to the lack of a suitable commercially available anti-GFP (humanised) antibody.

Therefore, another approach was adopted. An adenovirus was made by Colin Glover that expressed PO protein in frame with the V5 tag (Ad.CMV.POV5.WPRE), as specific anti-V5 antibodies exist that can be used for immunocytochemistry. As enzyme function may be altered as a consequence of the introduction of a tag, PO activity was measured in explants transduced with the PO native or V5-tagged viruses, as well as wild-type and PO null-mutant explants. Data showed that the V5 tag clearly decreased PO activity when compared with the PO untagged-transduced neurons (Fig. 5.9).

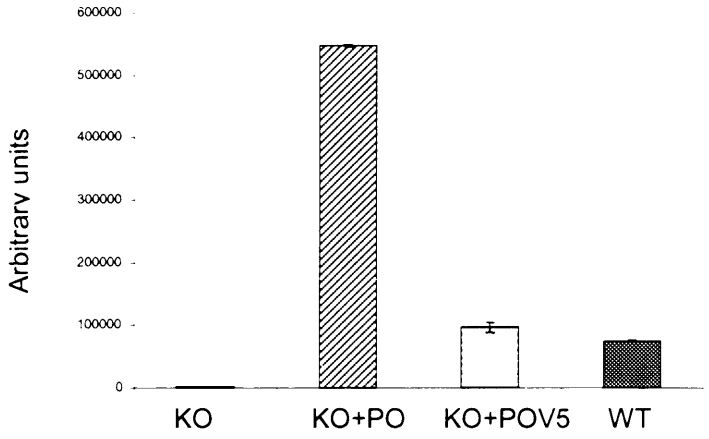

Fig. 5.9 PO activity in PO-transduced DRGs.
PO KO neurons were transduced with an adenovirus containing PO untagged or V5-tagged and analysed for PO activity 5 days after transduction. WT explants were used as a positive control. Ten DRGs were pooled per condition and 20 µl of homogenate were analysed in the PO activity assay as described in Materials and Methods (n = 4 replicates per condition, mean ± sem).

These results showed that the V5 tag decreases PO catalytic activity to levels that are similar to those observed in wild-type primary neurons. Viral transduction of PO null-mutant neurons with the PO untagged virus restores PO activity, and the levels were much higher than those measured in wild-type extracts, therefore suggesting that PO over-expression occurs. As we showed that the V5 tag alters PO enzymatic activity we decided to go back to the PO untagged virus and adopt a different strategy in order to perform growth cone area measurements.

A combination approach was therefore adopted, consisting of addition of the PO untagged adenovirus together with a CMV-EGFP adenovirus (Ad.CMV.EGFP.WPRE, generated by Colin Glover), previously shown to transduce explants efficiently, with the assumption that the two viruses should both transduce the same cells (James Uney and Colin Glover, personal communication). Transduction efficiency was determined by labelling the explants with an anti-GAP43 antibody, which labels all neurites, and scoring the GAP43-labelled as well as the GFP-fluorescent growth cones. The transduction rate was calculated between ~50-60%. Importantly, it became evident that the fluorescence, although quite strong, was not homogeneous along the neurite length and it was occasionally absent in the growth cone, therefore preventing reliable growth cone measurements (Fig. 5.10).

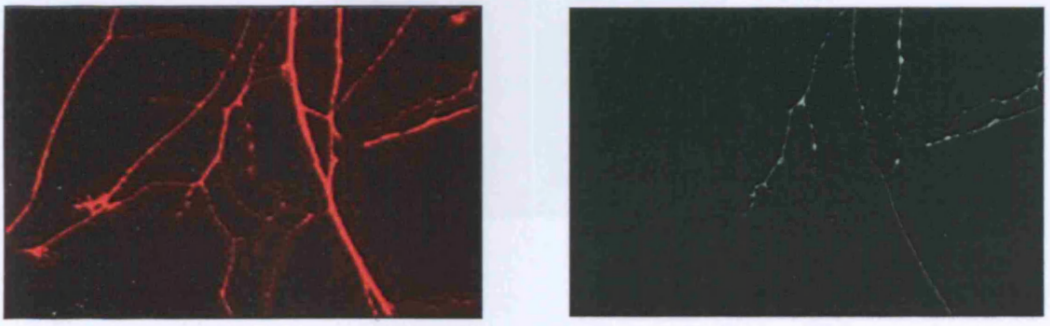

Fig. 5.10 Examples of adenoviral transduction of DRG explants.
Explants were labelled with an anti-GAP43 antibody (Abcam, 1:2,000) followed by the secondary antibody goat anti-rabbit Alexa594. GFP fluorescent images were also acquired in the same field.

In order to determine if the PO adenovirus was able to transduce sensory neurons and restore PO protein expression, lysates from PO-transduced, wild-type or PO null-mutant sensory neurons were analysed by Western blotting (Fig 5.11). PO is endogenously expressed in wild-type sensory neurons, whereas it is not expressed in PO null-mutant neurons. Transduction of PO null-mutant neurons with the PO adenovirus restored PO protein expression, whereas addition of the virus to wild-type cultures induced PO protein over-expression.

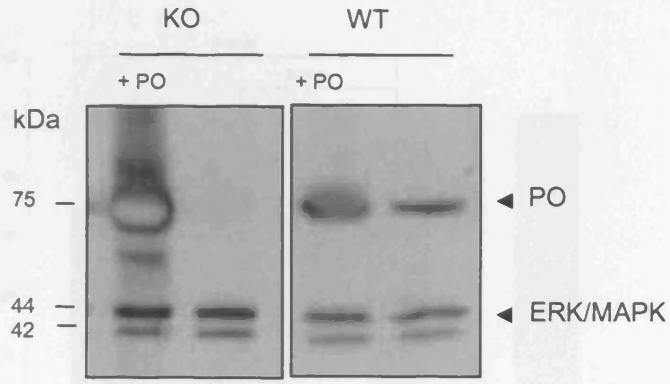

Fig. 5.11 PO protein expression in PO-transduced DRG.
Six DRGs from WT or PO KO mice transduced or not with the PO adenovirus (1 µl) were lysed 5 days after transduction in ~30 µl of lysis buffer. Western blotting was performed using the anti-PO antibody #1216 (1:1,000) (band of ~75 kDa). An anti-ERK/MAPK antibody (1:10,000) (bands of 44, 42 kDa) was used as a loading control.

Growth cone scoring was subsequently performed. GAP43-labelled cultures were analysed and a statistical approach was adopted in order to take into consideration that only 50% of the neurons were actually transduced. The statistical power calculation identified the number of replicates required in order to obtain statistically significant results (18-20 replicates needed). Therefore, four independent experiments were performed with a total of >20 replicates. Reintroduction of the PO native protein into the PO null-mutant sensory explants reversed the percentage of collapsed neurons to values that were similar to those observed in untreated wild-type neurons (KO: 35%; KO + EGFP: 36%; KO + EGFP +PO: 46%; WT: 51%) (Fig. 5.12).

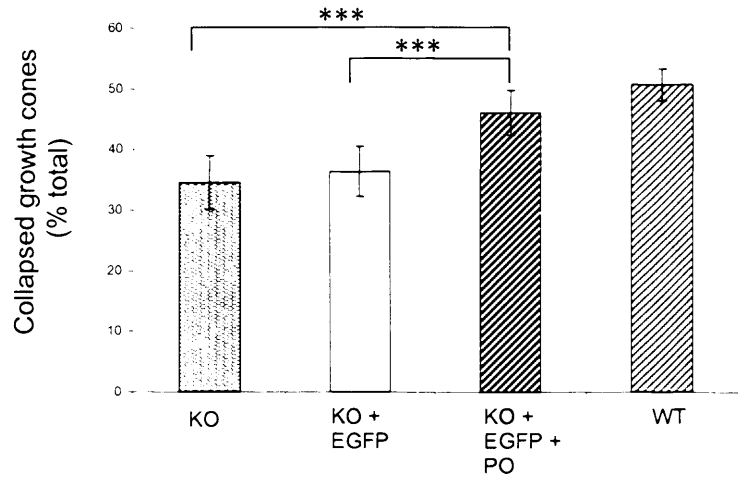

Fig. 5.12 Growth cone analysis of PO null-mutant sensory neuron transduced with PO native adenovirus. Explants were left untreated or they were transduced with an EGFP adenovirus or with the EGFP adenovirus together with the PO native untagged adenovirus (1 µl of virus/well). Explants were fixed 4 days post-infection, labelled with anti-GAP43 antibody and scored as collapsed or spread (n = 4 independent preparations, n>20 explants/condition). Mean ± sem are indicated, p***<0.001; Two-way ANOVA was performed.

These results show that PO is a key component in the nerve terminal where it affects processes involved in growth cone morphology.

5.2.8 Viral transduction studies in sensory neurons: catalytically-dead PO

Subsequently, in order to dissect the involvement of PO enzymatic activity in growth cone morphology, neurons were transduced with an adenovirus expressing catalytically-dead (Ser554Ala) PO (Ad.CMV.cat-deadPO_{IRES}hrGFPII.WPRE) (made by Colin Glover). Protein lysates were analysed to determine if the virus was able to induce PO protein expression in PO null-mutant sensory explants. Western blotting data showed that PO protein can be detected in PO null-mutant PO catalytically-dead-transduced sensory neurons (Fig. 5.13).

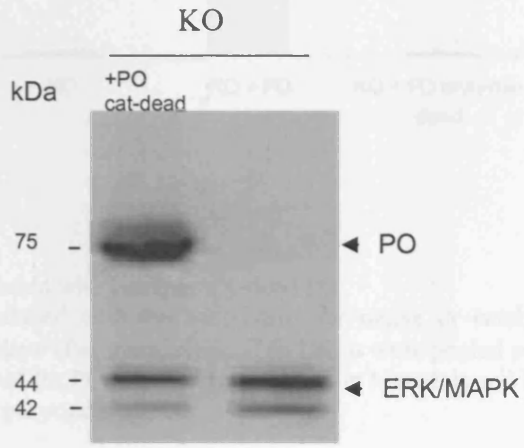

Fig. 5.13 PO protein expression in catalytically-dead PO-transduced DRG.
Six DRGs from PO KO mice transduced or not with the catalytically-dead PO adenovirus were lysed 5 days after transduction in ~30 µl of lysis buffer. Western blotting was performed using the anti-PO antibody #1216 (1:1,000) (band of ~75 kDa). An anti-ERK/MAPK antibody (1:10,000) (bands of 44, 42 kDa) was used as loading control.

PO enzymatic activity was also measured in DRG explants transduced with the catalytically-dead PO adenovirus, as well as native PO. Results in Fig. 5.14 show that the catalytically-dead PO is devoid of PO enzymatic activity, as expected.

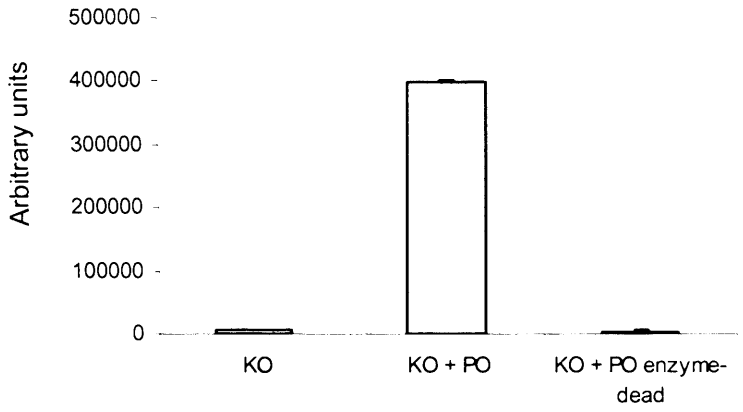

Fig. 5.14 PO activity in DRGs transduced with catalytically-dead PO.
PO KO DRGs were transduced with the adenovirus for native or catalytically-dead PO and analysed for PO activity 5 days after transduction. Ten DRGs were pooled per condition and 20 µl of homogenate were analysed for PO activity, as described in Materials and Methods. Mean ± sem are shown (n = 4 replicates per condition).

Following on from these experiments, which showed that the adenovirus expressing catalytically-dead PO is able to restore PO protein without inducing any increase in PO enzymatic activity, the catalytically-dead PO adenovirus was applied to sensory neurons dissected from the PO null-mutant mouse in combination with the EGFP expressing adenovirus and growth cones were scored as collapsed or spread. Explants transduced with the catalytically-dead PO showed an increase in the percentage of collapsed growth cones when compared with EGFP-transduced neurons or with PO null-mutant neurons (KO: 34%; KO + EGFP: 36%; KO + EGFP + PO dead: 57%) (Fig. 5.15).

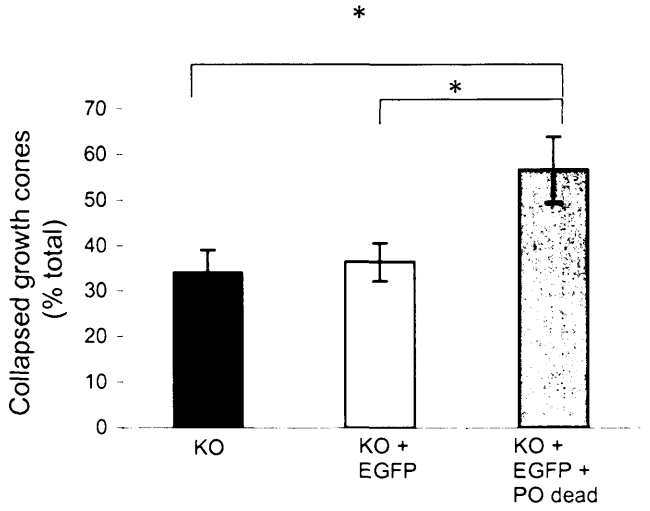

Fig. 5.15 Growth cone analysis of PO null-mutant sensory neuron transduced with a catalytically-dead PO adenovirus.
Explants were left untreated or they were transduced with an EGFP adenovirus or with the EGFP adenovirus together with the catalytically-dead PO adenovirus (1 µl of virus/well). Explants were fixed 4 days post-infection, labelled with an anti-GAP43 antibody and scored as collapsed or spread (n = 4 independent, n>20 explants/condition). Mean ± sem are indicated. Two-way ANOVA was performed, *$p<0.05$.

These results show that the PO null-mutant phenotype can be altered not only by re-introduction of the PO native enzyme, but also when the PO enzyme without the catalytic activity is expressed. This indicates that the PO enzymatic activity is not necessary for the effect of PO on growth cone morphology. These data are in agreement with the findings that treatment of wild-type explants with the PO inhibitor S-17092 does not alter growth cone morphology when added on its own (Fig. 5.2A).

A summary table of the viruses used and the issues encountered with each of them is presented below (Table 5.1):

Viruses used	Summary
Ad.CMV.PO$_{IRES}$hrGFPII.WPRE (cv 73, 1.5 x 10^{10} pfu/ml)	- Restores PO protein and activity - Weak hrGFP fluorescence - No suitable Ab anti-PO or anti-hrGFP for ICC - Can be used only if statistical approach applied
Ad.CMV.cat-deadPO$_{IRES}$hrGFPII.WPRE (cv 76, 2.23 x 10^{9} pfu/ml)	- Restores PO protein but not activity - Weak hrGFP fluorescence - No suitable Ab anti-PO or anti-hrGFP for ICC - Can be used only of statistical approach applied
Ad.CMV.POV5.WPRE (cv 79, 1.0 x 10^{10} pfu/ml)	- Growth cones can be visualised using an anti-V5 antibody - Restores PO protein but PO activity is compromised - Cannot be used
Ad.CMV.EGFP.WPRE (cv 31, 2.25 x 10^{9} pfu/ml)	- Good EGFP fluorescence, but sometimes fragmented

Table 5.1 Summary of viruses used in the study.

5.3 Discussion

PO has been implicated in the mechanism of action of mood stabilizers but the nature of the interaction remains largely unknown.

In this study we show that, unexpectedly, the growth cone morphology of sensory neurons dissected from PO null-mutant mice is altered; in particular, the percentage of collapsed growth cones is decreased to ~30% compared with wild-type neurons (~60%) and the percentage of enlarged growth cones is increased. These results suggest that PO plays a central role in growth cone dynamics.

When PO null-mutant neurons were treated with a mood stabilizer, no alterations in the percentage of growth cone collapse were observed, suggesting that PO modulates a pathway that is also affected by mood stabilizers, probably upstream of their action. In contrast, addition of a mood stabilizer to wild-type neurons increased the growth cone spread area and decreased the percentage of collapse. Furthermore, when the PO inhibitor was added in combination with the drugs it reversed/prevented the mood stabilizer effect (Table 5.2). The PO inhibitor alone, however, did not have any effect in wild-type neurons. It is possible, therefore, that mood stabilizers perturb PO interactions with putative target molecules and that PO inhibitors may have a further effect in combination with a mood stabilizer.

A WT growth cones

Treatment	Main phenotyp
Untreated	Collapsed
+PO inhibitor	Collapsed
+mood stabilizer	Spread
+PO inhibitor plus mood stabilizer	Collapsed

B KO growth cones

Treatment	Main phenotype
Untreated	Spread
+mood stabilizer	Spread
+PO native	Collapsed
+PO catalytically dead	Collapsed

Table 5.2 Summary of growth cone morphological changes in sensory neurons.
A WT neurons left untreated show a prevalence of collapsed growth cones. Treatment with the PO inhibitor, S-17092, does not alter the percentage of collapse. Treatment with a mood stabilizer increases the growth cone spread area, but co-application with the PO inhibitor restores the WT untreated phenotype.
B PO KO cultures left untreated show an increase in the percentage of enlarged growth cones when compared with WT and treatment with a mood stabilizer does not alter the morphology any further. Re-introduction of PO (native or catalytically-dead) restores the WT phenotype.

When the PO native enzyme was re-introduced in the PO null-mutant DRG, using an adenoviral approach, we found an increase in the percentage of collapse, which resembled values observed in wild-type untreated cultures. These results confirm that the morphological changes observed in the PO null-mutant mouse are due to the lack of PO protein and highlight the importance of this enzyme in growth cone morphology. Viral delivery has proven to be challenging in terms of growth cone visualisation due to the lack of selective PO antibodies for immunocytochemistry. It is worth mentioning that the homologous recombination in HEK293 cells was problematic and very inefficient for PO when compared with other proteins (1 week compared with 3 days with other proteins - personal communication from Colin Glover), therefore indicating some unusual properties of this enzyme that would be interesting to clarify.

When PO null-mutant DRGs were transduced with a catalytically-dead PO adenovirus, the percentage of collapsed growth cones increased in a statistically significant manner, when compared either to the PO null-mutant. These data lead us to conclude that the PO enzymatic activity on its own is not central to PO biological functions related to growth cone morphology. This is supported by the lack of effect of a PO inhibitor on the growth cone morphology of wild-type neurons. The catalytically-dead enzyme was also able to interact with GAP43, indicating that mutation of one amino acid does not alter the PO folding in such a way as to compromise its interactions and downstream functions and that catalytic activity is not critical for PO function.

Addition of *myo*-inositol did not modify the percentage of growth cone collapse in PO null-mutant neurons and inositol levels were not changed in sensory explants or brain of PO null-mutant mice when compared with wild-types. These latter findings were not unexpected as it seems highly unlikely to deplete the millimolar inositol concentration measured in neurons. Overall, it seems likely that inositol requires PO in order to exert any cellular effects. cAMP was recently shown to decrease the percentage of collapse and increase the spread area of sensory explants (Cheng *et al.*, 2005). The same study reported that PO inhibitors reversed the effects of cAMP, suggesting a functional link between these two molecules. It is possible that PO actions may involve modulation of the PKA/cAMP and/or the PIns signalling. To support the involvement of the PKA/cAMP pathway, a proteomic study performed at GlaxoSmithKline has identified several components of the PKA pathway whose expression may be altered in the PO null-mutant mouse brain. Further studies are, however, required to confirm these findings and determine their functional relevance. The changes in growth cone morphology observed suggest that alterations in actin and in the microtubule cytoskeleton may occur in the PO null-mutant mouse and, indeed, several cytoskeletal proteins were identified in the proteomic study as differentially expressed in the PO null-mutant (e.g. MAP2, 14-3-3 zeta etc.). Interestingly, α-tubulin was also reported as a PO interactor in another Y2H screen (Schulz *et al.*, 2005).

Overall, the observations in the PO null-mutant mouse are interesting as they shed light on PO intracellular functions that have not been previously reported. The observed increase in growth cone area could be due to alterations in expression levels of the growth cone protein GAP43, which we have reported to interact directly with PO. GAP43 phosphorylation levels are low in neurites of growth cones that have collapsed (Dent & Meiri, 1998) suggesting that phosphorylation of GAP43 by PKC could direct the functional behaviour of the growth cone. Moreover, it is known that phosphorylation of GAP43 weakens the binding of GAP43 to phosphoinositides and as a result, GAP43 interaction with lipid rafts is perturbed, therefore affecting axonal growth and guidance (Dent & Meiri, 1998). This was not, however, the case in our system as no changes in GAP43 or in P-GAP43 levels were detected at least at steady state, indicating that other GAP43 post-transtranslational modifications may be affected. It is possible that PO forms an intracellular complex with GAP43 and other proteins, which may be altered in the PO null-mutant mouse. We propose that GAP43 is a key molecule for further analysis in its

interactions with PO and link with the PIns pathway. GAP43 has been reported to inhibit PIP kinase, a key enzyme in the synthesis of PIP_2, and the interaction with PO suggests a possible link with the PIns signalling pathway. Our hypothesis is that PO interaction with GAP43 is key to regulate cellular processes, such as growth cone area enlargement; it is possible that mood stabilizers, as well as PO inhibitors may affect the interaction directly (Fig. 5.16).

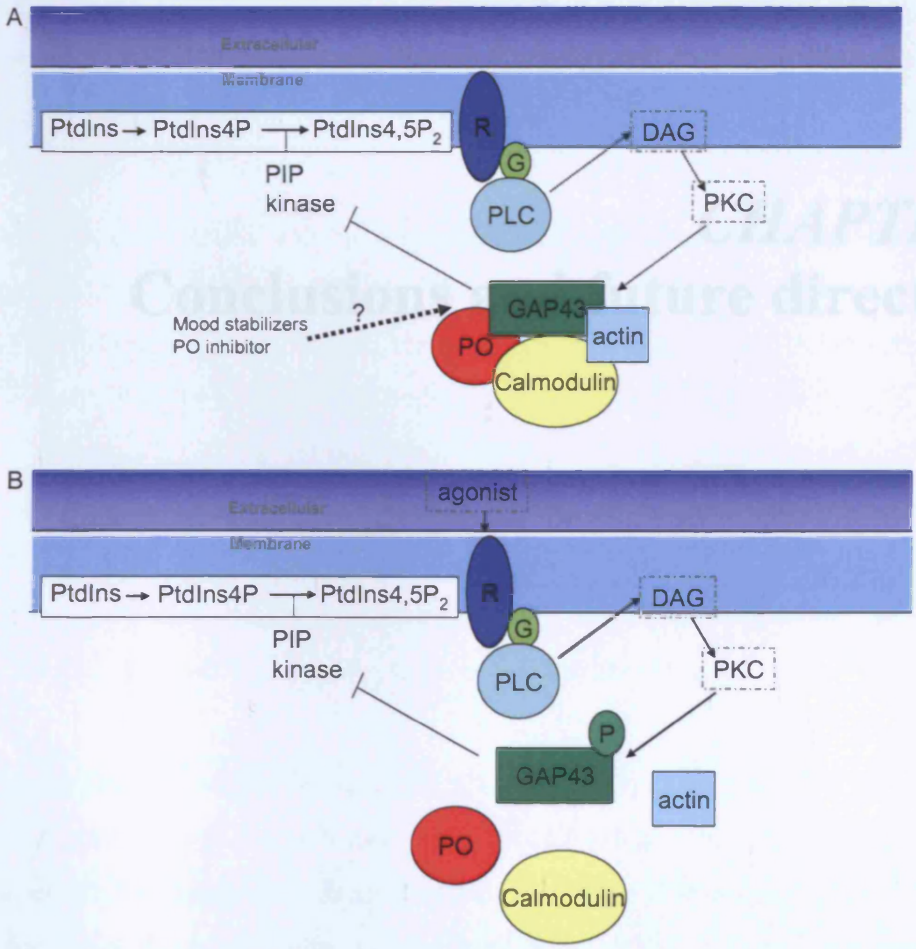

Fig. 5.16 Schematic of hypothesis for PO action in the growth cone.
A In resting conditions PO and GAP43 associate in a protein complex, which includes actin and calmodulin. Low level of PIPkinase inhibition is achieved. The unphosphorylated form of GAP43 has been associated with collapsed growth cones. It is possible that mood stabilizers and PO inhibitors may affect the protein interaction between PO, GAP43 and other proteins in the complex, therefore resulting in alterations in growth cone morphology.
B After stimulation of the PIns pathway (e.g. carbachol), GAP43 is phosphorylated on Ser41 by PKC. This results in inhibition of PIPkinase, which negatively regulates PIP_2 synthesis. P-GAP43 does not bind to calmodulin, therefore disrupting the protein complex. When the complex is disassembled, and the phosphorylated form of GAP43 predominates, an increase in growth cone spread area is observed. The same phenotype is observed when PO is not present in the complex (in the PO null-mutant mouse) and the protein complex is, therefore, affected.

CHAPTER 6
Conclusions and future directions

None of the drugs currently used to treat BD, such as lithium, VPA and CBZ, were developed with that use in mind. They do not seem to act by binding to extracellular receptors, rather they may modulate intracellular signalling molecules. It is not clear at present which pathways are modulated in relation to the therapeutic action or to the side-effects of the drugs.

One approach to better understand the therapeutic targets is to identify commonly-regulated molecules. It is, however, possible that each of these drugs modulates a common pathway, rather than a molecule, by acting at different levels in the pathway.

In this thesis the ERK/MAPK and the PIns signalling pathways were examined and I have also focused on the signalling molecule GSK3, as discussed in the relevant chapters. The ERK/MAPK pathway is implicated in neuronal survival and neurite outgrowth and it is activated by neurotrophins (Skaper & Walsh, 1998). Activation of ERK/MAPK has been shown for VPA and LiCl, but the mechanism of activation is still not clear. In fact, VPA and LiCl induce phosphorylation of ERK/MAPK and exert downstream effects on some ERK/MAPK targets, such as Elk1 (Di Daniel *et al.*, 2005). Direct activation of Ras/Raf and MEK have not, however, been demonstrated for any mood stabilizers. Moreover, the effects on ERK/MAPK activation seem to be cell-dependent *in vitro*.

In order to validate new targets and test new potential therapeutics for BD it is important to have good *in vitro* and/or *in vivo* models that predict efficacy in humans. Unfortunately, there are currently no useful animal models for BD and no useful drug screens for testing potential candidate drugs. There have been attempts to mimic different symptoms of the illness, such as hyper-activity (observed in mania) or prepulse inhibition (PPI) deficits (also common to schizophrenia) or lack of motivation (observed in depression). For BD and other psychiatric conditions it is very difficult to establish *in vitro* models as there are no obvious pathological/cellular abnormalities in BD brains that can be mimicked in a tissue culture environment.

The growth cone assay described here and previously (Williams et al., 2002) is the first assay to show a common effect of the three most widely-prescribed drugs for the treatment of BD. While the system uses sensory neurons, which are not relevant for the pathology, it

is important that by analysing the common effects of the drugs we may discover therapeutic targets. In this assay, inositol reverses the effects of the drugs, suggesting the PIns pathway as the key therapeutic pathway. Importantly, I have shown that the effects of the drugs are also observed in neurons from a more disease-relevant brain area - the cerebral cortex. These data give us confidence that by using the growth cone assay in sensory explants we may be able to extrapolate findings to the brain. Moreover, GPT and PTN, anticonvulsants that are not efficacious in the treatment of BD at least as monotherapy, did not produce inositol-reversible effects on growth cones, strengthening the hypothesis that alterations in the PIns pathway may specifically underlie BD. The growth cone assay, therefore, seems to be potentially useful for assessing new candidate drugs. Other anticonvulsant, antipsychotic or antidepressant drugs with efficacy in BD should be tested in this assay in order to validate this assay as predictive of BD efficacy. GSK3 inhibitors increased sensory neuron growth cone area, in particular by increasing the percentage of very large growth cones; an effect that was not reversed by addition of inositol. GSK3 inhibition does not seem to be a common effect of lithium, VPA and CBZ, as only lithium affected GSK3 downstream targets e.g. GS and tau. However, only two drug concentrations were chosen – 1 and 10 mM – and in future studies a concentration-response analysis should be performed to determine at which concentration the effects on GSK3 targets can be observed.

Increasing evidence points to the PIns signalling as the key pathway that is affected in BD and which may be critical to modulate with drugs in order to restore the physiological status. In particular, it has been proposed that hyper-activation of this pathway may be linked with mania and decreased activity (inhibition of PIns recycling rather than decreased levels of inositol) with depression and, therefore, normalisation of the activity of this pathway may be key to mood stabilization (Cheng *et al.*, 2005). We have analysed several components of the PIns pathway. One of these, IMPase has been previously analysed as a drug target by Merck Sharp & Dohme. The IMPase inhibitors developed were potent competitive inhibitors and produced similar *in vitro* effects to those observed with lithium (accumulation of inositol phosphates and CDP-DAG), although lithium is an uncompetitive inhibitor (Atack *et al.*, 1994). The compounds were not brain penetrant and for this reason they did not provide useful drug candidates (Atack *et al.*, 1993). Another critical component in the pathway is MIP-synthase. Both VPA and lithium increase the

expression of the MIP-synthase homologue INO-1 in yeast (Ju *et al.*, 2004; Vaden *et al.*, 2001) and *Dictyostelium discoideum* (Williams et al., 2002), although neurons appear to have evolved different mechanisms for regulating the availability of this important precursor for membrane PIns synthesis. This enzyme is unlikely to be a valid drug target as it is expressed in the vasculature (Wong *et al.*, 1987) and it is unclear whether it contributes to the inositol-dependent effects of mood stabilizers on neurons.

Recent focus has been given to the inositol transporters, in particular to SMIT and HMIT. Astrocytic SMIT activity was reported to be inhibited by lithium, VPA and CBZ after long-term treatment (8-14 days). Berry and colleagues reported that the fetal brains of mice with a SMIT1 gene deletion had normal levels of inositol phospholipids (Berry et al., 2004; Berry et al., 2003) and they raised the question of how neurons obtain their inositol for PIns synthesis. Moreover, SMIT1 heterozygous mice did not show any obvious behavioural abnormalities (forced swim, amphetamine-induced hyperactivity, elevated plus maze, apomorphine-induced stereotypic climbing and lithium-pilocarpine seizure tests) (Shaldubina *et al.*, 2006a). SMIT1 and SMIT2 are highly expressed in the periphery, in particular in the kidney. Lithium is known to induce kidney toxicity and this may be related to inhibition of SMIT (Kitamura *et al.*, 1998). Moreover, SMIT expression is upregulated by osmotic stress and it does not seem to contribute to the regulation of the PIns pathway in neurons. In contrast, HMIT is a neuronal transporter, expressed predominantly in the brain and at very low levels in the periphery, therefore representing a potential therapeutic target for mood disorders. HMIT is expressed in endosomal compartments and is thought to translocate to the plasma membrane in an activity-dependent manner. However, little information on HMIT neuronal localisation in resting and/or activated cells is available at present and it is critical to determine whether this transporter is expressed at the plasma membrane, where it could transport inositol from the CSF. It is also not known at present whether HMIT is regulated directly by mood stabilizers. In this thesis I have shown that primary neurons do not express SMIT1 or SMIT2 mRNA, but they express both HMIT mRNA and protein. In future studies it will be worth investigating the role of this transporter in mood stabilization and in the mechanism of action of mood stabilizers.

Another component of the PIns pathway that seems to be of therapeutic interest is the enzyme PO. PO null-mutant mice have been extensively characterised behaviourally and neurochemically at GlaxoSmithKline. They did not show any gross abnormalities in behaviour (e.g. locomotor activity, forced swim, PPI tests) or in brain monoamine levels. It would be interesting to analyse further their behaviour in stressful conditions or by crossing the mutant into a different strain. Analysis of mouse growth cone morphology in wild-type sensory neurons showed PO inhibitors to reverse the effect of mood stabilizers on the percentage of collapse, mimicking addition of *myo*-inositol. PO inhibitors have been reported to increase IP_3 levels (two-fold) in cells, therefore suggesting that PO modulates the PIns pathway. However, the biological significance of a two-fold change in IP_3 levels is unclear. Moreover, PO inhibitors reversed the effects of lithium on CDP-DAG accumulation in neurons (Thomas J. & Mudge A.W. personal communication). Growth cones from the PO null-mutant mice were analysed with the hypothesis that their morphology would have been resistant to the drug effects. Unexpectedly, PO null-mutant sensory neurons showed increased growth cone area and decreased percentage of collapse - two parameters that were measured independently. Moreover, treatment of the PO null-mutant cultures with the mood stabilizers lithium or VPA or CBZ did not alter the morphology any further. These data suggest that PO is critical for growth cone morphology and that mood stabilizers modulate a pathway that is common to PO.

Treatment of PO null-mutant cultures with inositol did not alter the percentage of collapse, in contrast to the effect observed in wild-type cultures treated with mood stabilizers, where inositol reversed the drug effects. We have measured inositol levels in the PO null-mutant brain and sensory explants and no differences were observed when compared with wild-type. It is possible that inositol levels themselves do not change, but it would be worth analysing levels/turnover of other inositol phosphates. Interestingly, lithium induced accumulation of CDP-DAG levels in the PO null-mutant neurons, as well as it did in wild-type neurons (Thomas J. & Mudge A.W. personal communication), suggesting that the PIns signalling is functional in the PO null-mutant mouse; however, lithium's concentration response in the PO null-mutant neurons was altered, indicating that the pathway is somehow compromised. Further studies are required in order to explain these observations.

Viral rescue studies were subsequently performed using an adenovirus expressing native PO. PO protein expression could be restored transducing PO null-mutant sensory explants with an adenovirus containing native PO or an adenovirus containing a catalytically-dead PO. PO activity was also restored with the PO native enzyme, but not with the catalytically-dead PO. Transduction with native or catalytically-dead PO virus induced a statistically significant increase in the percentage of growth cone collapse when compared with PO null-mutant neurons. These results propose that PO has a central role in growth cone morphology and that the enzymatic activity on its own is not critical for growth cone morphology. Moreover, it is possible that the alterations in growth cone morphology may be due to alterations in protein interaction with GAP43.

Questions that should be addressed in future experiments are:

- Can a mood stabilizer modulate the growth cone morphology in PO null-mutant neurons transduced with catalytically-dead PO?- *this would indicate that PO enzymatic activity is not key for the drug action*
- Do PO inhibitors modulate the growth cone morphology in PO null-mutant neurons transduced with catalytically-dead PO and treated with a mood stabilizer? – *this would indicate that PO inhibitors act at other sites apart from the catalytic one*
- Do mood stabilizers and PO inhibitors modulate PO-GAP43 interaction directly? - *this would indicate that drugs able to alter PO protein interactions should be designed*
- What is the cellular phenotype of neurons over-expressing PO? Is the percentage of collapse increased? – *this would strenghten our finding that PO is a key modulator of growth cone morphology*
- Is neurotransmitter release (e.g. measured using the lipophilic dye FM4-64) affected in the PO null-mutant mouse? – *the PIns signalling pathway modulates neurotranmitter release, therefore it is possible that this is altered in the PO null-mutant brain*

The growth cone alterations observed in the PO null-mutant neurons and the PO interaction with GAP43 provide novelty in that they highlight PO intracellular functions and thus move away from the proteolysis of neuropeptide theory that has dominated the PO field. While it is possible that PO cleaves peptides in the extracellular space, this would be restricted to the blood compartment only, where a PO-related enzyme ZIP exists. GAP43 may interact with inositol phospholipids and regulate actin dynamics. It seems likely, therefore, that PO modulates growth cone function via its interaction with GAP43.

To conclude, there is great need to develop better treatments for BD. New targets should be identified in the PIns pathway. PO is a candidate target and understanding of its site of action in the pathway is critical. Inositol transporters, in particular HMIT, also represent a tractable and interesting drug target and future experiments should address this hypothesis.

SUPPLEMENTARY
Other pathways implicated in BD and in the mechanism of action of mood stabilizers

The biogenic amine neurotransmitter systems have long been implicated in the pathophysiology of BD, but there is still controversy as to whether dysregulation of these systems exerts a primary role in the illness. I will briefly review the key reports of mood stabilizers on the main neurotransmitters in the brain.

Lithium affects the release of glutamate, serotonin (5-HT), and the activity of GABA receptors among others (Price & Heninger, 1994). Lithium has been reported to increase extracellular glutamate in monkey and in mouse cerebral cortical slices (Dixon *et al.*, 1994; Dixon & Hokin, 1998), perhaps by inhibiting presynaptic glutamate reuptake (Dixon & Hokin, 1998). Intriguingly, VPA can also increase extracellular glutamate by a mechanism that stimulates glutamate release (Dixon & Hokin, 1997). Glutamate activates NMDA receptors which, through the activation of PKC, leads to the accumulation of IP_3 in post-synaptic cells (Dixon *et al.*, 1994). Interestingly, it has been shown very recently that chronic treatment with LiCl and VPA also reduces synaptic expression of the AMPA (amino-3-hydroxy-5-methylisoxazole-4-propionic acid) receptor subunit GluR1 in the hippocampus, while treatment with the antidepressant imipramine enhances the synaptic expression of GluR1. Interestingly, LTG, which has a predominant antidepressant effect in BD, significantly enhanced the surface expression of GluR1 and GluR2 in a time - and concentration-dependent manner in cultured hippocampal neurons. This finding mimics the effects of the antidepressant drug imipramine and it is in contrast to VPA, which significantly reduces surface expression of GluR1 and GluR2. Regulation of GluR1/2 surface levels and function have therefore been suggested to be responsible for the different clinical profile of anticonvulsant drugs (antimanic or antidepressants) (Du *et al.*, 2006).

Lithium increases inhibitory neurotransmitter GABA signalling during chronic treatment by increasing the levels of $GABA_B$ receptors in the rat hippocampus (Motohashi, 1992). VPA also increases GABA neurotransmission by directly inhibiting enzymes that modulate GABA levels. In particular, VPA inhibits GABA transaminase *in vitro*, an enzyme involved in degrading GABA to succinic semialdehyde, and it also inhibits succinate semialdhyde dehydrogenase. Moreover, VPA increases GABA synthesis by activating glutamic acid decarboxylase, an enzyme that converts glutamic acid to GABA

(Johannessen, 2000). However, inhibition/activation of these enzymes *in vivo* has yet to be demonstrated.

Electrophysiological studies have shown that lithium increases the release of 5-HT to the synapse, possibly by inhibiting 5-HT1_A autoreceptors (Haddjeri *et al.*, 2000), which are localised on the soma and dendrites of 5-HT neurons and control their firing. Also 5-HT1_B receptors are localised on presynaptic neuron terminals and control 5-HT release. Activation of 5-HT1_B autoreceptors decreases release of 5-HT to the synaptic cleft. Massot *et al.* have shown that therapeutic concentrations of lithium, but not other metallic cations, induced specific inhibition of 5-HT1_B receptor binding in a membrane preparation (Massot *et al.*, 1999). Lithium has been shown to induce antidepressant effects in the mouse forced swim test and this effect has been suggested to be mediated by 5-HT1_B receptors (Redrobe & Bourin, 1999). However, other studies have related it to GSK3 inhibition. In fact, GSK3 heterozygote mice showed antidepressant-like effects in the forced swim test that were mimicked by potent GSK3 inhibitors (Gould *et al.*, 2004; O'Brien *et al.*, 2004).

Other pathways/signalling components not described in this thesis that deserve further study are briefly outlined below.

Lithium, VPA and CBZ have been shown to affect the arachidonic acid (AA) signalling pathway by modulating key molecules. AA is an important second messenger, which consists of a polyunsaturated fatty acid, esterified at the sn-2 position of phospholipids. Lithium, as well as VPA, have been shown to reduce specifically the turnover rate of AA (by 80% and 28-33%, respectively) in rat brain phospholipids (Chang *et al.*, 2001). Reduced AA turnover is accompanied by down-regulation of gene expression and protein levels of the AA-specific cytosolic phospholipase A2 (cPLA(2)). VPA, however, has no effect on cPLA(2) protein levels (Chang *et al.*, 2001; Rapoport & Bosetti, 2002). Moreover, chronic lithium administration to rats significantly reduces brain protein levels and enzyme activity of cyclooxygenase-2 (COX-2), without affecting COX-2 mRNA or COX-1. Lithium also reduces the brain concentration of prostaglandin E(2) (PGE(2)), a bioactive product of AA formed via the COX reaction (Bosetti *et al.*, 2002). VPA, instead, when chronically administered to rats significantly reduced brain protein levels of COX-1, as well as of COX-2, without altering the mRNA levels of these enzymes. COX activity

was also decreased, as were the brain concentrations of 11-dehydrothromboxane B2 and PGE2 (Bosetti *et al.*, 2003). Chronic treatment with CBZ also induced a decrease in PLA(2) activity, protein and mRNA levels in rat brain. COX activity was decreased in CBZ-treated rats, but COX-1 or COX-2 protein levels did not change. Brain PGE(2) concentration was also reduced. The protein levels of other AA metabolizing enzymes, 5-lipoxygenase and cytochrome P450 epoxygenase, were not significantly altered after CBZ treatment nor was the brain concentration of the 5-lipoxygenase product leukotriene B(4) (Ghelardoni *et al.*, 2004). Overall, each mood stabilizer affects the AA pathway, but the molecules involved are not always the same. However, the general effect produced by the drugs is down-regulation of the AA signalling. It is possible, therefore, that drugs that are effective in BD mania may act by downregulating the incorporation and turnover of AA (20:4n-6), but not of docosahexaenoic acid (DHA, 22:6n-3) in brain phospholipids (Bazinet *et al.*, 2005). Further studies are required in order to validate and extend these findings.

Another area of research that deserves attention is represented by the circadian clock. There are lines of evidence that circadian rhythms may be altered in BD e.g. sleep disturbances and precipitation of mania due to changes of time zones. Circadian rhythm affects many aspects of behaviour and physiology, including sleep-wake cycle, blood pressure, body temperature and metabolism. The central clock lies in the suprachiasmatic nucleus of the hypothalamus, which is reset daily by light, but peripheral clocks exist (e.g. liver). Chronotherapy, which consists of sleep deprivation and exposure to light, is currently used, in combination with drugs, to treat BD with very promising results (Pontiggia *et al.*, 2006). Among clock proteins, several transcription factors have been identified, such as CLOCK and PER. Interestingly, a recent study reported that the nuclear receptor Rev-ErbAα is a direct target of lithium, probably via GSK3 inhibition (Yin *et al.*, 2006). GSK3, in fact, phosphorylates and stabilises Rev-ErbAα. Lithium treatment, by inhibiting GSK3, therefore induces rapid proteosomal degradation of Rev-ErbAα and activation of the clock gene Bmal1. It is interesting to note that lithium affected Rev-ErbAα at 10 mM, but also at the therapeutic concentration of 1 mM. Genetic studies are also suggesting that some genes involved in circadian rhythm regulation may be modulated in BD (Nievergelt *et al.*, 2006; Mansour *et al.*, 2006; Mansour *et al.*, 2005), but these are

preliminary findings that remain to be confirmed in larger populations. Studies on circadian rhythms may reveal new therapeutic targets.

Word count: ~37,000

Please note that some of the work with mood stabilizers and ERK/MAPK had started before the registration for a PhD. However, additional experiments were performed after enrolling for the PhD. Due to the different focus of the study I have inserted the data as a supplementary publication.

PUBLICATIONS FROM THESIS RESEARCH

FULL PAPERS

Di Daniel E., Mudge A.W., Maycox P.R. Comparative analysis of the effects of four mood stabilizers in SH-SY5Y cells and in primary neurons. Bipolar Disorders 2005 Feb; 7(1):33-41.

Di Daniel E., Cheng L., Maycox P.R., Mudge A.W. The common inositol-reversible effect of mood stabilizers on neurons does not involve GSK3 inhibition, *myo*-inositol-1-phosphate synthase, or the sodium-dependent *myo*-inositol transporters. MCN 2006 May-Jun; 32(1-2):27-36.

ABSTRACTS

Di Daniel E., Tacconi S., Mudge A.W., Maycox P.R. Characterisation of prolyl oligopeptidase expression and activity-studies with a null mutant mouse – Poster presented at Society for Neuroscience, San Diego, 2004.

Di Daniel E., Mudge A.W., Maycox P.R. Neurons from prolyl oligopeptidase (PO) null mice have altered responses to mood stabilising drugs – Poster presented at Society for Neuroscience, Washinghton DC, 2005.

Di Daniel E., Mudge A.W., Maycox P.R. Analysis of prolyl oligopeptidase as a target for bipolar disorder-characterisation of PO null-mutant mice – Poster presented at ECNP, Nice, 2006.

Di Daniel E., White J., Sanderson H., Mudge A.W., Maycox P.R. A potential mechanism for the action of mood stabilizers involves prolyl oligopeptidase and its interaction with growth-associated protein-43 – Poster presented at the 2nd Biennial Conference for the International Society of Bipolar Disorder, Edinburgh, 2006.

REFERENCES

Adams, J. M. & Cory, S. (1998). The Bcl-2 protein family: arbiters of cell survival. *Science* **281**, 1322-1326.

Agam, G., Shamir, A., Shaltiel, G., & Greenberg, M. L. (2002). Myo-inositol-1-phosphate (MIP) synthase: a possible new target for antibipolar drugs. *Bipolar.Disord.* **4 Suppl 1**, 15-20.

Agirregoitia, N., Irazusta, A., Ruiz, F., Irazusta, J., & Gil, J. (2003). Ontogeny of soluble and particulate prolyl endopeptidase activity in several areas of the rat brain and in the pituitary gland. *Dev.Neurosci.* **25**, 316-323.

Agranoff, B. W. & Fisher, S. K. (2001). Inositol, lithium, and the brain. *Psychopharmacol.Bull.* **35**, 5-18.

Aigner, L., Arber, S., Kapfhammer, J. P., Laux, T., Schneider, C., Botteri, F., Brenner, H. R., & Caroni, P. (1995). Overexpression of the neural growth-associated protein GAP-43 induces nerve sprouting in the adult nervous system of transgenic mice. *Cell* **83**, 269-278.

Aigner, L. & Caroni, P. (1993). Depletion of 43-kD growth-associated protein in primary sensory neurons leads to diminished formation and spreading of growth cones. *J.Cell Biol.* **123**, 417-429.

Ali, A., Hoeflich, K. P., & Woodgett, J. R. (2001). Glycogen synthase kinase-3: properties, functions, and regulation. *Chem.Rev.* **101**, 2527-2540.

Allison, J. H. & Stewart, M. A. (1971). Reduced brain inositol in lithium-treated rats. *Nat.New Biol.* **233**, 267-268.

Altshuler, L. L., Post, R. M., Leverich, G. S., Mikalauskas, K., Rosoff, A., & Ackerman, L. (1995). Antidepressant-induced mania and cycle acceleration: a controversy revisited. *Am.J.Psychiatry* **152**, 1130-1138.

Altshuler, L. L., Ventura, J., van Gorp, W. G., Green, M. F., Theberge, D. C., & Mintz, J. (2004). Neurocognitive function in clinically stable men with bipolar I disorder or schizophrenia and normal control subjects. *Biol.Psychiatry* **56**, 560-569.

Atack, J. R., Broughton, H. B., & Pollack, S. J. (1995). Structure and mechanism of inositol monophosphatase. *FEBS Lett.* **361**, 1-7.

Atack, J. R., Cook, S. M., Watt, A. P., Fletcher, S. R., & Ragan, C. I. (1993). In vitro and in vivo inhibition of inositol monophosphatase by the bisphosphonate L-690,330. *J.Neurochem.* **60**, 652-658.

Atack, J. R., Prior, A. M., Fletcher, S. R., Quirk, K., McKernan, R., & Ragan, C. I. (1994). Effects of L-690,488, a prodrug of the bisphosphonate inositol monophosphatase inhibitor L-690,330, on phosphatidylinositol cycle markers. *J.Pharmacol.Exp.Ther.* **270**, 70-76.

Badenhop, R. F., Moses, M. J., Scimone, A., Mitchell, P. B., Ewen-White, K. R., Rosso, A., Donald, J. A., Adams, L. J., & Schofield, P. R. (2002). A genome screen of 13 bipolar affective disorder pedigrees provides evidence for susceptibility loci on chromosome 3 as well as chromosomes 9, 13 and 19. *Mol.Psychiatry* **7**, 851-859.

Badner, J. A. & Gershon, E. S. (2002). Meta-analysis of whole-genome linkage scans of bipolar disorder and schizophrenia. *Mol.Psychiatry* **7**, 405-411.

Barelli, H., Petit, A., Hirsch, E., Wilk, S., De Nanteuil, G., Morain, P., & Checler, F. (1999). S 17092-1, a highly potent, specific and cell permeant inhibitor of human proline endopeptidase. *Biochem.Biophys.Res.Commun.* **257**, 657-661.

Barrett, T. B., Hauger, R. L., Kennedy, J. L., Sadovnick, A. D., Remick, R. A., Keck, P. E., McElroy, S. L., Alexander, M., Shaw, S. H., & Kelsoe, J. R. (2003). Evidence that a single nucleotide polymorphism in the promoter of the G protein receptor kinase 3 gene is associated with bipolar disorder. *Mol.Psychiatry* **8**, 546-557.

Batty, I. H. & Downes, C. P. (1995). The mechanism of muscarinic receptor-stimulated phosphatidylinositol resynthesis in 1321N1 astrocytoma cells and its inhibition by Li+. *J.Neurochem.* **65**, 2279-2289.

Bazinet, R. P., Rao, J. S., Chang, L., Rapoport, S. I., & Lee, H. J. (2005). Chronic valproate does not alter the kinetics of docosahexaenoic acid within brain phospholipids of the unanesthetized rat. *Psychopharmacology (Berl)* **182**, 180-185.

Bebchuk, J. M., Arfken, C. L., Dolan-Manji, S., Murphy, J., Hasanat, K., & Manji, H. K. (2000). A preliminary investigation of a protein kinase C inhibitor in the treatment of acute mania. *Arch.Gen.Psychiatry* **57**, 95-97.

Bellemere, G., Vaudry, H., Mounien, L., Boutelet, I., & Jegou, S. (2004). Localization of the mRNA encoding prolyl endopeptidase in the rat brain and pituitary. *J.Comp Neurol.* **471**, 128-143.

Benedetti, F., Bernasconi, A., Lorenzi, C., Pontiggia, A., Serretti, A., Colombo, C., & Smeraldi, E. (2004a). A single nucleotide polymorphism in glycogen synthase kinase 3-beta promoter gene influences onset of illness in patients affected by bipolar disorder. *Neurosci.Lett.* **355**, 37-40.

Benedetti, F., Serretti, A., Colombo, C., Lorenzi, C., Tubazio, V., & Smeraldi, E. (2004b). A glycogen synthase kinase 3-beta promoter gene single nucleotide polymorphism is associated with age at onset and response to total sleep deprivation in bipolar depression. *Neurosci.Lett.* **368**, 123-126.

Benedetti, F., Serretti, A., Pontiggia, A., Bernasconi, A., Lorenzi, C., Colombo, C., & Smeraldi, E. (2005). Long-term response to lithium salts in bipolar illness is influenced by the glycogen synthase kinase 3-beta -50 T/C SNP. *Neurosci.Lett.* **376**, 51-55.

Bennett, M., Onnebo, S. M., Azevedo, C., & Saiardi, A. (2006). Inositol pyrophosphates: metabolism and signaling. *Cell Mol.Life Sci.* **63**, 552-564.

Benowitz, L. I. & Routtenberg, A. (1997). GAP-43: an intrinsic determinant of neuronal development and plasticity. *Trends Neurosci.* **20**, 84-91.

Berrettini, W. H., Ferraro, T. N., Goldin, L. R., Weeks, D. E., Detera-Wadleigh, S., Nurnberger, J. I., Jr., & Gershon, E. S. (1994). Chromosome 18 DNA markers and manic-depressive illness: evidence for a susceptibility gene. *Proc.Natl.Acad.Sci.U.S.A* **91**, 5918-5921.

Berridge, M. J., Downes, C. P., & Hanley, M. R. (1989). Neural and developmental actions of lithium: a unifying hypothesis. *Cell* **59**, 411-419.

Berridge, M. J. & Irvine, R. F. (1989). Inositol phosphates and cell signalling. *Nature* **341**, 197-205.

Berry, G. T., Wu, S., Buccafusca, R., Ren, J., Gonzales, L. W., Ballard, P. L., Golden, J. A., Stevens, M. J., & Greer, J. J. (2003). Loss of murine Na+/myo-inositol cotransporter leads to brain myo-inositol depletion and central apnea. *J.Biol.Chem.* **278**, 18297-18302.

Bhagwagar, Z. & Goodwin, G. M. (2005). Lamotrigine in the treatment of bipolar disorder. *Expert.Opin.Pharmacother.* **6**, 1401-1408.

Bianchi, M., Hagan, J. J., & Heidbreder, C. A. (2005). Neuronal plasticity, stress and depression: involvement of the cytoskeletal microtubular system? *Curr.Drug Targets.CNS.Neurol.Disord.* **4**, 597-611.

Bijur, G. N., De Sarno, P., & Jope, R. S. (2000). Glycogen synthase kinase-3beta facilitates staurosporine- and heat shock-induced apoptosis. Protection by lithium. *J.Biol.Chem.* **275**, 7583-7590.

Birney, Y. A. & O'Connor, B. F. (2001). Purification and characterization of a Z-pro-prolinal-insensitive Z-Gly-Pro-7-amino-4-methyl coumarin-hydrolyzing peptidase from bovine serum--a new proline-specific peptidase. *Protein Expr.Purif.* **22**, 286-298.

Bissonnette, P., Coady, M. J., & Lapointe, J. Y. (2004). Expression of the sodium-myo-inositol cotransporter SMIT2 at the apical membrane of Madin-Darby canine kidney cells. *J.Physiol* **558**, 759-768.

Blackwood, D. H., He, L., Morris, S. W., McLean, A., Whitton, C., Thomson, M., Walker, M. T., Woodburn, K., Sharp, C. M., Wright, A. F., Shibasaki, Y., St Clair, D. M., Porteous, D. J., & Muir, W. J. (1996). A locus for bipolar affective disorder on chromosome 4p. *Nat.Genet.* **12**, 427-430.

Blehar, M. C., DePaulo, J. R., Jr., Gershon, E. S., Reich, T., Simpson, S. G., & Nurnberger, J. I., Jr. (1998). Women with bipolar disorder: findings from the NIMH Genetics Initiative sample. *Psychopharmacol.Bull.* **34**, 239-243.

Bosetti, F., Rintala, J., Seemann, R., Rosenberger, T. A., Contreras, M. A., Rapoport, S. I., & Chang, M. C. (2002). Chronic lithium downregulates cyclooxygenase-2 activity and prostaglandin E(2) concentration in rat brain. *Mol.Psychiatry* **7**, 845-850.

Bosetti, F., Weerasinghe, G. R., Rosenberger, T. A., & Rapoport, S. I. (2003). Valproic acid down-regulates the conversion of arachidonic acid to eicosanoids via cyclooxygenase-1 and -2 in rat brain. *J.Neurochem.* **85**, 690-696.

Bottenstein, J. E. & Sato, G. H. (1979). Growth of a rat neuroblastoma cell line in serum-free supplemented medium. *Proc.Natl.Acad.Sci.U.S.A* **76**, 514-517.

Bowden, C. L. (1996). Dosing strategies and time course of response to antimanic drugs. *J.Clin.Psychiatry* **57 Suppl 13**, 4-9.

Bowden, C. L. (1998). New concepts in mood stabilization: evidence for the effectiveness of valproate and lamotrigine. *Neuropsychopharmacology* **19**, 194-199.

Bowden, C. L., Brugger, A. M., Swann, A. C., Calabrese, J. R., Janicak, P. G., Petty, F., Dilsaver, S. C., Davis, J. M., Rush, A. J., Small, J. G., & . (1994). Efficacy of divalproex vs lithium and placebo in the treatment of mania. The Depakote Mania Study Group. *JAMA* **271**, 918-924.

Breen, G., Harwood, A. J., Gregory, K., Sinclair, M., Collier, D., St Clair, D., & Williams, R. S. (2004). Two peptidase activities decrease in treated bipolar disorder not schizophrenic patients. *Bipolar.Disord.* **6**, 156-161.

Brewer, G. J., Torricelli, J. R., Evege, E. K., & Price, P. J. (1993). Optimized survival of hippocampal neurons in B27-supplemented Neurobasal, a new serum-free medium combination. *J.Neurosci.Res.* **35**, 567-576.

Brose, N., Betz, A., & Wegmeyer, H. (2004). Divergent and convergent signaling by the diacylglycerol second messenger pathway in mammals. *Curr.Opin.Neurobiol.* **14**, 328-340.

Bruno, V., Sortino, M. A., Scapagnini, U., Nicoletti, F., & Canonico, P. L. (1995). Antidegenerative effects of Mg(2+)-valproate in cultured cerebellar neurons. *Funct.Neurol.* **10**, 121-130.

Calabrese, B. and Halpain, S. Role of phosphatidylinositol-4,5-bisphosphate in maintaining dendritic spine morphology. Program No: 34.16, 2006 Abstract. Atlanta, Society for Neuroscience, 2006.

Calabrese, J. R., Fatemi, S. H., & Woyshville, M. J. (1996). Antidepressant effects of lamotrigine in rapid cycling bipolar disorder. *Am.J.Psychiatry* **153**, 1236.

Calabrese, J. R., Goldberg, J. F., Ketter, T. A., Suppes, T., Frye, M., White, R., DeVeaugh-Geiss, A., & Thompson, T. R. (2006). Recurrence in bipolar I disorder: a post hoc analysis excluding relapses in two double-blind maintenance studies. *Biol.Psychiatry* **59**, 1061-1064.

Calabrese, J. R. & Rapport, D. J. (1999). Mood stabilizers and the evolution of maintenance study designs in bipolar I disorder. *J.Clin.Psychiatry* **60 Suppl 5**, 5-13.

Calabrese, J. R., Shelton, M. D., Rapport, D. J., Kimmel, S. E., & Elhaj, O. (2002). Long-term treatment of bipolar disorder with lamotrigine. *J.Clin.Psychiatry* **63 Suppl 10**, 18-22.

Calabrese, J. R., Vieta, E., & Shelton, M. D. (2003). Latest maintenance data on lamotrigine in bipolar disorder. *Eur.Neuropsychopharmacol.* **13 Suppl 2**, S57-S66.

Calabrese, J. R. & Woyshville, M. J. (1995). Lithium therapy: limitations and alternatives in the treatment of bipolar disorders. *Ann.Clin.Psychiatry* **7**, 103-112.

Caroni, P. (2001). New EMBO members' review: actin cytoskeleton regulation through modulation of PI(4,5)P(2) rafts. *EMBO J.* **20**, 4332-4336.

Chadborn, N. H., Ahmed, A. I., Holt, M. R., Prinjha, R., Dunn, G. A., Jones, G. E., & Eickholt, B. J. (2006). PTEN couples Sema3A signalling to growth cone collapse. *J.Cell Sci.* **119**, 951-957.

Chalecka-Franaszek, E. & Chuang, D. M. (1999). Lithium activates the serine/threonine kinase Akt-1 and suppresses glutamate-induced inhibition of Akt-1 activity in neurons. *Proc.Natl.Acad.Sci.U.S.A* **96**, 8745-8750.

Chang, M. C., Contreras, M. A., Rosenberger, T. A., Rintala, J. J., Bell, J. M., & Rapoport, S. I. (2001). Chronic valproate treatment decreases the in vivo turnover of arachidonic acid in brain phospholipids: a possible common effect of mood stabilizers. *J.Neurochem.* **77**, 796-803.

Chau, J. F., Lee, M. K., Law, J. W., Chung, S. K., & Chung, S. S. (2005). Sodium/myo-inositol cotransporter-1 is essential for the development and function of the peripheral nerves. *FASEB J.* **19**, 1887-1889.

Chen, G., Huang, L. D., Jiang, Y. M., & Manji, H. K. (1999a). The mood-stabilizing agent valproate inhibits the activity of glycogen synthase kinase-3. *J.Neurochem.* **72**, 1327-1330.

Chen, G., Manji, H. K., Hawver, D. B., Wright, C. B., & Potter, W. Z. (1994). Chronic sodium valproate selectively decreases protein kinase C alpha and epsilon in vitro. *J.Neurochem.* **63**, 2361-2364.

Chen, G., Masana, M. I., & Manji, H. K. (2000a). Lithium regulates PKC-mediated intracellular cross-talk and gene expression in the CNS in vivo. *Bipolar.Disord.* **2**, 217-236.

Chen, G., Rajkowska, G., Du, F., Seraji-Bozorgzad, N., & Manji, H. K. (2000b). Enhancement of hippocampal neurogenesis by lithium. *J.Neurochem.* **75**, 1729-1734.

Chen, G., Zeng, W. Z., Yuan, P. X., Huang, L. D., Jiang, Y. M., Zhao, Z. H., & Manji, H. K. (1999b). The mood-stabilizing agents lithium and valproate robustly increase the levels of the neuroprotective protein bcl-2 in the CNS. *J.Neurochem.* **72**, 879-882.

Chen, R. W. & Chuang, D. M. (1999). Long term lithium treatment suppresses p53 and Bax expression but increases Bcl-2 expression. A prominent role in neuroprotection against excitotoxicity. *J.Biol.Chem.* **274**, 6039-6042.

Chen, Y. S., Akula, N., Detera-Wadleigh, S. D., Schulze, T. G., Thomas, J., Potash, J. B., DePaulo, J. R., McInnis, M. G., Cox, N. J., & McMahon, F. J. (2004). Findings in an independent sample support an association between bipolar affective disorder and the G72/G30 locus on chromosome 13q33. *Mol.Psychiatry* **9**, 87-92.

Cheng, L., Lumb, M., Polgar, L., & Mudge, A. W. (2005). How can the mood stabilizer VPA limit both mania and depression? *Mol.Cell Neurosci.* **29**, 155-161.

Cheng, L. & Mudge, A. W. (1996). Cultured Schwann cells constitutively express the myelin protein P0. *Neuron* **16**, 309-319.

Cho, J. H. & Johnson, G. V. (2003). Glycogen synthase kinase 3beta phosphorylates tau at both primed and unprimed sites. Differential impact on microtubule binding. *J.Biol.Chem.* **278**, 187-193.

Chong, L. D., Traynor-Kaplan, A., Bokoch, G. M., & Schwartz, M. A. (1994). The small GTP-binding protein Rho regulates a phosphatidylinositol 4-phosphate 5-kinase in mammalian cells. *Cell* **79**, 507-513.

Coady, M. J., Wallendorff, B., Gagnon, D. G., & Lapointe, J. Y. (2002). Identification of a novel Na+/myo-inositol cotransporter. *J.Biol.Chem.* **277**, 35219-35224.

Cockcroft, S. (2001). Phosphatidylinositol transfer proteins couple lipid transport to phosphoinositide synthesis. *Semin.Cell Dev.Biol.* **12**, 183-191.

Craddock, N., Dawson, E., Burge, S., Parfitt, L., Mant, B., Roberts, Q., Daniels, J., Gill, M., McGuffin, P., Powell, J., & . (1993). The gene for Darier's disease maps to chromosome 12q23-q24.1. *Hum.Mol.Genet.* **2**, 1941-1943.

Craddock, N. & Forty, L. (2006). Genetics of affective (mood) disorders. *Eur.J.Hum.Genet.* **14**, 660-668.

Craddock, N., O'Donovan, M. C., & Owen, M. J. (2005). The genetics of schizophrenia and bipolar disorder: dissecting psychosis. *J.Med.Genet.* **42**, 193-204.

Cross, D. A., Alessi, D. R., Cohen, P., Andjelkovich, M., & Hemmings, B. A. (1995). Inhibition of glycogen synthase kinase-3 by insulin mediated by protein kinase B. *Nature* **378**, 785-789.

Cross, D. A., Culbert, A. A., Chalmers, K. A., Facci, L., Skaper, S. D., & Reith, A. D. (2001). Selective small-molecule inhibitors of glycogen synthase kinase-3 activity protect primary neurones from death. *J.Neurochem.* **77**, 94-102.

Crowder, R. J. & Freeman, R. S. (2000). Glycogen synthase kinase-3 beta activity is critical for neuronal death caused by inhibiting phosphatidylinositol 3-kinase or Akt but not for death caused by nerve growth factor withdrawal. *J.Biol.Chem.* **275**, 34266-34271.

Cryns, K., Shamir, A., Shapiro, J., Daneels, G., Goris, I., Van Craenendonck, H., Straetemans, R., Belmaker, R. H., Agam, G., Moechars, D., & Steckler, T. (2006). Lack of Lithium-Like Behavioral and Molecular Effects in IMPA2 Knockout Mice. *Neuropsychopharmacology* 1-11.

Cunningham, D. F. & O'Connor, B. (1997). Identification and initial characterisation of a N-benzyloxycarbonyl-prolyl-prolinal (Z-Pro-prolinal)-insensitive 7-(N-benzyloxycarbonyl-glycyl-prolyl-amido)-4-methylcoumarin (Z-Gly-Pro-NH-Mec)-hydrolysing peptidase in bovine serum. *Eur.J.Biochem.* **244**, 900-903.

Dando, T. M. & Keating, G. M. (2006). Spotlight on quetiapine in acute mania and depression associated with bipolar disorder. *CNS.Drugs* **20**, 429-431.

De Sarno, P., Li, X., & Jope, R. S. (2002). Regulation of Akt and glycogen synthase kinase-3 beta phosphorylation by sodium valproate and lithium. *Neuropharmacology* **43**, 1158-1164.

Dent, E. W. & Kalil, K. (2001). Axon branching requires interactions between dynamic microtubules and actin filaments. *J.Neurosci.* **21**, 9757-9769.

Dent, E. W. & Meiri, K. F. (1998). Distribution of phosphorylated GAP-43 (neuromodulin) in growth cones directly reflects growth cone behavior. *J.Neurobiol.* **35**, 287-299.

Di Daniel, E., Cheng, L., Maycox, P. R., & Mudge, A. W. (2006). The common inositol-reversible effect of mood stabilizers on neurons does not involve GSK3 inhibition, myo-inositol-1-phosphate synthase or the sodium-dependent myo-inositol transporters. *Mol.Cell Neurosci.* **32**, 27-36.

Di Daniel, E., Mudge, A. W., & Maycox, P. R. (2005). Comparative analysis of the effects of four mood stabilizers in SH-SY5Y cells and in primary neurons. *Bipolar.Disord.* **7**, 33-41.

Di Paolo, G. & De Camilli, P. (2006). Phosphoinositides in cell regulation and membrane dynamics. *Nature* **443**, 651-657.

Dixon, J. F. & Hokin, L. E. (1997). The antibipolar drug valproate mimics lithium in stimulating glutamate release and inositol 1,4,5-trisphosphate accumulation in brain cortex slices but not accumulation of inositol monophosphates and bisphosphates. *Proc.Natl.Acad.Sci.U.S.A* **94**, 4757-4760.

Dixon, J. F. & Hokin, L. E. (1998). Lithium acutely inhibits and chronically up-regulates and stabilizes glutamate uptake by presynaptic nerve endings in mouse cerebral cortex. *Proc.Natl.Acad.Sci.U.S.A* **95**, 8363-8368.

Dixon, J. F., Los, G. V., & Hokin, L. E. (1994). Lithium stimulates glutamate "release" and inositol 1,4,5-trisphosphate accumulation via activation of the N-methyl-D-aspartate receptor in monkey and mouse cerebral cortex slices. *Proc.Natl.Acad.Sci.U.S.A* **91**, 8358-8362.

DSM-IV (2000). American Psychiatric Association: Diagnostic and Statistical Manual of Mental Disorders , Washington DC: APA ed.

Du, J., Suzuki, K., Wei, Y., Wang, Y., Blumenthal, R., Chen, Z., Falke, C., Zarate, C. A., Jr., & Manji, H. K. (2006). The Anticonvulsants Lamotrigine, Riluzole, and Valproate Differentially Regulate AMPA Receptor Membrane Localization: Relationship to Clinical Effects in Mood Disorders. *Neuropsychopharmacology* 1-10.

Duman, R. S., Malberg, J., Nakagawa, S., & D'Sa, C. (2000). Neuronal plasticity and survival in mood disorders. *Biol.Psychiatry* **48**, 732-739.

Egan, M. F., Kojima, M., Callicott, J. H., Goldberg, T. E., Kolachana, B. S., Bertolino, A., Zaitsev, E., Gold, B., Goldman, D., Dean, M., Lu, B., & Weinberger, D. R. (2003). The BDNF val66met polymorphism affects activity-dependent secretion of BDNF and human memory and hippocampal function. *Cell* **112**, 257-269.

Eickholt, B. J., Towers, G. J., Ryves, W. J., Eikel, D., Adley, K., Ylinen, L. M., Chadborn, N. H., Harwood, A. J., Nau, H., & Williams, R. S. (2005). Effects of valproic acid derivatives on inositol trisphosphate depletion, teratogenicity, glycogen synthase kinase-3beta inhibition, and viral replication: a screening approach for new bipolar disorder drugs derived from the valproic acid core structure. *Mol.Pharmacol.* **67**, 1426-1433.

Eickholt, B. J., Walsh, F. S., & Doherty, P. (2002). An inactive pool of GSK-3 at the leading edge of growth cones is implicated in Semaphorin 3A signaling. *J.Cell Biol.* **157**, 211-217.

Einat, H., Yuan, P., Gould, T. D., Li, J., Du, J., Zhang, L., Manji, H. K., & Chen, G. (2003). The role of the extracellular signal-regulated kinase signaling pathway in mood modulation. *J.Neurosci.* **23**, 7311-7316.

El Badri, S. M., Ashton, C. H., Moore, P. B., Marsh, V. R., & Ferrier, I. N. (2001). Electrophysiological and cognitive function in young euthymic patients with bipolar affective disorder. *Bipolar.Disord.* **3**, 79-87.

Fang, X., Yu, S. X., Lu, Y., Bast, R. C., Jr., Woodgett, J. R., & Mills, G. B. (2000). Phosphorylation and inactivation of glycogen synthase kinase 3 by protein kinase A. *Proc.Natl.Acad.Sci.U.S.A* **97**, 11960-11965.

Fink, M. (2006). ECT in therapy-resistant mania: does it have a place? *Bipolar.Disord.* **8**, 307-309.

Fisher, S. K., Novak, J. E., & Agranoff, B. W. (2002). Inositol and higher inositol phosphates in neural tissues: homeostasis, metabolism and functional significance. *J.Neurochem.* **82**, 736-754.

Fujita, Y., Sasaki, T., Fukui, K., Kotani, H., Kimura, T., Hata, Y., Sudhof, T. C., Scheller, R. H., & Takai, Y. (1996). Phosphorylation of Munc-18/n-Sec1/rbSec1 by protein kinase C: its implication in regulating the interaction of Munc-18/n-Sec1/rbSec1 with syntaxin. *J.Biol.Chem.* **271**, 7265-7268.

Fulop, V., Bocskei, Z., & Polgar, L. (1998). Prolyl oligopeptidase: an unusual beta-propeller domain regulates proteolysis. *Cell* **94**, 161-170.

Fuxreiter, M., Magyar, C., Juhasz, T., Szeltner, Z., Polgar, L., & Simon, I. (2005). Flexibility of prolyl oligopeptidase: molecular dynamics and molecular framework analysis of the potential substrate pathways. *Proteins* **60**, 504-512.

Geddes, J. R., Goodwin, G. M., Huffman R, Paska W, Evoniuk G, & Leadbetter, R. (2006). Lamotrigine for acute treatment of bipolar depression: individual patient data meta-analysis of 5 randomized trials conducted by GSK. *Bipolar.Disord.* **8**, 32.

Gee, N. S., Ragan, C. I., Watling, K. J., Aspley, S., Jackson, R. G., Reid, G. G., Gani, D., & Shute, J. K. (1988). The purification and properties of myo-inositol monophosphatase from bovine brain. *Biochem.J.* **249**, 883-889.

Ghaemi, S. N. (2000). New treatments for bipolar disorder: the role of atypical neuroleptic agents. *J.Clin.Psychiatry* **61 Suppl 14**, 33-42.

Ghaemi, S. N. (2001). On defining 'mood stabilizer'. *Bipolar.Disord.* **3**, 154-158.

Ghaemi, S. N., Boiman, E. E., & Goodwin, F. K. (2000). Diagnosing bipolar disorder and the effect of antidepressants: a naturalistic study. *J.Clin.Psychiatry* **61**, 804-808.

Ghaemi, S. N., Hsu, D. J., Soldani, F., & Goodwin, F. K. (2003). Antidepressants in bipolar disorder: the case for caution. *Bipolar.Disord.* **5**, 421-433.

Ghaemi, S. N., Rosenquist, K. J., Ko, J. Y., Baldassano, C. F., Kontos, N. J., & Baldessarini, R. J. (2004). Antidepressant treatment in bipolar versus unipolar depression. *Am.J.Psychiatry* **161**, 163-165.

Ghelardoni, S., Tomita, Y. A., Bell, J. M., Rapoport, S. I., & Bosetti, F. (2004). Chronic carbamazepine selectively downregulates cytosolic phospholipase A2 expression and cyclooxygenase activity in rat brain. *Biol.Psychiatry* **56**, 248-254.

Goodwin, F. K. (2003). Rationale for using lithium in combination with other mood stabilizers in the management of bipolar disorder. *J.Clin.Psychiatry* **64 Suppl 5**, 18-24.

Goodwin, F. K. & Jamison, K. R. (1990). Manic-depressive illness, Oxford University Press ed. New York.

Goodwin, G. M., Bowden, C. L., Calabrese, J. R., Grunze, H., Kasper, S., White, R., Greene, P., & Leadbetter, R. (2004). A pooled analysis of 2 placebo-controlled 18-month

trials of lamotrigine and lithium maintenance in bipolar I disorder. *J.Clin.Psychiatry* **65**, 432-441.

Goodwin, G. M. & Young, A. H. (2003). The British Association for Psychopharmacology guidelines for treatment of bipolar disorder: a summary. *J.Psychopharmacol.* **17**, 3-6.

Goold, R. G., Owen, R., & Gordon-Weeks, P. R. (1999). Glycogen synthase kinase 3beta phosphorylation of microtubule-associated protein 1B regulates the stability of microtubules in growth cones. *J.Cell Sci.* **112 (Pt 19)**, 3373-3384.

Goossens, F., De, M., I, Vanhoof, G., Hendriks, D., Vriend, G., & Scharpe, S. (1995). The purification, characterization and analysis of primary and secondary-structure of prolyl oligopeptidase from human lymphocytes. Evidence that the enzyme belongs to the alpha/beta hydrolase fold family. *Eur.J.Biochem.* **233**, 432-441.

Goossens, F. J., Wauters, J. G., Vanhoof, G. C., Bossuyt, P. J., Schatteman, K. A., Loens, K., & Scharpe, S. L. (1996). Subregional mapping of the human lymphocyte prolyl oligopeptidase gene (PREP) to human chromosome 6q22. *Cytogenet.Cell Genet.* **74**, 99-101.

Gould, T. D., Einat, H., Bhat, R., & Manji, H. K. (2004). AR-A014418, a selective GSK-3 inhibitor, produces antidepressant-like effects in the forced swim test. *Int.J.Neuropsychopharmacol.* **7**, 387-390.

Gould, T. D. & Manji, H. K. (2005). Glycogen synthase kinase-3: a putative molecular target for lithium mimetic drugs. *Neuropsychopharmacology* **30**, 1223-1237.

Gow, I. F. & Ellis, D. (1996). Transmembrane movement of lithium ions in isolated sheep heart Purkinje fibres. *J.Mol.Cell Cardiol.* **28**, 299-310.

Grafe, P., Rimpel, J., Reddy, M. M., & ten Bruggencate, G. (1982). Lithium distribution across the membrane of motoneurons in the isolated frog spinal cord. *Pflugers Arch.* **393**, 297-301.

Green, E. & Craddock, N. (2003). Brain-derived neurotrophic factor as a potential risk locus for bipolar disorder: evidence, limitations, and implications. *Curr.Psychiatry Rep.* **5**, 469-476.

Green, E. K., Raybould, R., Macgregor, S., Gordon-Smith, K., Heron, J., Hyde, S., Grozeva, D., Hamshere, M., Williams, N., Owen, M. J., O'Donovan, M. C., Jones, L., Jones, I., Kirov, G., & Craddock, N. (2005). Operation of the schizophrenia susceptibility gene, neuregulin 1, across traditional diagnostic boundaries to increase risk for bipolar disorder. *Arch.Gen.Psychiatry* **62**, 642-648.

Green, E. K., Raybould, R., Macgregor, S., Hyde, S., Young, A. H., O'Donovan, M. C., Owen, M. J., Kirov, G., Jones, L., Jones, I., & Craddock, N. (2006). Genetic variation of brain-derived neurotrophic factor (BDNF) in bipolar disorder: case-control study of over 3000 individuals from the UK. *Br.J.Psychiatry* **188**, 21-25.

Greenwood, T. A., Schork, N. J., Eskin, E., & Kelsoe, J. R. (2006). Identification of additional variants within the human dopamine transporter gene provides further evidence for an association with bipolar disorder in two independent samples. *Mol.Psychiatry* **11**, 125-33, 115.

Grimes, C. A. & Jope, R. S. (2001). The multifaceted roles of glycogen synthase kinase 3beta in cellular signaling. *Prog.Neurobiol.* **65**, 391-426.

Guo, W., Shimada, S., Tajiri, H., Yamauchi, A., Yamashita, T., Okada, S., & Tohyama, M. (1997). Developmental regulation of Na+ / myo-inositol cotransporter gene expression. *Brain Res.Mol.Brain Res.* **51**, 91-96.

Gurvich, N., Berman, M. G., Wittner, B. S., Gentleman, R. C., Klein, P. S., & Green, J. B. (2005). Association of valproate-induced teratogenesis with histone deacetylase inhibition in vivo. *FASEB J.* **19**, 1166-1168.

Gutkind, J. S. (1998). The pathways connecting G protein-coupled receptors to the nucleus through divergent mitogen-activated protein kinase cascades. *J.Biol.Chem.* **273**, 1839-1842.

Haddjeri, N., Szabo, S. T., de Montigny, C., & Blier, P. (2000). Increased tonic activation of rat forebrain 5-HT(1A) receptors by lithium addition to antidepressant treatments. *Neuropsychopharmacology* **22**, 346-356.

Hall, A. C., Brennan, A., Goold, R. G., Cleverley, K., Lucas, F. R., Gordon-Weeks, P. R., & Salinas, P. C. (2002). Valproate regulates GSK-3-mediated axonal remodeling and synapsin I clustering in developing neurons. *Mol.Cell Neurosci.* **20**, 257-270.

Hall, A. C., Lucas, F. R., & Salinas, P. C. (2000). Axonal remodeling and synaptic differentiation in the cerebellum is regulated by WNT-7a signaling. *Cell* **100**, 525-535.

Hallcher, L. M. & Sherman, W. R. (1980). The effects of lithium ion and other agents on the activity of myo-inositol-1-phosphatase from bovine brain. *J.Biol.Chem.* **255**, 10896-10901.

Halstead, J. R., Jalink, K., & Divecha, N. (2005). An emerging role for PtdIns(4,5)P2-mediated signalling in human disease. *Trends Pharmacol.Sci.* **26**, 654-660.

Hao, Y., Creson, T., Zhang, L., Li, P., Du, F., Yuan, P., Gould, T. D., Manji, H. K., & Chen, G. (2004). Mood stabilizer valproate promotes ERK pathway-dependent cortical neuronal growth and neurogenesis. *J.Neurosci.* **24**, 6590-6599.

Harrison, D. C., Medhurst, A. D., Bond, B. C., Campbell, C. A., Davis, R. P., & Philpott, K. L. (2000). The use of quantitative RT-PCR to measure mRNA expression in a rat

model of focal ischemia--caspase-3 as a case study. *Brain Res.Mol.Brain Res.* **75**, 143-149.

Harwood, A. J. (2003). Neurodevelopment and mood stabilizers. *Curr.Mol.Med.* **3**, 472-482.

Harwood, A. J. (2005). Lithium and bipolar mood disorder: the inositol-depletion hypothesis revisited. *Mol.Psychiatry* **10**, 117-126.

Harwood, A. J. & Agam, G. (2003). Search for a common mechanism of mood stabilizers. *Biochem.Pharmacol.* **66**, 179-189.

Harwood, V. J., Denson, J. D., Robinson-Bidle, K. A., & Schreier, H. J. (1997). Overexpression and characterization of a prolyl endopeptidase from the hyperthermophilic archaeon Pyrococcus furiosus. *J.Bacteriol.* **179**, 3613-3618.

Hattori, E., Liu, C., Badner, J. A., Bonner, T. I., Christian, S. L., Maheshwari, M., Detera-Wadleigh, S. D., Gibbs, R. A., & Gershon, E. S. (2003). Polymorphisms at the G72/G30 gene locus, on 13q33, are associated with bipolar disorder in two independent pedigree series. *Am.J.Hum.Genet.* **72**, 1131-1140.

He, Q., Dent, E. W., & Meiri, K. F. (1997). Modulation of actin filament behavior by GAP-43 (neuromodulin) is dependent on the phosphorylation status of serine 41, the protein kinase C site. *J.Neurosci.* **17**, 3515-3524.

Heacock, A. M. & Agranoff, B. W. (1997). CDP-diacylglycerol synthase from mammalian tissues. *Biochim.Biophys.Acta* **1348**, 166-172.

Hedgepeth, C. M., Conrad, L. J., Zhang, J., Huang, H. C., Lee, V. M., & Klein, P. S. (1997). Activation of the Wnt signaling pathway: a molecular mechanism for lithium action. *Dev.Biol.* **185**, 82-91.

Hetman, M., Cavanaugh, J. E., Kimelman, D., & Xia, Z. (2000). Role of glycogen synthase kinase-3beta in neuronal apoptosis induced by trophic withdrawal. *J.Neurosci.* **20**, 2567-2574.

Horschitz, S., Hummerich, R., Lau, T., Rietschel, M., & Schloss, P. (2005). A dopamine transporter mutation associated with bipolar affective disorder causes inhibition of transporter cell surface expression. *Mol.Psychiatry* **10**, 1104-1109.

Hughes, K., Nikolakaki, E., Plyte, S. E., Totty, N. F., & Woodgett, J. R. (1993). Modulation of the glycogen synthase kinase-3 family by tyrosine phosphorylation. *EMBO J.* **12**, 803-808.

Ilouz, R., Kaidanovich, O., Gurwitz, D., & Eldar-Finkelman, H. (2002). Inhibition of glycogen synthase kinase-3beta by bivalent zinc ions: insight into the insulin-mimetic action of zinc. *Biochem.Biophys.Res.Commun.* **295**, 102-106.

Irazusta, J., Larrinaga, G., Gonzalez-Maeso, J., Gil, J., Meana, J. J., & Casis, L. (2002). Distribution of prolyl endopeptidase activities in rat and human brain. *Neurochem.Int.* **40**, 337-345.

Irvine, R. F. (2005). Inositide evolution - towards turtle domination? *J.Physiol* **566**, 295-300.

Irvine, R. F., Lloyd-Burton, S. M., Yu, J. C., Letcher, A. J., & Schell, M. J. (2006). The regulation and function of inositol 1,4,5-trisphosphate 3-kinases. *Adv.Enzyme Regul.* **46**, 314-323.

Jamison, K. R. (1995). Manic-depressive illness and creativity. *Sci.Am.* **272**, 62-67.

Jamison, K. R. (1996). Touched With Fire: Manic Depressive Illness and the Artistic Temperament, New York, The Free Press ed.

Jin, N., Kovacs, A. D., Sui, Z., Dewhurst, S., & Maggirwar, S. B. (2005). Opposite effects of lithium and valproic acid on trophic factor deprivation-induced glycogen synthase kinase-3 activation, c-Jun expression and neuronal cell death. *Neuropharmacology* **48**, 576-583.

Johannessen, C. U. (2000). Mechanisms of action of valproate: a commentatory. *Neurochem.Int.* **37**, 103-110.

Jope, R. S. (2003). Lithium and GSK-3: one inhibitor, two inhibitory actions, multiple outcomes. *Trends Pharmacol.Sci.* **24**, 441-443.

Jope, R. S. & Bijur, G. N. (2002). Mood stabilizers, glycogen synthase kinase-3beta and cell survival. *Mol.Psychiatry* **7 Suppl 1**, S35-S45.

Jope, R. S. & Johnson, G. V. (2004). The glamour and gloom of glycogen synthase kinase-3. *Trends Biochem.Sci.* **29**, 95-102.

Ju, S., Shaltiel, G., Shamir, A., Agam, G., & Greenberg, M. L. (2004). Human 1-D-myo-inositol-3-phosphate synthase is functional in yeast. *J.Biol.Chem.* **279**, 21759-21765.

Judd, L. L., Akiskal, H. S., Schettler, P. J., Coryell, W., Maser, J., Rice, J. A., Solomon, D. A., & Keller, M. B. (2003a). The comparative clinical phenotype and long term longitudinal episode course of bipolar I and II: a clinical spectrum or distinct disorders? *J.Affect.Disord.* **73**, 19-32.

Judd, L. L., Schettler, P. J., Akiskal, H. S., Maser, J., Coryell, W., Solomon, D., Endicott, J., & Keller, M. (2003b). Long-term symptomatic status of bipolar I vs. bipolar II disorders. *Int.J.Neuropsychopharmacol.* **6**, 127-137.

Juhasz, T., Szeltner, Z., Fulop, V., & Polgar, L. (2005). Unclosed beta-propellers display stable structures: implications for substrate access to the active site of prolyl oligopeptidase. *J.Mol.Biol.* **346**, 907-917.

Kakee, A., Takanaga, H., Hosoya, K., Sugiyama, Y., & Terasaki, T. (2002). In vivo evidence for brain-to-blood efflux transport of valproic acid across the blood-brain barrier. *Microvasc.Res.* **63**, 233-238.

Kalidas, S., Santosh, V., Shareef, M. M., Shankar, S. K., Christopher, R., & Shetty, K. T. (2000). Expression of p67 (Munc-18) in adult human brain and neuroectodermal tumors of human central nervous system. *Acta Neuropathol.(Berl)* **99**, 191-198.

Kato, T., Okada, M., & Nagatsu, T. (1980). Distribution of post-proline cleaving enzyme in human brain and the peripheral tissues. *Mol.Cell Biochem.* **32**, 117-121.

Kessing, L. V., Sondergard, L., Kvist, K., & Andersen, P. K. (2005). Suicide risk in patients treated with lithium. *Arch.Gen.Psychiatry* **62**, 860-866.

Kim, A. J., Shi, Y., Austin, R. C., & Werstuck, G. H. (2005a). Valproate protects cells from ER stress-induced lipid accumulation and apoptosis by inhibiting glycogen synthase kinase-3. *J.Cell Sci.* **118**, 89-99.

Kim, H., McGrath, B. M., & Silverstone, P. H. (2005b). A review of the possible relevance of inositol and the phosphatidylinositol second messenger system (PI-cycle) to psychiatric disorders--focus on magnetic resonance spectroscopy (MRS) studies. *Hum.Psychopharmacol.* **20**, 309-326.

Kim, W. Y., Zhou, F. Q., Zhou, J., Yokota, Y., Wang, Y. M., Yoshimura, T., Kaibuchi, K., Woodgett, J. R., Anton, E. S., & Snider, W. D. (2006). Essential roles for GSK-3s and GSK-3-primed substrates in neurotrophin-induced and hippocampal axon growth. *Neuron* **52**, 981-996.

Kimura, A., Yoshida, I., Takagi, N., & Takahashi, T. (1999). Structure and localization of the mouse prolyl oligopeptidase gene. *J.Biol.Chem.* **274**, 24047-24053.

Kitamura, H., Yamauchi, A., Sugiura, T., Matsuoka, Y., Horio, M., Tohyama, M., Shimada, S., Imai, E., & Hori, M. (1998). Inhibition of myo-inositol transport causes acute renal failure with selective medullary injury in the rat. *Kidney Int.* **53**, 146-153.

Klein, P. S. & Melton, D. A. (1996). A molecular mechanism for the effect of lithium on development. *Proc.Natl.Acad.Sci.U.S.A* **93**, 8455-8459.

Koida, M. & Walter, R. (1976). Post-proline cleaving enzyme. Purification of this endopeptidase by affinity chromatography. *J.Biol.Chem.* **251**, 7593-7599.

Kopnisky, K. L., Chalecka-Franaszek, E., Gonzalez-Zulueta, M., & Chuang, D. M. (2003). Chronic lithium treatment antagonizes glutamate-induced decrease of phosphorylated CREB in neurons via reducing protein phosphatase 1 and increasing MEK activities. *Neuroscience* **116**, 425-435.

Kusuhara, M., Hachisuka, H., Nakano, S., & Sasai, Y. (1993). Purification and characterization of prolyl endopeptidase from rat skin. *J.Dermatol.Sci.* **6**, 138-145.

Lai, J. S., Zhao, C., Warsh, J. J., & Li, P. P. (2006). Cytoprotection by lithium and valproate varies between cell types and cellular stresses. *Eur.J.Pharmacol.* **539**, 18-26.

Laux, T., Fukami, K., Thelen, M., Golub, T., Frey, D., & Caroni, P. (2000). GAP43, MARCKS, and CAP23 modulate PI(4,5)P(2) at plasmalemmal rafts, and regulate cell cortex actin dynamics through a common mechanism. *J.Cell Biol.* **149**, 1455-1472.

Lee, C. W., Lau, K. F., Miller, C. C., & Shaw, P. C. (2003). Glycogen synthase kinase-3 beta-mediated tau phosphorylation in cultured cell lines. *Neuroreport* **14**, 257-260.

Lenox, R. H., Watson, D. G., Patel, J., & Ellis, J. (1992). Chronic lithium administration alters a prominent PKC substrate in rat hippocampus. *Brain Res.* **570**, 333-340.

Leverich, G. S., McElroy, S. L., Suppes, T., Keck, P. E., Jr., Denicoff, K. D., Nolen, W. A., Altshuler, L. L., Rush, A. J., Kupka, R., Frye, M. A., Autio, K. A., & Post, R. M. (2002). Early physical and sexual abuse associated with an adverse course of bipolar illness. *Biol.Psychiatry* **51**, 288-297.

Li, X., Rosborough, K. M., Friedman, A. B., Zhu, W., & Roth, K. A. (2006). Regulation of mouse brain glycogen synthase kinase-3 by atypical antipsychotics. *Int.J.Neuropsychopharmacol.* 1-13.

Lovestone, S., Davis, D. R., Webster, M. T., Kaech, S., Brion, J. P., Matus, A., & Anderton, B. H. (1999). Lithium reduces tau phosphorylation: effects in living cells and in neurons at therapeutic concentrations. *Biol.Psychiatry* **45**, 995-1003.

Lu, R., Song, L., & Jope, R. S. (1999). Lithium attenuates p53 levels in human neuroblastoma SH-SY5Y cells. *Neuroreport* **10**, 1123-1125.

Lubrich, B. & van Calker, D. (1999). Inhibition of the high affinity myo-inositol transport system: a common mechanism of action of antibipolar drugs? *Neuropsychopharmacology* **21**, 519-529.

Lucas, F. R., Goold, R. G., Gordon-Weeks, P. R., & Salinas, P. C. (1998). Inhibition of GSK-3beta leading to the loss of phosphorylated MAP-1B is an early event in axonal remodelling induced by WNT-7a or lithium. *J.Cell Sci.* **111 (Pt 10)**, 1351-1361.

Lucas, F. R. & Salinas, P. C. (1997). WNT-7a induces axonal remodeling and increases synapsin I levels in cerebellar neurons. *Dev.Biol.* **192**, 31-44.

Luo, Y., Raible, D., & Raper, J. A. (1993). Collapsin: a protein in brain that induces the collapse and paralysis of neuronal growth cones. *Cell* **75**, 217-227.

MacKinnon, D. F., Jamison, K. R., & DePaulo, J. R. (1997). Genetics of manic depressive illness. *Annu.Rev.Neurosci.* **20**, 355-373.

Maes, M., Goossens, F., Scharpe, S., Calabrese, J., Desnyder, R., & Meltzer, H. Y. (1995). Alterations in plasma prolyl endopeptidase activity in depression, mania, and schizophrenia: effects of antidepressants, mood stabilizers, and antipsychotic drugs. *Psychiatry Res.* **58**, 217-225.

Maes, M., Goossens, F., Scharpe, S., Meltzer, H. Y., D'Hondt, P., & Cosyns, P. (1994). Lower serum prolyl endopeptidase enzyme activity in major depression: further evidence that peptidases play a role in the pathophysiology of depression. *Biol.Psychiatry* **35**, 545-552.

Maggirwar, S. B., Tong, N., Ramirez, S., Gelbard, H. A., & Dewhurst, S. (1999). HIV-1 Tat-mediated activation of glycogen synthase kinase-3beta contributes to Tat-mediated neurotoxicity. *J.Neurochem.* **73**, 578-586.

Mai, L., Jope, R. S., & Li, X. (2002). BDNF-mediated signal transduction is modulated by GSK3beta and mood stabilizing agents. *J.Neurochem.* **82**, 75-83.

Maier, D. L., Mani, S., Donovan, S. L., Soppet, D., Tessarollo, L., McCasland, J. S., & Meiri, K. F. (1999). Disrupted cortical map and absence of cortical barrels in growth-associated protein (GAP)-43 knockout mice. *Proc.Natl.Acad.Sci.U.S.A* **96**, 9397-9402.

Malhi, G. S., Mitchell, P. B., & Salim, S. (2003). Bipolar depression: management options. *CNS.Drugs* **17**, 9-25.

Manji, H. K. & Chen, G. (2002). PKC, MAP kinases and the bcl-2 family of proteins as long-term targets for mood stabilizers. *Mol.Psychiatry* **7 Suppl 1**, S46-S56.

Manji, H. K., Moore, G. J., & Chen, G. (2000). Lithium up-regulates the cytoprotective protein Bcl-2 in the CNS in vivo: a role for neurotrophic and neuroprotective effects in manic depressive illness. *J.Clin.Psychiatry* **61 Suppl 9**, 82-96.

Mansour, H. A., Monk, T. H., & Nimgaonkar, V. L. (2005). Circadian genes and bipolar disorder. *Ann.Med.* **37**, 196-205.

Mansour, H. A., Wood, J., Logue, T., Chowdari, K. V., Dayal, M., Kupfer, D. J., Monk, T. H., Devlin, B., & Nimgaonkar, V. L. (2006). Association study of eight circadian genes with bipolar I disorder, schizoaffective disorder and schizophrenia. *Genes Brain Behav.* **5**, 150-157.

Mark, R. J., Ashford, J. W., Goodman, Y., & Mattson, M. P. (1995). Anticonvulsants attenuate amyloid beta-peptide neurotoxicity, Ca2+ deregulation, and cytoskeletal pathology. *Neurobiol.Aging* **16**, 187-198.

Massot, O., Rousselle, J. C., Fillion, M. P., Januel, D., Plantefol, M., & Fillion, G. (1999). 5-HT1B receptors: a novel target for lithium. Possible involvement in mood disorders. *Neuropsychopharmacology* **21**, 530-541.

McDonald, C., Zanelli, J., Rabe-Hesketh, S., Ellison-Wright, I., Sham, P., Kalidindi, S., Murray, R. M., & Kennedy, N. (2004). Meta-analysis of magnetic resonance imaging brain morphometry studies in bipolar disorder. *Biol.Psychiatry* **56**, 411-417.

McGuffin, P., Rijsdijk, F., Andrew, M., Sham, P., Katz, R., & Cardno, A. (2003). The heritability of bipolar affective disorder and the genetic relationship to unipolar depression. *Arch.Gen.Psychiatry* **60**, 497-502.

McLaughlin, S. & Murray, D. (2005). Plasma membrane phosphoinositide organization by protein electrostatics. *Nature* **438**, 605-611.

McQueen, M. B., Devlin, B., Faraone, S. V., Nimgaonkar, V. L., Sklar, P., Smoller, J. W., Abou, J. R., Albus, M., Bacanu, S. A., Baron, M., Barrett, T. B., Berrettini, W., Blacker, D., Byerley, W., Cichon, S., Coryell, W., Craddock, N., Daly, M. J., DePaulo, J. R., Edenberg, H. J., Foroud, T., Gill, M., Gilliam, T. C., Hamshere, M., Jones, I., Jones, L., Juo, S. H., Kelsoe, J. R., Lambert, D., Lange, C., Lerer, B., Liu, J., Maier, W., Mackinnon,

J. D., McInnis, M. G., McMahon, F. J., Murphy, D. L., Nothen, M. M., Nurnberger, J. I., Pato, C. N., Pato, M. T., Potash, J. B., Propping, P., Pulver, A. E., Rice, J. P., Rietschel, M., Scheftner, W., Schumacher, J., Segurado, R., Van Steen, K., Xie, W., Zandi, P. P., & Laird, N. M. (2005). Combined analysis from eleven linkage studies of bipolar disorder provides strong evidence of susceptibility loci on chromosomes 6q and 8q. *Am.J.Hum.Genet.* **77**, 582-595.

Medhurst, A. D., Harrison, D. C., Read, S. J., Campbell, C. A., Robbins, M. J., & Pangalos, M. N. (2000). The use of TaqMan RT-PCR assays for semiquantitative analysis of gene expression in CNS tissues and disease models. *J.Neurosci.Methods* **98**, 9-20.

Meiri, K. F. & Gordon-Weeks, P. R. (1990). GAP-43 in growth cones is associated with areas of membrane that are tightly bound to substrate and is a component of a membrane skeleton subcellular fraction. *J.Neurosci.* **10**, 256-266.

Micheva, K. D., Holz, R. W., & Smith, S. J. (2001). Regulation of presynaptic phosphatidylinositol 4,5-biphosphate by neuronal activity. *J.Cell Biol.* **154**, 355-368.

Moller, H. J. & Grunze, H. (2000). Have some guidelines for the treatment of acute bipolar depression gone too far in the restriction of antidepressants? *Eur.Arch.Psychiatry Clin.Neurosci.* **250**, 57-68.

Moore, G. J., Bebchuk, J. M., Hasanat, K., Chen, G., Seraji-Bozorgzad, N., Wilds, I. B., Faulk, M. W., Koch, S., Glitz, D. A., Jolkovsky, L., & Manji, H. K. (2000). Lithium increases N-acetyl-aspartate in the human brain: in vivo evidence in support of bcl-2's neurotrophic effects? *Biol.Psychiatry* **48**, 1-8.

Moore, G. J., Bebchuk, J. M., Parrish, J. K., Faulk, M. W., Arfken, C. L., Strahl-Bevacqua, J., & Manji, H. K. (1999). Temporal dissociation between lithium-induced changes in frontal lobe myo-inositol and clinical response in manic-depressive illness. *Am.J.Psychiatry* **156**, 1902-1908.

Mora, A., Sabio, G., Alonso, J. C., Soler, G., & Centeno, F. (2002). Different dependence of lithium and valproate on PI3K/PKB pathway. *Bipolar.Disord.* **4**, 195-200.

Morain, P., Lestage, P., De Nanteuil, G., Jochemsen, R., Robin, J. L., Guez, D., & Boyer, P. A. (2002). S 17092: a prolyl endopeptidase inhibitor as a potential therapeutic drug for memory impairment. Preclinical and clinical studies. *CNS.Drug Rev.* **8**, 31-52.

Morain, P., Robin, J. L., De Nanteuil, G., Jochemsen, R., Heidet, V., & Guez, D. (2000). Pharmacodynamic and pharmacokinetic profile of S 17092, a new orally active prolyl endopeptidase inhibitor, in elderly healthy volunteers. A phase I study. *Br.J.Clin.Pharmacol.* **50**, 350-359.

Moss, D. J., Fernyhough, P., Chapman, K., Baizer, L., Bray, D., & Allsopp, T. (1990). Chicken growth-associated protein GAP-43 is tightly bound to the actin-rich neuronal membrane skeleton. *J.Neurochem.* **54**, 729-736.

Motohashi, N. (1992). GABA receptor alterations after chronic lithium administration. Comparison with carbamazepine and sodium valproate. *Prog.Neuropsychopharmacol.Biol.Psychiatry* **16**, 571-579.

Muller-Oerlinghausen, B., Felber, W., Berghofer, A., Lauterbach, E., & Ahrens, B. (2005). The impact of lithium long-term medication on suicidal behavior and mortality of bipolar patients. *Arch.Suicide Res.* **9**, 307-319.

Munoz-Montano, J. R., Lim, F., Moreno, F. J., Avila, J., & Diaz-Nido, J. (1999). Glycogen Synthase Kinase-3 Modulates Neurite Outgrowth in Cultured Neurons: Possible Implications for Neurite Pathology in Alzheimer's Disease. *J.Alzheimers.Dis.* **1**, 361-378.

Murray, M. & Greenberg, M. L. (2000). Expression of yeast INM1 encoding inositol monophosphatase is regulated by inositol, carbon source and growth stage and is decreased by lithium and valproate. *Mol.Microbiol.* **36**, 651-661.

Muzina, D. J., Elhaj, O., Gajwani, P., Gao, K., & Calabrese, J. R. (2005). Lamotrigine and antiepileptic drugs as mood stabilizers in bipolar disorder. *Acta Psychiatr.Scand.Suppl* 21-28.

Nahorski, S. R., Ragan, C. I., & Challiss, R. A. (1991). Lithium and the phosphoinositide cycle: an example of uncompetitive inhibition and its pharmacological consequences. *Trends Pharmacol.Sci.* **12**, 297-303.

Nakajima, T., Ono, Y., Kato, A., Maeda, J., & Ohe, T. (1992). Y-29794--a non-peptide prolyl endopeptidase inhibitor that can penetrate into the brain. *Neurosci.Lett.* **141**, 156-160.

Nasrallah, H. A., Ketter, T. A., & Kalali, A. H. (2006). Carbamazepine and valproate for the treatment of bipolar disorder: a review of the literature. *J.Affect.Disord.*

Nemanov, L., Ebstein, R. P., Belmaker, R. H., Osher, Y., & Agam, G. (1999). Effect of bipolar disorder on lymphocyte inositol monophosphatase mRNA levels. *Int.J.Neuropsychopharmcol.* **2**, 25-29.

Neve, R. L., Perrone-Bizzozero, N. I., Finklestein, S., Zwiers, H., Bird, E., Kurnit, D. M., & Benowitz, L. I. (1987). The neuronal growth-associated protein GAP-43 (B-50, F1): neuronal specificity, developmental regulation and regional distribution of the human and rat mRNAs. *Brain Res.* **388**, 177-183.

Nievergelt, C. M., Kripke, D. F., Barrett, T. B., Burg, E., Remick, R. A., Sadovnick, A. D., McElroy, S. L., Keck, P. E., Jr., Schork, N. J., & Kelsoe, J. R. (2006). Suggestive evidence for association of the circadian genes PERIOD3 and ARNTL with bipolar disorder. *Am.J.Med.Genet.B Neuropsychiatr.Genet.* **141**, 234-241.

Nishizuka, Y. (1995). Protein kinase C and lipid signaling for sustained cellular responses. *FASEB J.* **9**, 484-496.

Nonaka, S. & Chuang, D. M. (1998). Neuroprotective effects of chronic lithium on focal cerebral ischemia in rats. *Neuroreport* **9**, 2081-2084.

Novak, A. & Dedhar, S. (1999). Signaling through beta-catenin and Lef/Tcf. *Cell Mol.Life Sci.* **56**, 523-537.

O'Brien, W. T., Harper, A. D., Jove, F., Woodgett, J. R., Maretto, S., Piccolo, S., & Klein, P. S. (2004). Glycogen synthase kinase-3beta haploinsufficiency mimics the behavioral and molecular effects of lithium. *J.Neurosci.* **24**, 6791-6798.

O'Day, P. M. & Phillips, C. L. (1991). Effects of external lithium on the physiology of Limulus ventral photoreceptors. *Vis.Neurosci.* **7**, 251-258.

O'Leary, R. M., Gallagher, S. P., & O'Connor, B. (1996). Purification and characterization of a novel membrane-bound form of prolyl endopeptidase from bovine brain. *Int.J.Biochem.Cell Biol.* **28**, 441-449.

O'Leary, R. M. & O'Connor, B. (1995). Identification and localisation of a synaptosomal membrane prolyl endopeptidase from bovine brain. *Eur.J.Biochem.* **227**, 277-283.

Oestreicher, A. B. & Gispen, W. H. (1986). Comparison of the immunocytochemical distribution of the phosphoprotein B-50 in the cerebellum and hippocampus of immature and adult rat brain. *Brain Res.* **375**, 267-279.

Ohnishi, T., Ohba, H., Seo, K., Im, J., Sato, Y., Iwiyama, Y., Furuichi, T., Chung, S., Yoshikawa, T. (2006). Biochemical properties that distinguish a second myoinositol monophosphatase, Impa2 from Impa1. Abstract 191, Atlanta, Society for Neuroscience.

Okuma, T., Yamashita, I., Takahashi, R., Itoh, H., Otsuki, S., Watanabe, S., Sarai, K., Hazama, H., & Inanaga, K. (1990). Comparison of the antimanic efficacy of carbamazepine and lithium carbonate by double-blind controlled study. *Pharmacopsychiatry* **23**, 143-150.

Osborne, S. L., Meunier, F. A., & Schiavo, G. (2001). Phosphoinositides as key regulators of synaptic function. *Neuron* **32**, 9-12.

Owen, R. & Gordon-Weeks, P. R. (2003). Inhibition of glycogen synthase kinase 3beta in sensory neurons in culture alters filopodia dynamics and microtubule distribution in growth cones. *Mol.Cell Neurosci.* **23**, 626-637.

Owens, M. J. & Nemeroff, C. B. (2003). Pharmacology of valproate. *Psychopharmacol.Bull.* **37 Suppl 2**, 17-24.

Pap, M. & Cooper, G. M. (1998). Role of glycogen synthase kinase-3 in the phosphatidylinositol 3-Kinase Akt cell survival pathway. *J.Biol.Chem.* **273**, 19929-19932.

Pardo, R., Andreolotti, A. G., Ramos, B., Picatoste, F., & Claro, E. (2003). Opposed effects of lithium on the MEK-ERK pathway in neural cells: inhibition in astrocytes and stimulation in neurons by GSK3 independent mechanisms. *J.Neurochem.* **87**, 417-426.

Parthasarathy, L., Vadnal, R. E., Parthasarathy, R., & Devi, C. S. (1994). Biochemical and molecular properties of lithium-sensitive myo-inositol monophosphatase. *Life Sci.* **54**, 1127-1142.

Peifer, M. & Polakis, P. (2000). Wnt signaling in oncogenesis and embryogenesis--a look outside the nucleus. *Science* **287**, 1606-1609.

Phiel, C. J. & Klein, P. S. (2001). Molecular targets of lithium action. *Annu.Rev.Pharmacol.Toxicol.* **41**, 789-813.

Phiel, C. J., Zhang, F., Huang, E. Y., Guenther, M. G., Lazar, M. A., & Klein, P. S. (2001). Histone deacetylase is a direct target of valproic acid, a potent anticonvulsant, mood stabilizer, and teratogen. *J.Biol.Chem.* **276**, 36734-36741.

Phillis, J. W. & O'Regan, M. H. (2004). A potentially critical role of phospholipases in central nervous system ischemic, traumatic, and neurodegenerative disorders. *Brain Res.Brain Res.Rev.* **44**, 13-47.

Plyte, S. E., Hughes, K., Nikolakaki, E., Pulverer, B. J., & Woodgett, J. R. (1992). Glycogen synthase kinase-3: functions in oncogenesis and development. *Biochim.Biophys.Acta* **1114**, 147-162.

Polgar, L. (2002). The prolyl oligopeptidase family. *Cell Mol.Life Sci.* **59**, 349-362.

Pollard, T. D. & Borisy, G. G. (2003). Cellular motility driven by assembly and disassembly of actin filaments. *Cell* **112**, 453-465.

Pontiggia, A., Benedetti, F., Barbini B, Cigala Furgosi M, Colombo, C., Dallaspezia S, & Smeraldi, E. (2006). Long term outcome of drug-resistant bipolar depression: a 9 months prospective follow-up after chronotherapeutics. *Eur.Neuropsychopharmacol.* **S72**.

Post, R. M., Denicoff, K. D., Leverich, G. S., Altshuler, L. L., Frye, M. A., Suppes, T. M., Rush, A. J., Keck, P. E., Jr., McElroy, S. L., Luckenbaugh, D. A., Pollio, C., Kupka, R., & Nolen, W. A. (2003a). Morbidity in 258 bipolar outpatients followed for 1 year with daily prospective ratings on the NIMH life chart method. *J.Clin.Psychiatry* **64**, 680-690.

Post, R. M., Leverich, G. S., Altshuler, L. L., Frye, M. A., Suppes, T. M., Keck, P. E., Jr., McElroy, S. L., Kupka, R., Nolen, W. A., Grunze, H., & Walden, J. (2003b). An overview of recent findings of the Stanley Foundation Bipolar Network (Part I). *Bipolar.Disord.* **5**, 310-319.

Price, L. H. & Heninger, G. R. (1994). Lithium in the treatment of mood disorders. *N.Engl.J.Med.* **331**, 591-598.

Ragan, C. I., Watling, K. J., Gee, N. S., Aspley, S., Jackson, R. G., Reid, G. G., Baker, R., Billington, D. C., Barnaby, R. J., & Leeson, P. D. (1988). The dephosphorylation of

inositol 1,4-bisphosphate to inositol in liver and brain involves two distinct Li+-sensitive enzymes and proceeds via inositol 4-phosphate. *Biochem.J.* **249**, 143-148.

Rapoport, S. I. & Bosetti, F. (2002). Do lithium and anticonvulsants target the brain arachidonic acid cascade in bipolar disorder? *Arch.Gen.Psychiatry* **59**, 592-596.

Redrobe, J. P. & Bourin, M. (1999). Evidence of the activity of lithium on 5-HT1B receptors in the mouse forced swimming test: comparison with carbamazepine and sodium valproate. *Psychopharmacology (Berl)* **141**, 370-377.

Ren, X. D. & Schwartz, M. A. (1998). Regulation of inositol lipid kinases by Rho and Rac. *Curr.Opin.Genet.Dev.* **8**, 63-67.

Riccio, A., Ahn, S., Davenport, C. M., Blendy, J. A., & Ginty, D. D. (1999). Mediation by a CREB family transcription factor of NGF-dependent survival of sympathetic neurons. *Science* **286**, 2358-2361.

Ridley, A. J. (2006). Rho GTPases and actin dynamics in membrane protrusions and vesicle trafficking. *Trends Cell Biol.* **16**, 522-529.

Roberson, E. D., English, J. D., Adams, J. P., Selcher, J. C., Kondratick, C., & Sweatt, J. D. (1999). The mitogen-activated protein kinase cascade couples PKA and PKC to cAMP response element binding protein phosphorylation in area CA1 of hippocampus. *J.Neurosci.* **19**, 4337-4348.

Robinson, L. J., Thompson, J. M., Gallagher, P., Goswami, U., Young, A. H., Ferrier, I. N., & Moore, P. B. (2006). A meta-analysis of cognitive deficits in euthymic patients with bipolar disorder. *J.Affect.Disord.* **93**, 105-115.

Roh, M. S., Kang, U. G., Shin, S. Y., Lee, Y. H., Jung, H. Y., Juhnn, Y. S., & Kim, Y. S. (2003). Biphasic changes in the Ser-9 phosphorylation of glycogen synthase kinase-3beta

after electroconvulsive shock in the rat brain. *Prog.Neuropsychopharmacol.Biol.Psychiatry* **27**, 1-5.

Rohatgi, R., Ho, H. Y., & Kirschner, M. W. (2000). Mechanism of N-WASP activation by CDC42 and phosphatidylinositol 4, 5-bisphosphate. *J.Cell Biol.* **150**, 1299-1310.

Rossner, S., Schulz, I., Zeitschel, U., Schliebs, R., Bigl, V., & Demuth, H. U. (2005). Brain prolyl endopeptidase expression in aging, APP transgenic mice and Alzheimer's disease. *Neurochem.Res.* **30**, 695-702.

Ryan, M. M., Lockstone, H. E., Huffaker, S. J., Wayland, M. T., Webster, M. J., & Bahn, S. (2006). Gene expression analysis of bipolar disorder reveals downregulation of the ubiquitin cycle and alterations in synaptic genes. *Mol.Psychiatry*.

Rybakowski, J. K., Borkowska, A., Czerski, P. M., Skibinska, M., & Hauser, J. (2003). Polymorphism of the brain-derived neurotrophic factor gene and performance on a cognitive prefrontal test in bipolar patients. *Bipolar.Disord.* **5**, 468-472.

Rybakowski, J. K., Suwalska, A., Skibinska, M., Szczepankiewicz, A., Leszczynska-Rodziewicz, A., Permoda, A., Czerski, P. M., & Hauser, J. (2005). Prophylactic lithium response and polymorphism of the brain-derived neurotrophic factor gene. *Pharmacopsychiatry* **38**, 166-170.

Ryves, W. J., Dajani, R., Pearl, L., & Harwood, A. J. (2002). Glycogen synthase kinase-3 inhibition by lithium and beryllium suggests the presence of two magnesium binding sites. *Biochem.Biophys.Res.Commun.* **290**, 967-972.

Ryves, W. J., Dalton, E. C., Harwood, A. J., & Williams, R. S. (2005). GSK-3 activity in neocortical cells is inhibited by lithium but not carbamazepine or valproic acid. *Bipolar.Disord.* **7**, 260-265.

Ryves, W. J. & Harwood, A. J. (2001). Lithium inhibits glycogen synthase kinase-3 by competition for magnesium. *Biochem.Biophys.Res.Commun.* **280**, 720-725.

Sachs, G. S. (1996). Bipolar mood disorder: practical strategies for acute and maintenance phase treatment. *J.Clin.Psychopharmacol.* **16**, 32S-47S.

Sang, H., Lu, Z., Li, Y., Ru, B., Wang, W., & Chen, J. (2001). Phosphorylation of tau by glycogen synthase kinase 3beta in intact mammalian cells influences the stability of microtubules. *Neurosci.Lett.* **312**, 141-144.

Schneider, J. S., Giardiniere, M., & Morain, P. (2002). Effects of the prolyl endopeptidase inhibitor S 17092 on cognitive deficits in chronic low dose MPTP-treated monkeys. *Neuropsychopharmacology* **26**, 176-182.

Schulz, I., Gerhartz, B., Neubauer, A., Holloschi, A., Heiser, U., Hafner, M., & Demuth, H. U. (2002). Modulation of inositol 1,4,5-triphosphate concentration by prolyl endopeptidase inhibition. *Eur.J.Biochem.* **269**, 5813-5820.

Schulz, I., Zeitschel, U., Rudolph, T., Ruiz-Carrillo, D., Rahfeld, J. U., Gerhartz, B., Bigl, V., Demuth, H. U., & Rossner, S. (2005). Subcellular localization suggests novel functions for prolyl endopeptidase in protein secretion. *J.Neurochem.* **94**, 970-979.

Schumacher, J., Jamra, R. A., Freudenberg, J., Becker, T., Ohlraun, S., Otte, A. C., Tullius, M., Kovalenko, S., Bogaert, A. V., Maier, W., Rietschel, M., Propping, P., Nothen, M. M., & Cichon, S. (2004). Examination of G72 and D-amino-acid oxidase as genetic risk factors for schizophrenia and bipolar affective disorder. *Mol.Psychiatry* **9**, 203-207.

Segurado, R., Detera-Wadleigh, S. D., Levinson, D. F., Lewis, C. M., Gill, M., Nurnberger, J. I., Jr., Craddock, N., DePaulo, J. R., Baron, M., Gershon, E. S., Ekholm, J., Cichon, S., Turecki, G., Claes, S., Kelsoe, J. R., Schofield, P. R., Badenhop, R. F., Morissette, J., Coon, H., Blackwood, D., McInnes, L. A., Foroud, T., Edenberg, H. J.,

Reich, T., Rice, J. P., Goate, A., McInnis, M. G., McMahon, F. J., Badner, J. A., Goldin, L. R., Bennett, P., Willour, V. L., Zandi, P. P., Liu, J., Gilliam, C., Juo, S. H., Berrettini, W. H., Yoshikawa, T., Peltonen, L., Lonnqvist, J., Nothen, M. M., Schumacher, J., Windemuth, C., Rietschel, M., Propping, P., Maier, W., Alda, M., Grof, P., Rouleau, G. A., Del Favero, J., Van Broeckhoven, C., Mendlewicz, J., Adolfsson, R., Spence, M. A., Luebbert, H., Adams, L. J., Donald, J. A., Mitchell, P. B., Barden, N., Shink, E., Byerley, W., Muir, W., Visscher, P. M., Macgregor, S., Gurling, H., Kalsi, G., McQuillin, A., Escamilla, M. A., Reus, V. I., Leon, P., Freimer, N. B., Ewald, H., Kruse, T. A., Mors, O., Radhakrishna, U., Blouin, J. L., Antonarakis, S. E., & Akarsu, N. (2003). Genome scan meta-analysis of schizophrenia and bipolar disorder, part III: Bipolar disorder. *Am.J.Hum.Genet.* **73**, 49-62.

Shaldubina, A., Buccafusca, R., Johanson, R. A., Agam, G., Belmaker, R. H., Berry, G. T., & Bersudsky, Y. (2006a). Behavioural phenotyping of sodium-myo-inositol cotransporter heterozygous knockout mice with reduced brain inositol. *Genes Brain Behav.* 1-7.

Shaldubina, A., Johanson, R. A., O'Brien, W. T., Buccafusca, R., Agam, G., Belmaker, R. H., Klein, P. S., Bersudsky, Y., & Berry, G. T. (2006b). SMIT1 haploinsufficiency causes brain inositol deficiency without affecting lithium-sensitive behavior. *Mol.Genet.Metab* **88**, 384-388.

Shaltiel, G., Shamir, A., Shapiro, J., Ding, D., Dalton, E., Bialer, M., Harwood, A. J., Belmaker, R. H., Greenberg, M. L., & Agam, G. (2004). Valproate decreases inositol biosynthesis. *Biol.Psychiatry* **56**, 868-874.

Shamir, A., Sjoholt, G., Ebstein, R. P., Agam, G., & Steen, V. M. (2001). Characterization of two genes, Impa1 and Impa2 encoding mouse myo-inositol monophosphatases. *Gene* **271**, 285-291.

Shaw, P. C., Davies, A. F., Lau, K. F., Garcia-Barcelo, M., Waye, M. M., Lovestone, S., Miller, C. C., & Anderton, B. H. (1998). Isolation and chromosomal mapping of human glycogen synthase kinase-3 alpha and -3 beta encoding genes. *Genome* **41**, 720-727.

Shaywitz, A. J. & Greenberg, M. E. (1999). CREB: a stimulus-induced transcription factor activated by a diverse array of extracellular signals. *Annu.Rev.Biochem.* **68**, 821-861.

Shetty, H. U., Holloway, H. W., & Rapoport, S. I. (1995). Capillary gas chromatography combined with ion trap detection for quantitative profiling of polyols in cerebrospinal fluid and plasma. *Anal.Biochem.* **224**, 279-285.

Shifman, S., Bronstein, M., Sternfeld, M., Pisante, A., Weizman, A., Reznik, I., Spivak, B., Grisaru, N., Karp, L., Schiffer, R., Kotler, M., Strous, R. D., Swartz-Vanetik, M., Knobler, H. Y., Shinar, E., Yakir, B., Zak, N. B., & Darvasi, A. (2004). COMT: a common susceptibility gene in bipolar disorder and schizophrenia. *Am.J.Med.Genet.B Neuropsychiatr.Genet.* **128**, 61-64.

Shinoda, M., Miyazaki, A., & Toide, K. (1999). Effect of a novel prolyl endopeptidase inhibitor, JTP-4819, on spatial memory and on cholinergic and peptidergic neurons in rats with ibotenate-induced lesions of the nucleus basalis magnocellularis. *Behav.Brain Res.* **99**, 17-25.

Shinoda, M., Okamiya, K., & Toide, K. (1995). Effect of a novel prolyl endopeptidase inhibitor, JTP-4819, on thyrotropin-releasing hormone-like immunoreactivity in the cerebral cortex and hippocampus of aged rats. *Jpn.J.Pharmacol.* **69**, 273-276.

Silverstone, P. H., Wu, R. H., O'Donnell, T., Ulrich, M., Asghar, S. J., & Hanstock, C. C. (2002). Chronic treatment with both lithium and sodium valproate may normalize phosphoinositol cycle activity in bipolar patients. *Hum.Psychopharmacol.* **17**, 321-327.

Sjoholt, G., Ebstein, R. P., Lie, R. T., Berle, J. O., Mallet, J., Deleuze, J. F., Levinson, D. F., Laurent, C., Mujahed, M., Bannoura, I., Murad, I., Molven, A., & Steen, V. M. (2004). Examination of IMPA1 and IMPA2 genes in manic-depressive patients: association between IMPA2 promoter polymorphisms and bipolar disorder. *Mol.Psychiatry* **9**, 621-629.

Skaper, S. D. & Walsh, F. S. (1998). Neurotrophic molecules: strategies for designing effective therapeutic molecules in neurodegeneration. *Mol.Cell Neurosci.* **12**, 179-193.

Skene, J. H. & Virag, I. (1989). Posttranslational membrane attachment and dynamic fatty acylation of a neuronal growth cone protein, GAP-43. *J.Cell Biol.* **108**, 613-624.

Sklar, P., Gabriel, S. B., McInnis, M. G., Bennett, P., Lim, Y. M., Tsan, G., Schaffner, S., Kirov, G., Jones, I., Owen, M., Craddock, N., DePaulo, J. R., & Lander, E. S. (2002). Family-based association study of 76 candidate genes in bipolar disorder: BDNF is a potential risk locus. Brain-derived neutrophic factor. *Mol.Psychiatry* **7**, 579-593.

Slepnev, V. I. & De Camilli, P. (2000). Accessory factors in clathrin-dependent synaptic vesicle endocytosis. *Nat.Rev.Neurosci.* **1**, 161-172.

Stine, O. C., Xu, J., Koskela, R., McMahon, F. J., Gschwend, M., Friddle, C., Clark, C. D., McInnis, M. G., Simpson, S. G., Breschel, T. S., & . (1995). Evidence for linkage of bipolar disorder to chromosome 18 with a parent-of-origin effect. *Am.J.Hum.Genet.* **57**, 1384-1394.

Straub, R. E., Lehner, T., Luo, Y., Loth, J. E., Shao, W., Sharpe, L., Alexander, J. R., Das, K., Simon, R., Fieve, R. R., & . (1994). A possible vulnerability locus for bipolar affective disorder on chromosome 21q22.3. *Nat.Genet.* **8**, 291-296.

Suppes, T. (2002). Review of the use of topiramate for treatment of bipolar disorders. *J.Clin.Psychopharmacol.* **22**, 599-609.

Sutherland, C., Leighton, I. A., & Cohen, P. (1993). Inactivation of glycogen synthase kinase-3 beta by phosphorylation: new kinase connections in insulin and growth-factor signalling. *Biochem.J.* **296 (Pt 1)**, 15-19.

Swann, A. C., Bowden, C. L., Morris, D., Calabrese, J. R., Petty, F., Small, J., Dilsaver, S. C., & Davis, J. M. (1997). Depression during mania. Treatment response to lithium or divalproex. *Arch.Gen.Psychiatry* **54**, 37-42.

Szeltner, Z., Alshafee, I., Juhasz, T., Parvari, R., & Polgar, L. (2005). The PREPL A protein, a new member of the prolyl oligopeptidase family, lacking catalytic activity. *Cell Mol.Life Sci.* **62**, 2376-2381.

Szeltner, Z., Renner, V., & Polgar, L. (2000). The noncatalytic beta-propeller domain of prolyl oligopeptidase enhances the catalytic capability of the peptidase domain. *J.Biol.Chem.* **275**, 15000-15005.

Tessier-Lavigne, M. (2002). Wiring the brain: the logic and molecular mechanisms of axon guidance and regeneration. *Harvey Lect.* **98**, 103-143.

Tessier-Lavigne, M. & Goodman, C. S. (1996). The molecular biology of axon guidance. *Science* **274**, 1123-1133.

Thomson, P. A., Wray, N. R., Millar, J. K., Evans, K. L., Hellard, S. L., Condie, A., Muir, W. J., Blackwood, D. H., & Porteous, D. J. (2005). Association between the TRAX/DISC locus and both bipolar disorder and schizophrenia in the Scottish population. *Mol.Psychiatry* **10**, 657-68, 616.

Toide, K., Okamiya, K., Iwamoto, Y., & Kato, T. (1995). Effect of a novel prolyl endopeptidase inhibitor, JTP-4819, on prolyl endopeptidase activity and substance P- and arginine-vasopressin-like immunoreactivity in the brains of aged rats. *J.Neurochem.* **65**, 234-240.

Toide, K., Shinoda, M., Iwamoto, Y., Fujiwara, T., Okamiya, K., & Uemura, A. (1997). A novel prolyl endopeptidase inhibitor, JTP-4819, with potential for treating Alzheimer's disease. *Behav.Brain Res.* **83**, 147-151.

Tolias, K. F., Couvillon, A. D., Cantley, L. C., & Carpenter, C. L. (1998). Characterization of a Rac1- and RhoGDI-associated lipid kinase signaling complex. *Mol.Cell Biol.* **18**, 762-770.

Tsai, G. & Coyle, J. T. (1995). N-acetylaspartate in neuropsychiatric disorders. *Prog.Neurobiol.* **46**, 531-540.

Uldry, M., Ibberson, M., Horisberger, J. D., Chatton, J. Y., Riederer, B. M., & Thorens, B. (2001). Identification of a mammalian H(+)-myo-inositol symporter expressed predominantly in the brain. *EMBO J.* **20**, 4467-4477.

Uldry, M., Steiner, P., Zurich, M. G., Beguin, P., Hirling, H., Dolci, W., & Thorens, B. (2004). Regulated exocytosis of an H+/myo-inositol symporter at synapses and growth cones. *EMBO J.* **23**, 531-540.

Vaden, D. L., Ding, D., Peterson, B., & Greenberg, M. L. (2001). Lithium and valproate decrease inositol mass and increase expression of the yeast INO1 and INO2 genes for inositol biosynthesis. *J.Biol.Chem.* **276**, 15466-15471.

Vadnal, R. & Parthasarathy, R. (1995). Myo-inositol monophosphatase: diverse effects of lithium, carbamazepine, and valproate. *Neuropsychopharmacology* **12**, 277-285.

van Calker, D. & Belmaker, R. H. (2000). The high affinity inositol transport system--implications for the pathophysiology and treatment of bipolar disorder. *Bipolar.Disord.* **2**, 102-107.

Van Dongen, C. J., Zwiers, H., De Graan, P. N., & Gispen, W. H. (1985). Modulation of the activity of purified phosphatidylinositol 4-phosphate kinase by phosphorylated and dephosphorylated B-50 protein. *Biochem.Biophys.Res.Commun.* **128**, 1219-1227.

Van Hooff, C. O., De Graan, P. N., Oestreicher, A. B., & Gispen, W. H. (1988). B-50 phosphorylation and polyphosphoinositide metabolism in nerve growth cone membranes. *J.Neurosci.* **8**, 1789-1795.

Venalainen, J. I., Juvonen, R. O., Forsberg, M. M., Garcia-Horsman, A., Poso, A., Wallen, E. A., Gynther, J., & Mannisto, P. T. (2002). Substrate-dependent, non-hyperbolic kinetics of pig brain prolyl oligopeptidase and its tight binding inhibition by JTP-4819. *Biochem.Pharmacol.* **64**, 463-471.

Venalainen, J. I., Juvonen, R. O., & Mannisto, P. T. (2004). Evolutionary relationships of the prolyl oligopeptidase family enzymes. *Eur.J.Biochem.* **271**, 2705-2715.

Verhaagen, J., Hermens, W. T., Oestreicher, A. B., Gispen, W. H., Rabkin, S. D., Pfaff, D. W., & Kaplitt, M. G. (1994). Expression of the growth-associated protein B-50/GAP43 via a defective herpes-simplex virus vector results in profound morphological changes in non-neuronal cells. *Brain Res.Mol.Brain Res.* **26**, 26-36.

Vestergaard, P. (2004). Guidelines for maintenance treatment of bipolar disorder: are there discrepancies between European and North American recommendations? *Bipolar.Disord.* **6**, 519-522.

Virdee, K., Xue, L., Hemmings, B. A., Goemans, C., Heumann, R., & Tolkovsky, A. M. (1999). Nerve growth factor-induced PKB/Akt activity is sustained by phosphoinositide 3-kinase dependent and independent signals in sympathetic neurons. *Brain Res.* **837**, 127-142.

Wang, J. F., Azzam, J. E., & Young, L. T. (2003). Valproate inhibits oxidative damage to lipid and protein in primary cultured rat cerebrocortical cells. *Neuroscience* **116**, 485-489.

Wang, Q. M., Fiol, C. J., DePaoli-Roach, A. A., & Roach, P. J. (1994). Glycogen synthase kinase-3 beta is a dual specificity kinase differentially regulated by tyrosine and serine/threonine phosphorylation. *J.Biol.Chem.* **269**, 14566-14574.

Watson, D. G. & Lenox, R. H. (1996). Chronic lithium-induced down-regulation of MARCKS in immortalized hippocampal cells: potentiation by muscarinic receptor activation. *J.Neurochem.* **67**, 767-777.

Weissman, M. M., Bland, R. C., Canino, G. J., Faravelli, C., Greenwald, S., Hwu, H. G., Joyce, P. R., Karam, E. G., Lee, C. K., Lellouch, J., Lepine, J. P., Newman, S. C., Rubio-Stipec, M., Wells, J. E., Wickramaratne, P. J., Wittchen, H., & Yeh, E. K. (1996). Cross-national epidemiology of major depression and bipolar disorder. *JAMA* **276**, 293-299.

Werstuck, G. H., Kim, A. J., Brenstrum, T., Ohnmacht, S. A., Panna, E., & Capretta, A. (2004). Examining the correlations between GSK-3 inhibitory properties and anti-convulsant efficacy of valproate and valproate-related compounds. *Bioorg.Med.Chem.Lett.* **14**, 5465-5467.

Williams, R. S., Cheng, L., Mudge, A. W., & Harwood, A. J. (2002). A common mechanism of action for three mood-stabilizing drugs. *Nature* **417**, 292-295.

Williams, R. S., Eames, M., Ryves, W. J., Viggars, J., & Harwood, A. J. (1999). Loss of a prolyl oligopeptidase confers resistance to lithium by elevation of inositol (1,4,5) trisphosphate. *EMBO J.* **18**, 2734-2745.

Willmroth, F., Drieling, T., Lamla, U., Marcushen, M., Wark, H. J., & van Calker, D. (2006). Sodium-myo-inositol co-transporter (SMIT-1) mRNA is increased in neutrophils of patients with bipolar 1 disorder and down-regulated under treatment with mood stabilizers. *Int.J.Neuropsychopharmacol.* 1-9.

Wong, Y. H., Kalmbach, S. J., Hartman, B. K., & Sherman, W. R. (1987). Immunohistochemical staining and enzyme activity measurements show myo-inositol-1-phosphate synthase to be localized in the vasculature of brain. *J.Neurochem.* **48**, 1434-1442.

Xiao, J. & Liu, Y. (2003). Differential roles of ERK and JNK in early and late stages of neuritogenesis: a study in a novel PC12 model system. *J.Neurochem.* **86**, 1516-1523.

Xiao, J., Pradhan, A., & Liu, Y. (2006). Functional role of JNK in neuritogenesis of PC12-N1 cells. *Neurosci.Lett.* **392**, 231-234.

Xu, C., Macciardi, F., Li, P. P., Yoon, I. S., Cooke, R. G., Hughes, B., Parikh, S. V., McIntyre, R. S., Kennedy, J. L., & Warsh, J. J. (2006). Association of the putative susceptibility gene, transient receptor potential protein melastatin type 2, with bipolar disorder. *Am.J.Med.Genet.B Neuropsychiatr.Genet.* **141**, 36-43.

Yamauchi, A., Miyai, A., Shimada, S., Minami, Y., Tohyama, M., Imai, E., Kamada, T., & Ueda, N. (1995). Localization and rapid regulation of Na+/myo-inositol cotransporter in rat kidney. *J.Clin.Invest* **96**, 1195-1201.

Yatham, L. N. (2004). Newer anticonvulsants in the treatment of bipolar disorder. *J.Clin.Psychiatry* **65 Suppl 10**, 28-35.

Yatham, L. N., Kusumakar, V., Calabrese, J. R., Rao, R., Scarrow, G., & Kroeker, G. (2002). Third generation anticonvulsants in bipolar disorder: a review of efficacy and summary of clinical recommendations. *J.Clin.Psychiatry* **63**, 275-283.

Yin, L., Wang, J., Klein, P. S., & Lazar, M. A. (2006). Nuclear receptor Rev-erbalpha is a critical lithium-sensitive component of the circadian clock. *Science* **311**, 1002-1005.

Yoon, I. S., Li, P. P., Siu, K. P., Kennedy, J. L., Macciardi, F., Cooke, R. G., Parikh, S. V., & Warsh, J. J. (2001). Altered TRPC7 gene expression in bipolar-I disorder. *Biol.Psychiatry* **50**, 620-626.

Yuan, P. X., Huang, L. D , Jiang, Y. M., Gutkind, J. S., Manji, H. K., & Chen, G. (2001). The mood stabilizer valproic acid activates mitogen-activated protein kinases and promotes neurite growth. *J.Biol.Chem.* **276**, 31674-31683.